Theoretical Foundations for Designing an Autonomous Power Grid:

PMU Data Science for Blackout and Cyber-Attack Early Warning

Paul Bogdan, Edmond Jonckheere,
Laith Shalalfeh, Jayson Sia

Dept. of Electrical Engineering
University of Southern California
Los Angeles, CA 90089
{pbogdan,jonckhee,shalalfe,jsia}@usc.edu

USC Viterbi
School of Engineering

University of Southern California

Plan of Action

- Part 1: Modeling
  - Part 1A: Data-driven and "First-principle"
  - Part 1B: General Introduction to Fractality
- Part 2: Security

The Smart Grid has Many Facets

- Large movement of power across geographically large areas
- Economic dispatch
- Line overloading
- Stochastic fluctuations induced by renewables
- Storage elements
- Integration with electric vehicles
- Phasor Measurement Unit (PMU) technology
- Privacy concern over smart meters
- Security (“black energy”)
- etc.

Lots of mathematics & new concepts

- Is that all???

Plan of Action: Part 1A – Modeling

- Data driven modeling
  - Detrended Fluctuation Analysis (DFA)
  - Auto-Regressive Fractionally Integrated (ARFIMA) modeling
  - Berg model (Scandinavian grid)
- *"First principles"* modeling
  - Load aggregation
  - Falsification of swing equation by PMU data

Long-Range Dependence or Memory (in PMU data)

- **Long-range memory** is one of the characteristics of fractal patterns. It relates to slow decay of the correlation as the lag between samples increase.

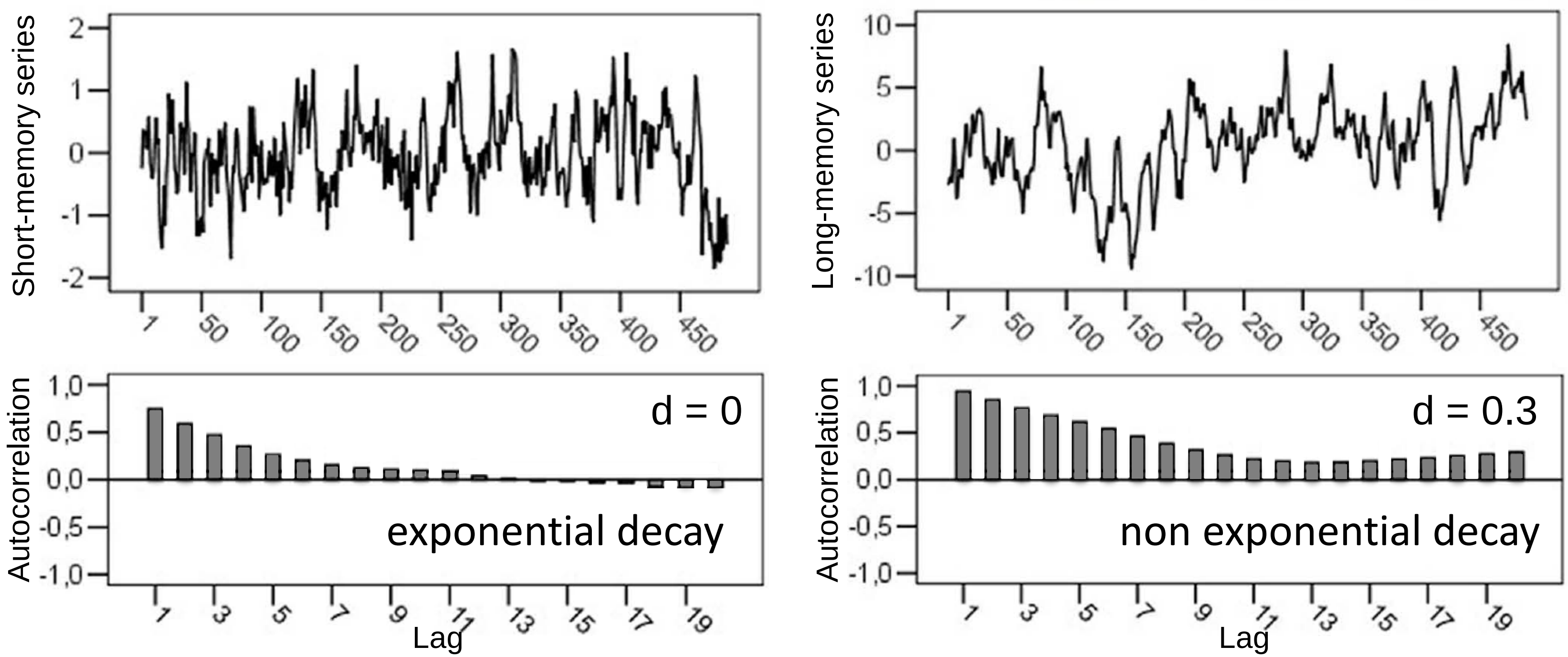

Long-Range Dependence or Memory

- There are several parameters that quantify the severity of the fractal behavior in a time series:

  - Number of incrementation or differentiation steps (d):

    $$\text{ARFIMA:} \quad \left(1-\sum_{i=1}^{p}\phi_i B^i\right)(1-B)^d X_t = \left(1+\sum_{i=1}^{q}\theta_i B^i\right)\varepsilon_t, \quad \phi_1 = \text{AR}(1)$$

  - Power Spectral Density exponent (β):

    $$S(f) \propto \frac{1}{f^{\beta}}$$

  - Hurst exponent (α):
    It relates to the autocorrelation of time series and the rate at which these decrease as the lag increases.

$(2d+1)/2 = \alpha = (\beta+1)/2$

Plan of Action: Part 1A – Modeling

- Data driven modeling
  - Detrended Fluctuation Analysis (DFA)
  - Auto-Regressive Fractionally Integrated (ARFIMA) modeling
  - Berg model (Scandinavian grid)
- *"First principles"* modeling
  - Load aggregation
  - Falsification of swing equation by PMU data

Detrended Fluctuation Analysis (DFA)

- Steps:
  1. Subtract average and integrate the data set:

$$y_{int}(k) = \sum_{i=1}^{k} (y(i) - y_{avg})$$

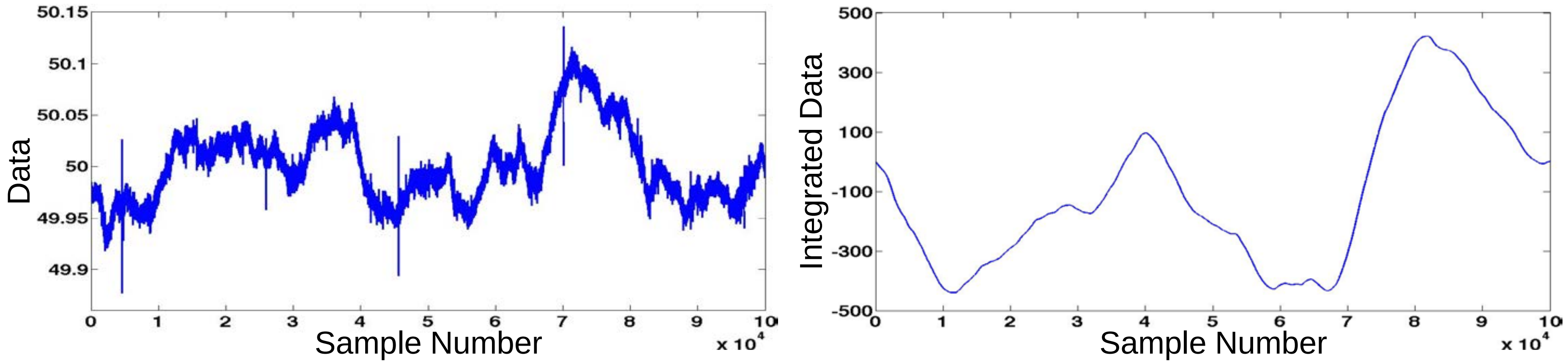

Detrended Fluctuation Analysis (DFA)

2. Divide the data into equal-sized boxes rach of size *n* and find the Linear Least Squares (LLS) line inside each box.
3. Subtract the LLS fitting from the integrated data to generate the detrended data:

$$y_{int}(k) - y_n(k) = y_d(k)$$

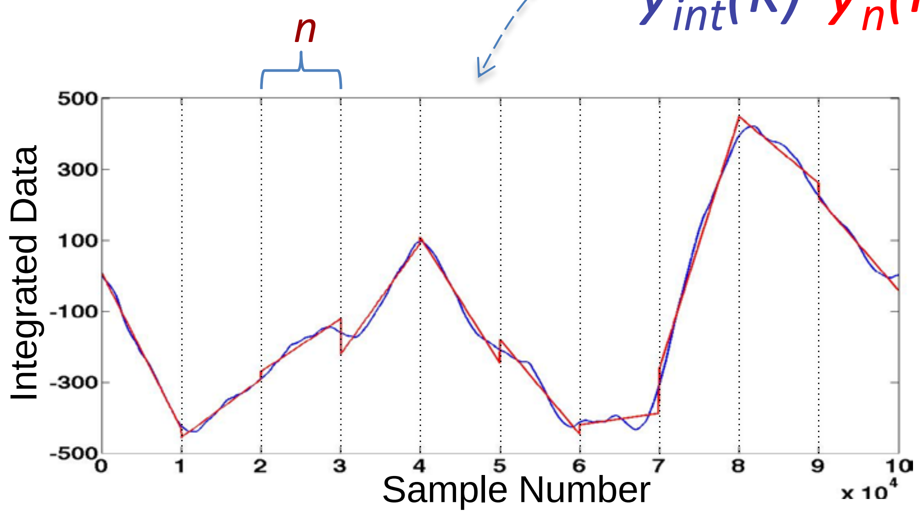

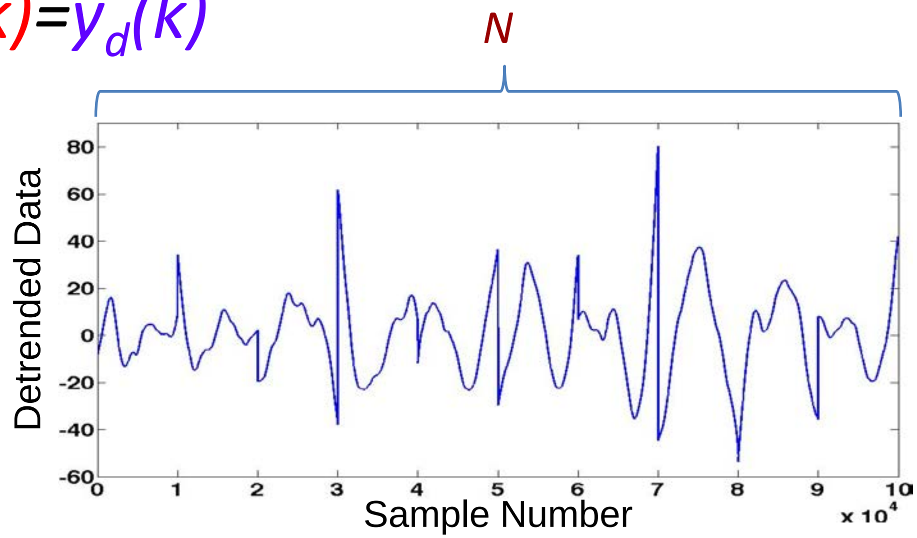

Detrended Fluctuation Analysis (DFA)

4. Find the Root Mean Square (RMS) fluctuation of the detrended data:

$$F(n) = \sqrt{\frac{1}{N}\sum_{k=1}^{N}\left(y_d(k)\right)^2}$$

4. The second and third steps are repeated at different box sizes:

$$\alpha = \lim_{n\to\infty} \frac{\log_{10}(F(n))}{\log_{10}(n)}$$

$$F(n) \sim n^{\alpha}$$

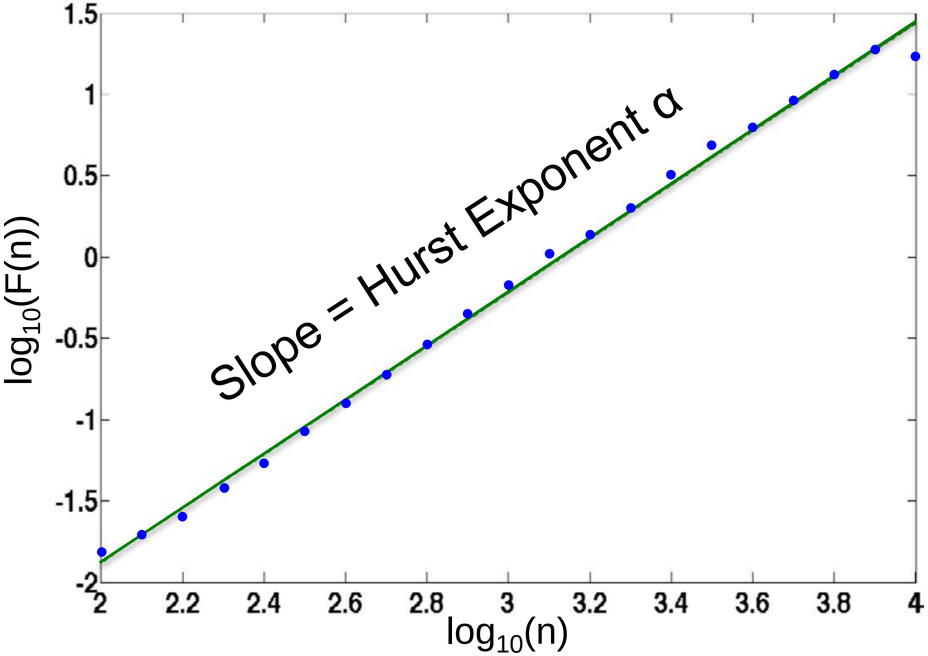

Interpretation of Hurst Exponent

- For white noise, $\alpha = 0.5$
- Long range process with power law: $0.5 < \alpha < 1$
- For $P(f) = f^{-1}$ pink noise, $\alpha = 1$
  - For $P(f) = f^{-\beta}$, $\alpha = \frac{\beta+1}{2}$
- For Brownian motion, $\alpha = 1.5$

Texas Synchrophasor Network

- Several PMUs are installed at 120V and 69KV over several locations:
  - Baylor University (Waco),
  - Harris Substation, and
  - McDonald Observatory.
- The data we analyzed here are
  - voltage magnitude,
  - frequency, and
  - phase angle.
- The sampling rate of the data is 30 samples/second.

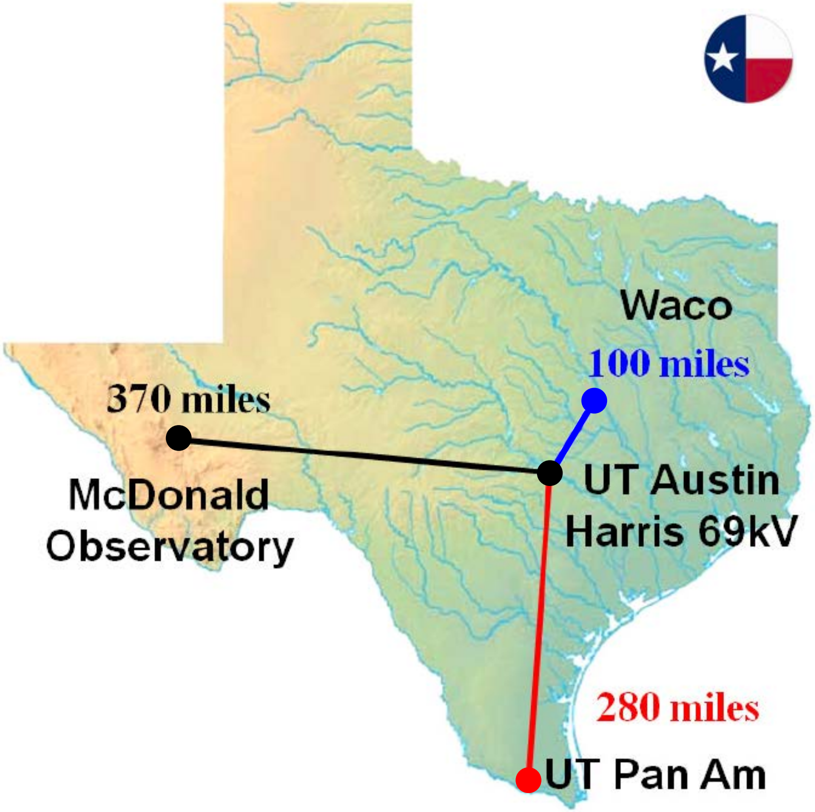

PMU Time Series (Texas)

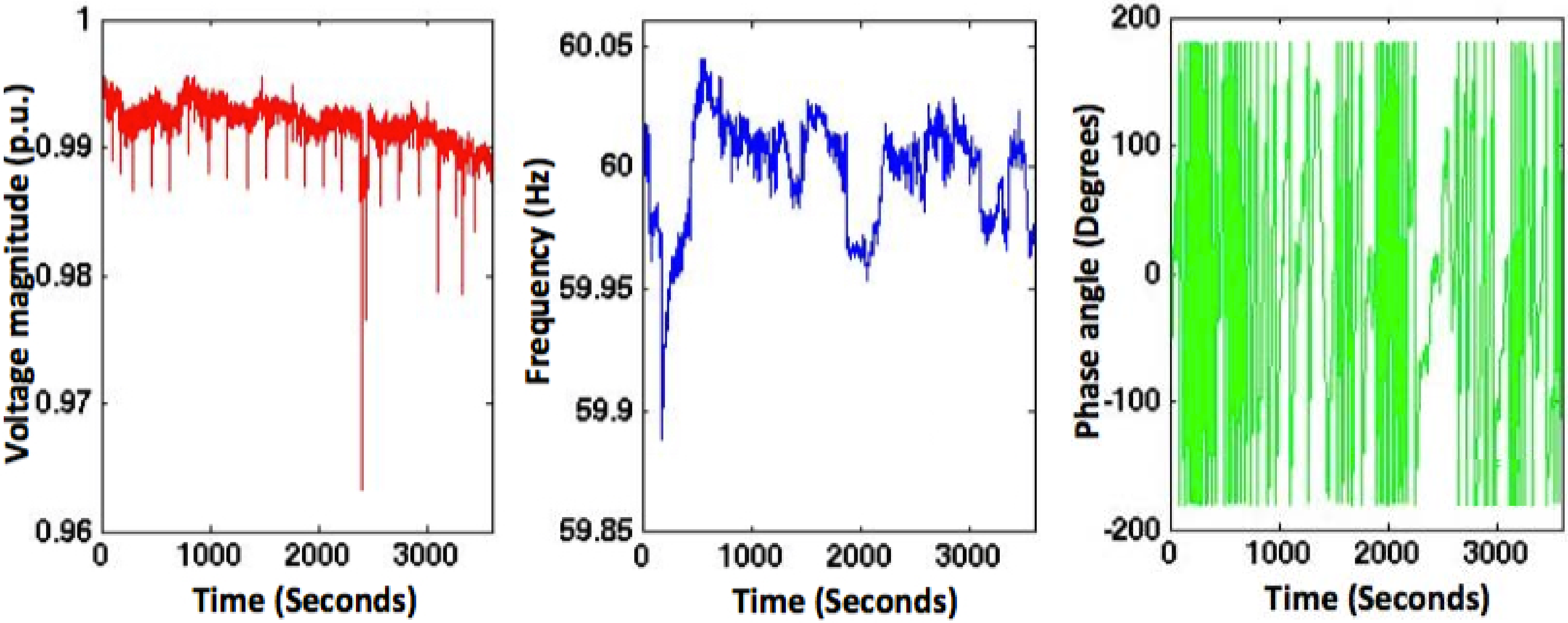

Laith Shalalfe, Paul Bogdan and Edmond Jonckheere, Evidence of Long-Range Dependence in Power Grid, IEEE Power and Energy Society General Meeting, 2016.

Details of Long-Range Dependence in PMU Data

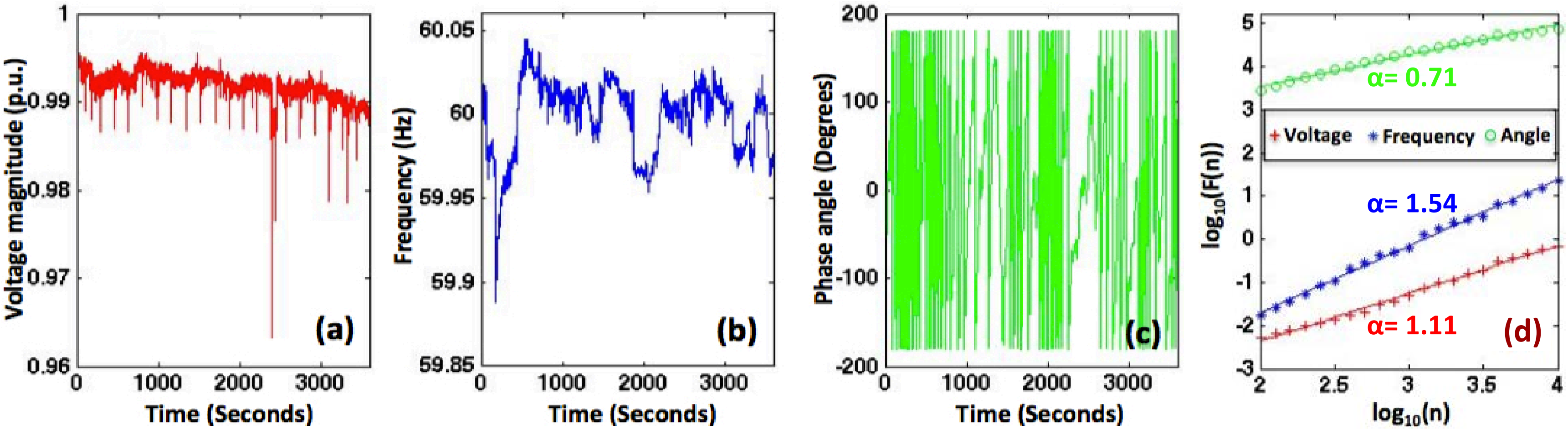

- Voltage Magnitude (V) → α ≈ 1.00 → Pink noise $(1/f)$
- Frequency (f) → α ≈ 1.50 → Brownian noise $(1/f^2)$
- Phase Angle (θ) → α ≈ 0.70 → Long-range/Power-law

$$\beta = 2\alpha - 1$$

Laith Shalalfe, Paul Bogdan and Edmond Jonckheere, Evidence of Long-Range Dependence in Power Grid, IEEE Power and Energy Society General Meeting, 2016.

Hurst Exponent (Texas)

$$0.5 \le \alpha \le 1: \quad \text{long range with power law}$$

$$\alpha > 1: \quad \text{long range but no power law}$$

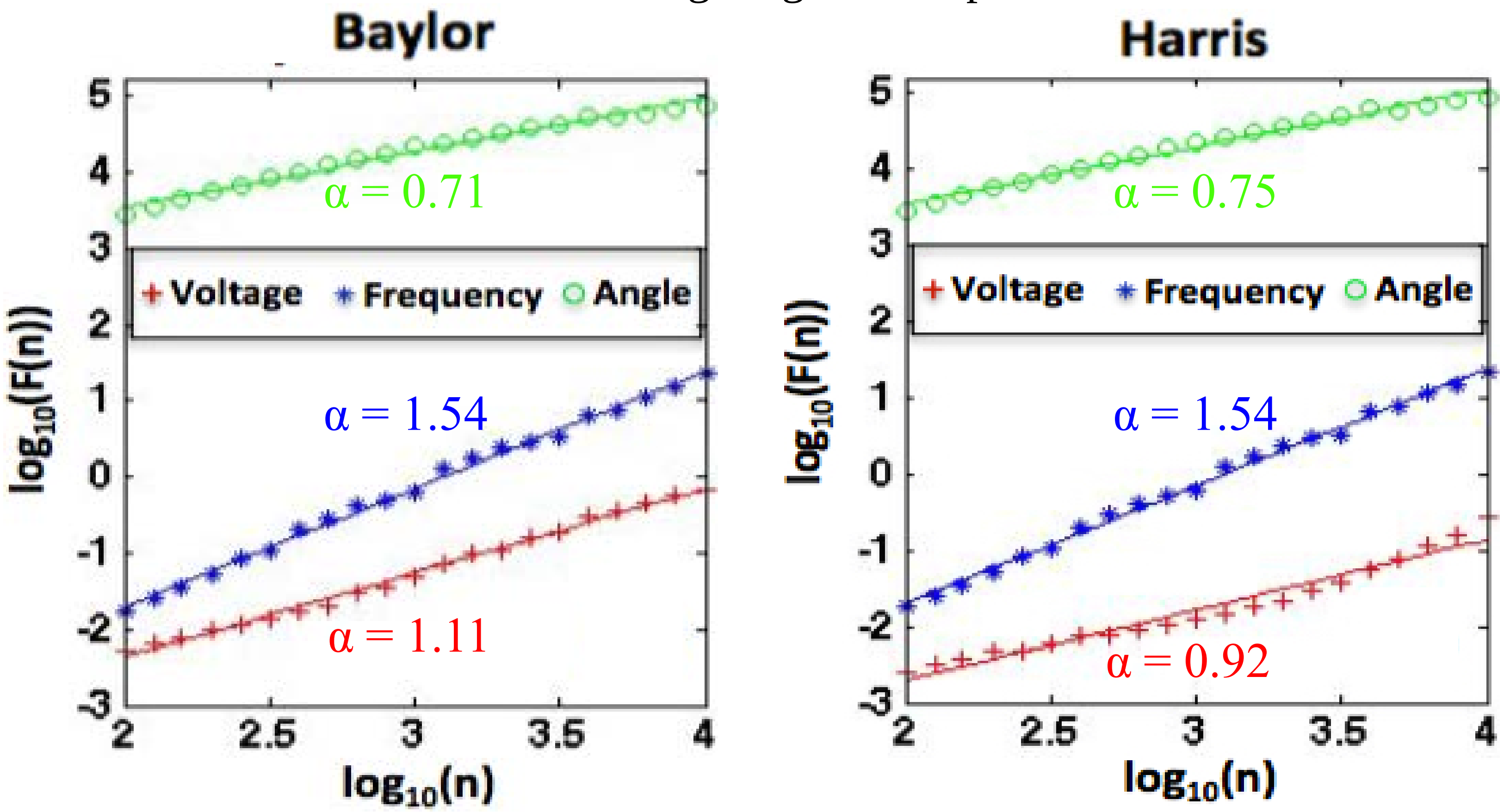

Laith Shalalfe, Paul Bogdan and Edmond Jonckheere, Evidence of Long-Range Dependence in Power Grid, IEEE Power and Energy Society General Meeting, 2016.

Hurst Exponent (Texas)

Data Set	Baylor			Harris			McDonald		
	V	f	θ	V	f	θ	V	f	θ
#1	1.11	1.54	0.71	0.92	1.54	0.75	1.32	1.54	0.74
#2	1.11	1.53	0.66	0.81	1.53	0.63	1.30	1.53	0.64
#3	1.05	1.45	0.67	0.91	1.45	0.76	1.37	1.45	0.73
#4	0.91	1.49	0.63	0.89	1.49	0.64	1.32	1.49	0.64

- Frequency and angle data are consistent across the 3 stations.
- Voltage definitely has higher Hurst exponent at McDonald… Why???
  - Proximity of wind farm?
  - Is the Hurst exponent of voltage a sign of *penetration of renewables* in the larger grid?

PMU-Based Monitoring in EPFL
(Ecole Polytechnique Fédérale de Lausanne)

- PMUs installed in EPFL campus perform real time monitoring of the EPFL pilot smart grid.
- The PMUs were installed on medium voltage buses (12KV)
- The sampling rate is 50 samples/second

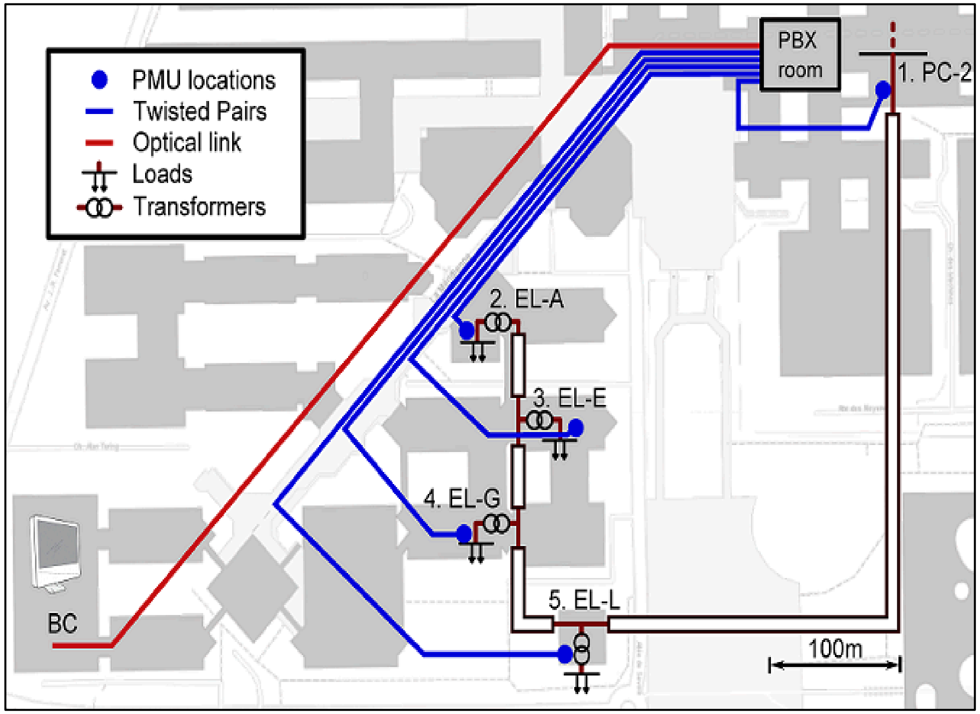

PMU Time Series (EPFL)

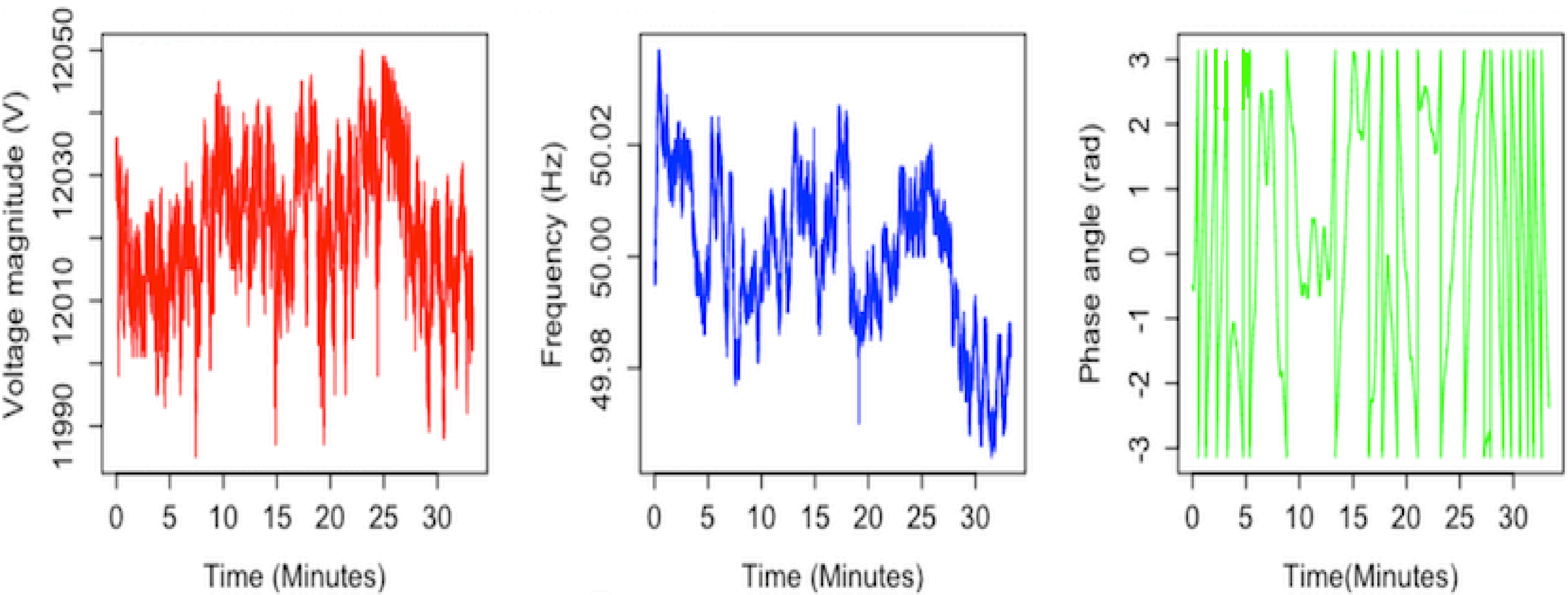

Laith Shalalfe, Paul Bogdan and Edmond Jonckheere, Kendall's Tau of Frequency Hurst Exponent as Blackout Proximity Margin, IEEE International Conference on Smart Grid Communications (SmartGridComm), 2016.

Hurst Exponents (EPFL)

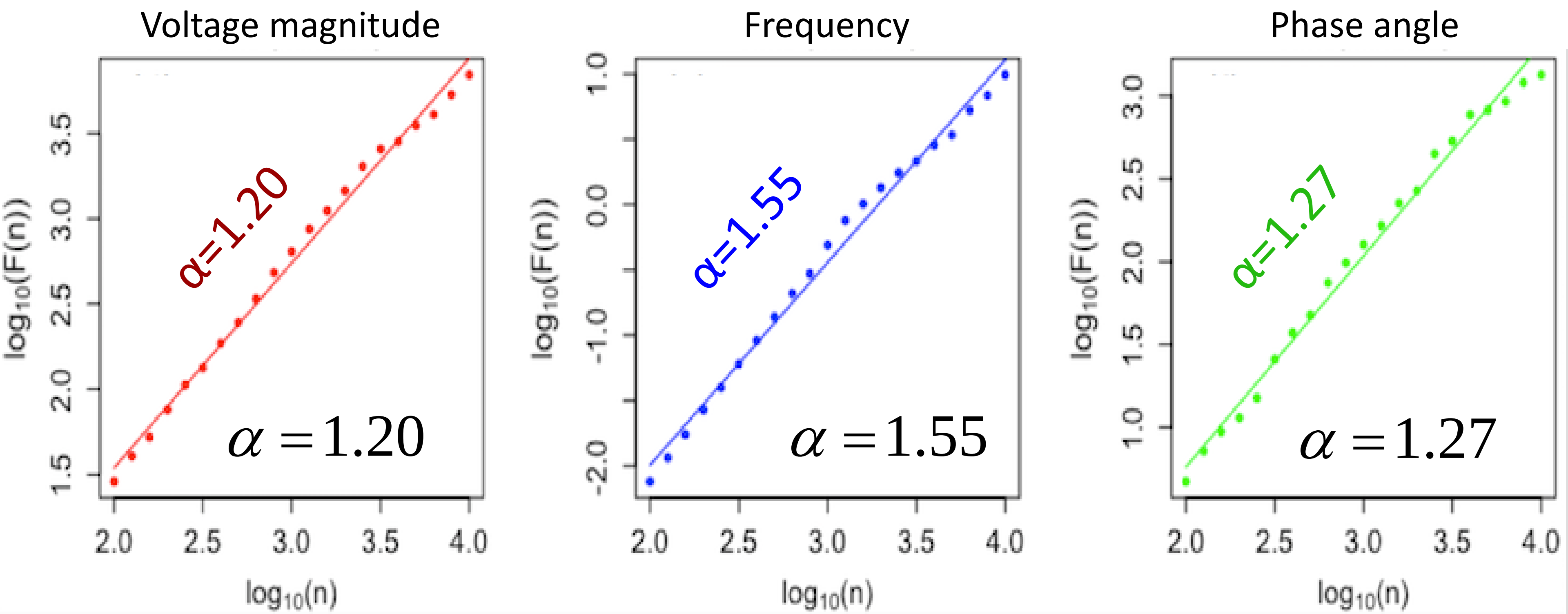

Amazing consistency between the frequency α in Texas (1.54) and Switzerland (1.55)

Laith Shalalfe, Paul Bogdan and Edmond Jonckheere, Kendall's Tau of Frequency Hurst Exponent as Blackout Proximity Margin, IEEE International Conference on Smart Grid Communications (SmartGridComm), 2016.

Hurst Exponent Histograms (EPFL)

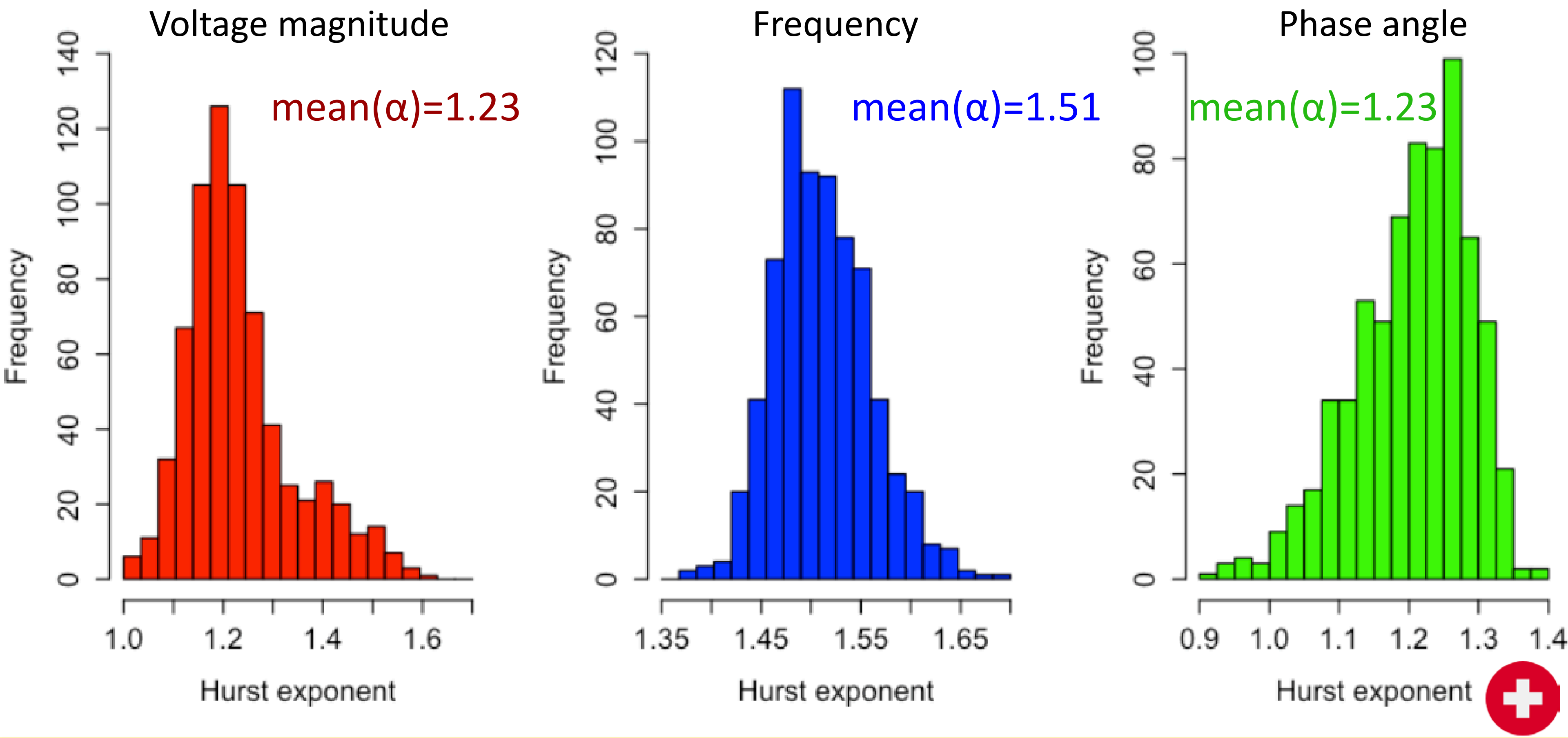

Laith Shalalfe, Paul Bogdan and Edmond Jonckheere, Kendall's Tau of Frequency Hurst Exponent as Blackout Proximity Margin, IEEE International Conference on Smart Grid Communications (SmartGridComm), 2016.

Part I: Summary

Empirical

Single Exponent

↓

DFA

Plan of Action: Part 1A – Modeling

- Data driven modeling
  - Detrended Fluctuation Analysis (DFA)
  - Auto-Regressive Fractionally Integrated (ARFIMA) modeling
  - Berg model (Scandinavian grid)
- *"First principles"* modeling
  - Load aggregation
  - Falsification of swing equation by PMU data

Autoregressive Fractionally Integrated Moving Average (ARFIMA) Model

- **ARFIMA** model:

  The model is a generalization of the ARIMA model (d is integer) provided by Box and Jenkins in the sense that the *differencing parameter (d)* could have a fractional (non-integer) values.

$$\left(1-\sum_{i=1}^{p}\Phi_i B^i\right)(1-B)^d X_t=\left(1+\sum_{j=1}^{q}\Theta_j B^j\right)\epsilon_t$$

- $ARMA\ Model \Leftrightarrow d=0$
- $ARIMA\ Model \Leftrightarrow d\ is\ intger$
- $ARFIMA\ Model \Leftrightarrow d\ is\ non\text{-}integer\ (fractional)$

PMU Time Series from EPFL

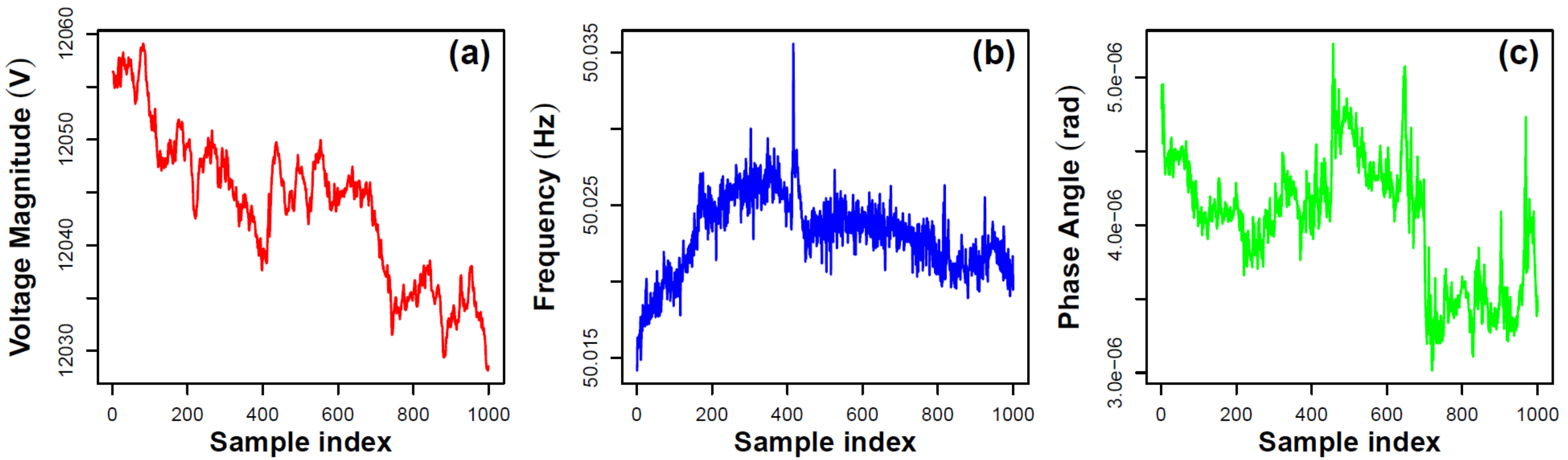

Fractality Parameters

- There are several parameters that quantify the severity of the fractal behavior in a time series:
  1. Scaling exponent (α): [$acf \sim k^{(2\alpha-2)}$]
     It relates to the autocorrelation of time series and the rate at which these decrease as the lag increases.
  2. Power exponent (β): [$S(f) \sim f^{-\beta}$]
  3. Differencing parameter (d) :
     The number of incrementation or differentiation steps.

$$\left(1 - \sum_{i=1}^{p} \Phi_i B^i\right)(1-B)^d X_t = \left(1 + \sum_{j=1}^{q} \Theta_j B^j\right)\epsilon_t$$

$$d = \alpha - 0.5 = \beta/2$$

Slow (Non-exponential) Decay of Autocorrelation Functions of PMU data

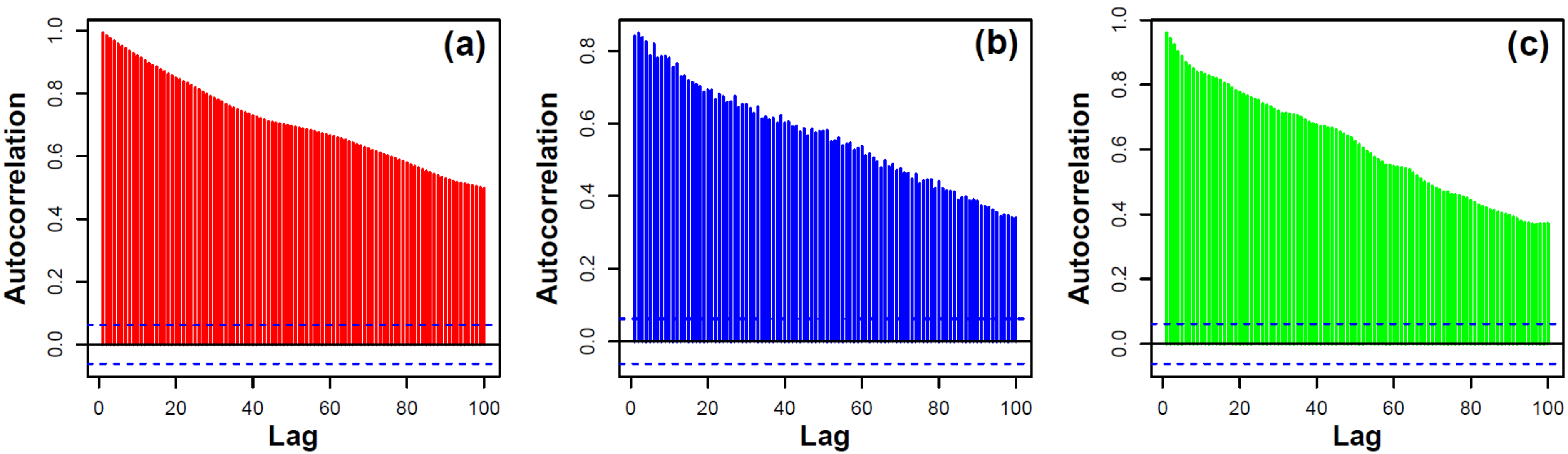

Voltage magnitude

Frequency

Phase Angle

Fractality Parameters

- There are several parameters that quantify the severity of the fractal behavior in a time series:
  1. Scaling exponent (α): [$acf \sim k^{(2\alpha-2)}$]
     It relates to the autocorrelation of time series and the rate at which these decrease as the lag increases.
  2. Power exponent (β): [$S(f) \sim f^{-\beta}$]
  3. Differencing parameter (d) :
     The number of incrementation or differentiation steps.

$$\left(1-\sum_{i=1}^{p}\Phi_i B^i\right)(1-B)^d X_t = \left(1+\sum_{j=1}^{q}\Theta_j B^j\right)\epsilon_t$$

Root of unity

$$d = \alpha - 0.5 = \beta/2$$

Root of Unity (Non-Stationarity) of PMU Data

- Augmented Dickey–Fuller (ADF) Test:
  - Null hypothesis (H_0) → unit root exists → Non-Stationary
  - Alternative hypothesis (H_1) → unit root does NOT exist → Stationary
- Kwiatkowski-Phillips-Schmidt-Shin (KPSS) Test:
  - Null hypothesis (H_0) → unit root does NOT exist → Stationary
  - Alternative hypothesis (H_1) → unit root exists → Non-Stationary

	ADF		*KPSS*	
	$p > 0.01$	$p \leq 0.01$	$p > 0.01$	$p \leq 0.01$
Voltage	88.16%	11.84%	05.48%	94.52%
Frequency	96.86%	03.14%	00.30%	99.70%
Angle	45.88%	54.12%	21.37%	78.63%

Fractality of PMU Data

➢ We estimate the fractality parameters of the PMU data using three methods:

1. Detrended Fluctuation Analysis (DFA) method: α
2. Geweke and Porter-Hudak (GPH) method: d
3. Power Spectral Density (PSD) method: β

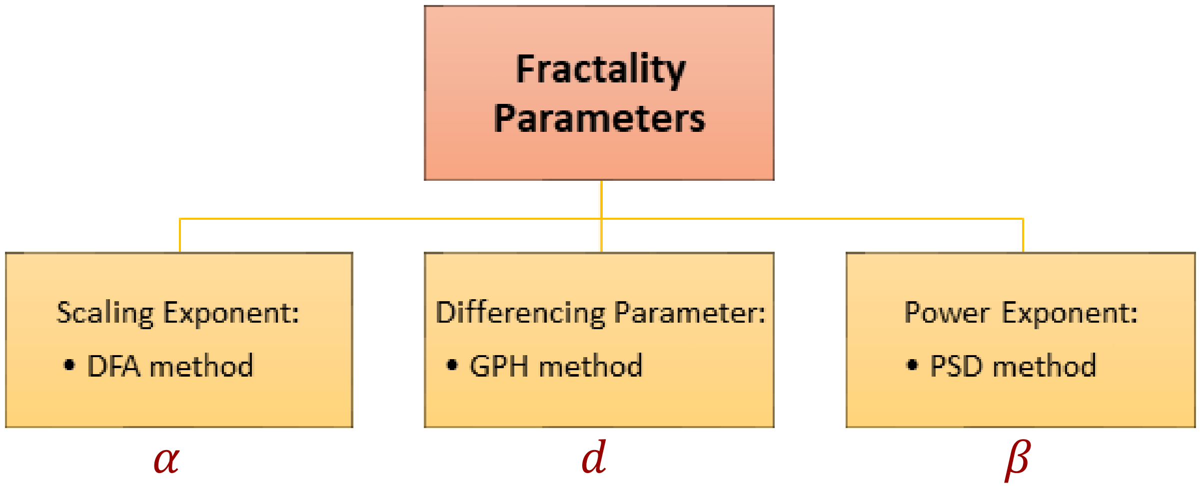

Differencing Parameters of PMU Data DFA-GPH-PSD Consistency

$$d = \alpha - 0.5 = \beta/2$$

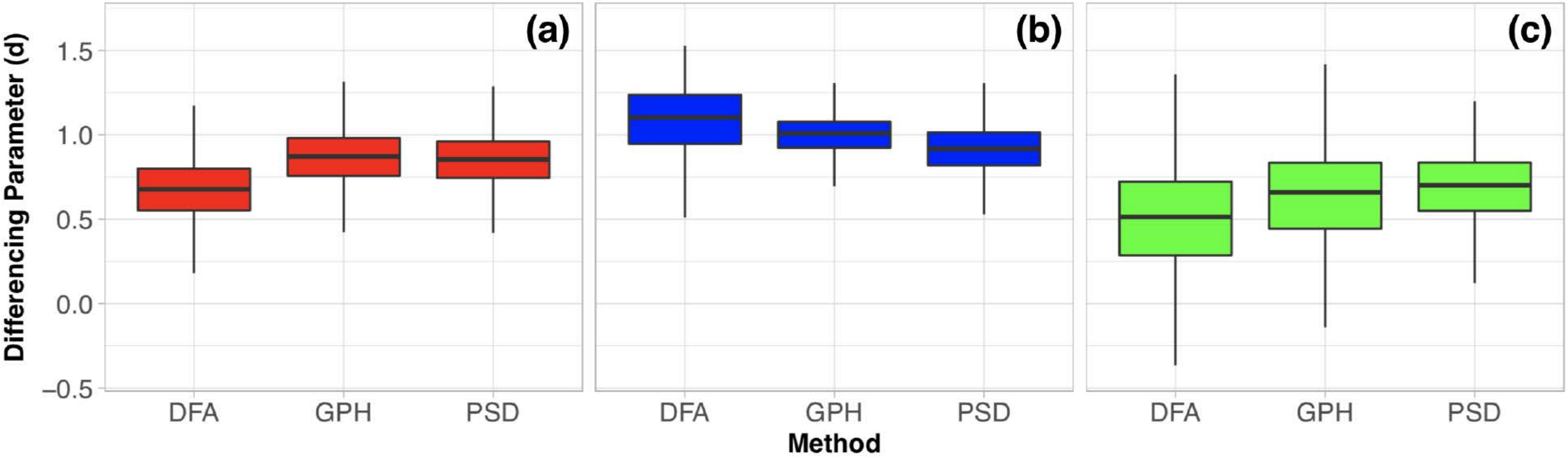

Voltage magnitude Frequency Phase Angle

Fractality Parameters

- There are several parameters that quantify the severity of the fractal behavior in a time series:

1. Scaling exponent (α): [$acf \sim k^{(2\alpha-2)}$]
   It relates to the autocorrelation of time series and the rate at which these decrease as the lag increases.
2. Power exponent (β): [$S(f) \sim f^{-\beta}$]
3. Differencing parameter (d) :
   The number of incrementation or differentiation steps.

$$\left(1 - \sum_{i=1}^{p} \Phi_i B^i\right)(1-B)^d X_t = \left(1 + \sum_{j=1}^{q} \Theta_j B^j\right)\epsilon_t$$

Root of unity

$$d = \alpha - 0.5 = \beta/2$$

Consistency of Fractality Parameters of PMU Data

$$d = \alpha - 0.5 = \beta/2$$

	Voltage	*Frequency*	*Angle*
Scaling exponent (α)	1.18 (0.18)	1.58 (0.21)	1.00 (0.27)
Diff. parameter (d)	0.86 (0.17)	1.00 (0.14)	0.63 (0.26)
Power exponent (β)	1.70 (0.33)	1.83 (0.29)	1.36 (0.40)

mean (standard deviation)

AR and MA Parameters

- There are several parameters that quantify the severity of the fractal behavior in a time series:
  1. Scaling exponent (α): [$acf \sim k^{(2\alpha-2)}$]
     It relates to the autocorrelation of time series and the rate at which these decrease as the lag increases.
  2. Power exponent (β): [$S(f) \sim f^{-\beta}$]
  3. Differencing parameter (d) :
     The number of incrementation or differentiation steps.

$$\left(1 - \sum_{i=1}^{p} \Phi_i B^i\right)(1-B)^d X_t = \left(1 + \sum_{j=1}^{q} \Theta_j B^j\right)\epsilon_t$$

Auto-Regressive (AR) parameter

$$d = \alpha - 0.5 = \beta/2$$

Moving-Average (MA) parameter

ARFIMA Model of Voltage (V) Time Series (Information Criterion)

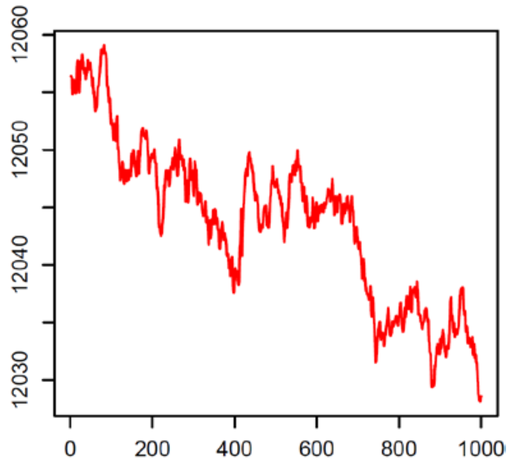

- The best model of 1000-sample voltage time series is ARFIMA (0,0.83,1):

$$(1-B)^{0.89}X_t = (1-0.63B)\epsilon_t$$

Model	AR parameters (Φ_1, Φ_2)	MA parameters (Θ_1, Θ_2)	Differencing parameter (d)	AIC	BIC
$(0, d, 0)$	$(0.00, 0.00)$	$(0.00, 0.00)$	1.23	− 739.8	− 725.0
$(1, d, 0)$	$(0.48, 0.00)$	$(0.00, 0.00)$	0.85	− 832.2	− 812.6
$(0, d, 1)$	**$(0.00, 0.00)$**	**$(-0.63, 0.00)$**	**0.89**	**− 946.9**	**− 927.3**
$(1, d, 1)$	$(0.03, 0.00)$	$(-0.62, 0.00)$	0.87	− 945.1	− 920.5
$(2, d, 0)$	$(0.41, -0.31)$	$(0.00, 0.00)$	1.07	− 915.9	− 891.3
$(0, d, 2)$	$(0.00, 0.00)$	$(-0.65, -0.02)$	0.87	− 945.1	− 920.6
$(2, d, 1)$	$(0.04, -0.06)$	$(-0.57, 0.00)$	0.91	− 944.0	− 914.6
$(1, d, 2)$	$(-0.88, 0.00)$	$(-1.54, -0.59)$	0.88	− 946.0	− 916.5
$(2, d, 2)$	$(-0.73, -0.07)$	$(-1.35, -0.50)$	0.90	− 944.3	− 909.9

ARFIMA Model of Frequency (f) Time Series (Information Criterion)

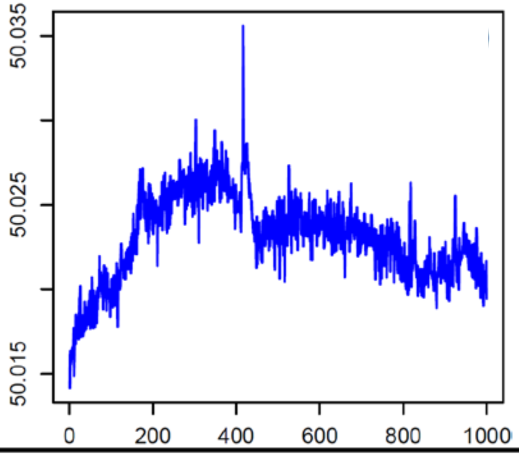

- The best model of 1000-sample frequency time series is ARFIMA (1,0.94,2):

$$(1+0.92B)(1-B)^{0.94}X_t = (1-0.18B+0.61B^2)\epsilon_t$$

Model	AR parameters (Φ_1, Φ_2)	MA parameters (Θ_1, Θ_2)	Differencing parameter (d)	AIC	BIC
$(0, d, 0)$	$(0.00, 0.00)$	$(0.00, 0.00)$	0.47	−13512.0	−13497.3
$(1, d, 0)$	$(-0.36, 0.00)$	$(0.00, 0.00)$	0.62	−13607.7	−13588.1
$(0, d, 1)$	$(0.00, 0.00)$	$(0.61, 0.00)$	0.84	−13633.0	−13613.4
$(1, d, 1)$	$(-0.08, 0.00)$	$(0.62, 0.00)$	0.88	−13634.6	−13610.1
$(2, d, 0)$	$(-0.51, -0.18)$	$(0.00, 0.00)$	0.70	−13628.0	−13603.5
$(0, d, 2)$	$(0.00, 0.00)$	$(0.65, -0.05)$	0.83	−13634.1	−13609.6
$(2, d, 1)$	$(-0.04, 0.06)$	$(0.72, 0.00)$	0.94	−13633.7	−13604.3
$(1, d, 2)$	**$(-0.92, 0.00)$**	**$(-0.18, 0.61)$**	**0.94**	**−13645.5**	**−13616.0**
$(2, d, 2)$	$(-0.89, 0.02)$	$(-0.16, 0.60)$	0.93	−13643.7	−13609.4

ARFIMA Model of Phase Angle (θ) Time Series (Information Criterion)

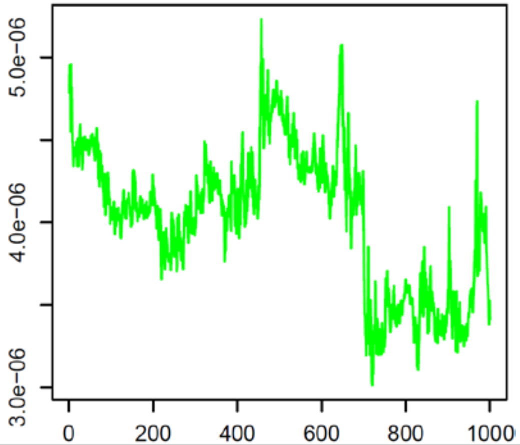

- The best model of 1000-sample phase angle time series is ARFIMA (1,0.83,1):

$$(1 + 0.18B)(1 - B)^{0.83} X_t = (1 + 0.18B)\epsilon_t$$

Mode	AR parameters (Φ_1, Φ_2)	MA parameters (Θ_1, Θ_2)	Differencing parameter (d)	AIC	BIC
$(0, d, 0)$	$(0.00, 0.00)$	$(0.00, 0.00)$	0.17	−29399.1	−29384.3
$(1, d, 0)$	$(-0.18, 0.00)$	$(0.00, 0.00)$	0.83	−29418.7	−29399.1
$(0, d, 1)$	$(0.00, 0.00)$	$(0.18, 0.00)$	0.83	−29420.8	−29401.2
$\mathbf{(1, d, 1)}$	$\mathbf{(-0.18, 0.00)}$	$\mathbf{(0.18, 0.00)}$	**0.83**	**−29543.0**	**−29518.5**
$(2, d, 0)$	$(-0.18, 0.02)$	$(0.00, 0.00)$	0.83	−29414.1	−29389.6
$(0, d, 2)$	$(0.00, 0.00)$	$(0.18, -0.02)$	0.83	−29418.5	−29394.0
$(2, d, 1)$	$(-0.18, 0.02)$	$(0.18, 0.00)$	0.83	−29537.4	−29507.9
$(1, d, 2)$	$(-0.18, 0.00)$	$(0.18, -0.02)$	0.83	−29538.6	−29509.1
$(2, d, 2)$	$(-0.18, 0.02)$	$(0.18, -0.02)$	0.83	−29532.5	−29498.2

Conclusions

- PMU data are non-stationarity based on the two unit root tests (ADF and KPSS).
- The fractality parameters prove the existence of long-range memory in PMU data.
- Estimating the differencing parameter is consistent among different methods (DFA, GPH, and PSD).
- The next challenge is to formulate some *“first principles”* that could justify the ARFIMA model.

L. Shalalfeh, P. Bodgan, and E. Jonckheere, ``Modeling of PMU data using ARFIMA models, Clemson University Power System Conference, Paper Session T-M II: Phasor Measurement Units (PMUs), Charleston, SC, September, 2018.

Part I: Summary

Empirical

Single Exponent

↓

DFA

ARIMA   ARFIMA

$$\left(1-\sum_{i=1}^{p}\phi_i B^i\right)(1-B)^d X_t=\left(1+\sum_{i=1}^{q}\theta_i B^i\right)\varepsilon_t$$

Plan of Action: Part 1A – Modeling

- Data driven modeling
  - Detrended Fluctuation Analysis (DFA)
  - Auto-Regressive Fractionally Integrated (ARFIMA) modeling
  - Berg model (Scandinavian grid)
- *"First principles"* modeling
  - Load aggregation
  - Falsification of swing equation by PMU data

Static versus Dynamic Load Models

- Static load model:

$$P_L = K_p V_L^{p_v} \qquad Q_L = K_q V_L^{q_v}$$

  - Constant Power ➡ $p_v = q_v = 0$
  - Constant Current ➡ $p_v = q_v = 1$
  - Constant Impedance ➡ $p_v = q_v = 2$

- Dynamic load model (Hill):

$$T_P \dot{P}_d + P_d = P_s(V_L) + k_p(V_L)\dot{V}_L$$

Should be

$$P_L(V_L, \omega)$$

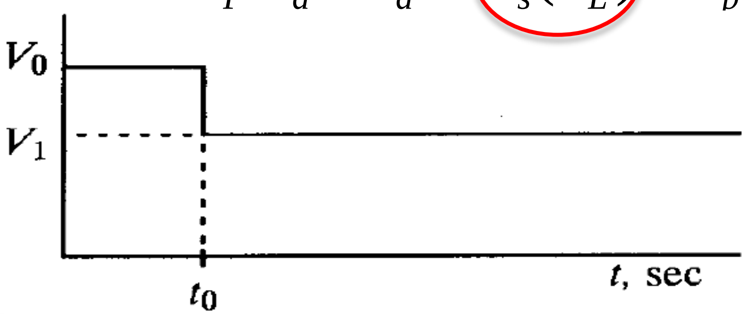

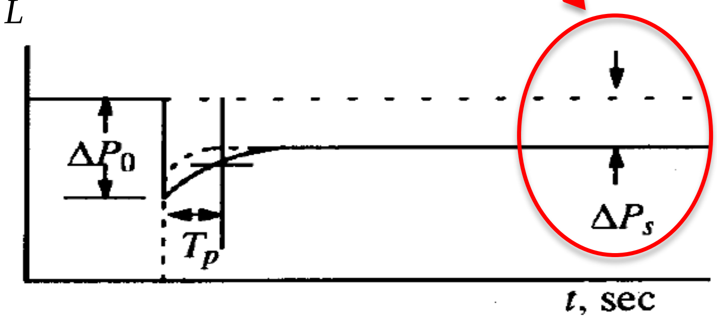

Berg Data-Driven Load Modeling Experiment in a Real Microgrid

Electric Reduction Furnace (Berg)

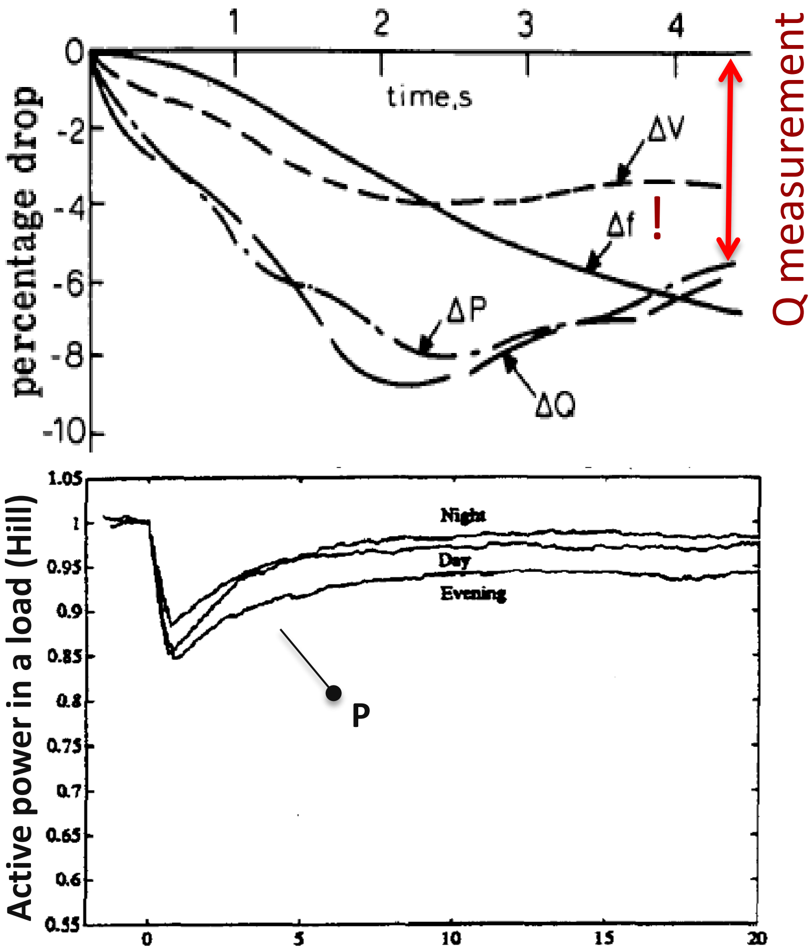

Mechanical Plant (Berg)

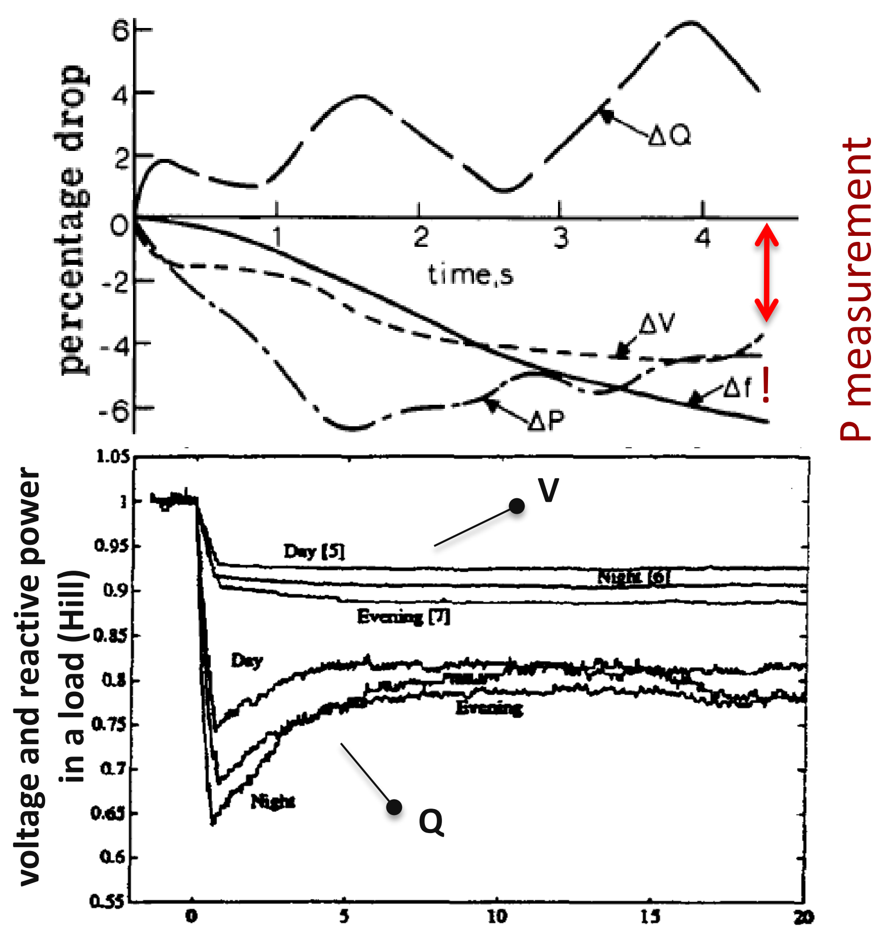

Berg Load Model Involves Frequency to a Non-integer Exponent

$$\vec{S}_L = P_L + jQ_L \qquad P_L = K_P V_L^{p_v} \omega^{p_\omega} \qquad Q_L = K_Q V_L^{q_v} \omega^{q_\omega}$$

Load Type	p_v	p_ω	q_v	q_ω
Filament lamp	1.6	0	0	0
Fluorescent lamp	1.2	-1.0	3.0	-2.8
Heater	2.0	0	0	0
Induction motor (HL)	0.2	1.5	1.6	-0.3
Induction motor (FL)	0.1	2.8	0.6	1.8
Reduction furnace	1.9	-0.5	2.1	0
Aluminum plant	1.8	-0.3	2.2	0.6
Regulated aluminum plant	2.4	0.4	1.6	0.7

Impedance Describing Function

$$\vec{Z}_L = \frac{\vec{V}_L}{\vec{I}_L} = \frac{\vec{V}_L \vec{V}_L^*}{\vec{I}_L \vec{V}_L^*} = \frac{V_L^2}{\vec{S}_L^*} = \frac{V_L^2}{P_L - jQ_L} = \frac{1}{K_p V_L^{p_v-2} \omega^{p_\omega} - jK_q V_L^{q_v-2} \omega^{q_\omega}}$$

Load Type	Describing Function
Filament lamp	$(K_p V_L^{-0.4} - jK_q V_L^{-2})^{-1}$
Fluorescent lamp	$(K_p V_L^{-0.8} \omega^{-1} - jK_q V_L \omega^{-2.8})^{-1}$
Heater	$(K_p - jK_q V_L^{-2})^{-1}$
Induction motor (HL)	$(K_p V_L^{-1.8} \omega^{1.5} - jK_q V_L^{-0.4} \omega^{-0.3})^{-1}$
Induction motor (FL)	$(K_p V_L^{-1.9} \omega^{2.8} - jK_q V_L^{-1.4} \omega^{1.8})^{-1}$
Reduction furnace	$(K_p V_L^{-0.1} \omega^{-0.5} - jK_q V_L^{0.1})^{-1}$
Aluminum plant	$(K_p V_L^{-0.2} \omega^{-0.3} - jK_q V_L^{0.2} \omega^{0.6})^{-1}$
Regulated aluminum plant	$(K_p V_L^{0.4} \omega^{0.4} - jK_q V_L^{-0.4} \omega^{0.7})^{-1}$

Analytic Extension of Describing Function

$$Y_L = \frac{1}{Z_L} = L(V_L)\omega^p + jW(V_L)\omega^q$$

<u>Crude way:</u>
Leaves some coefficients complex, not completely in line with formal circuit theory

$$\omega \rightarrow \omega - j\sigma$$

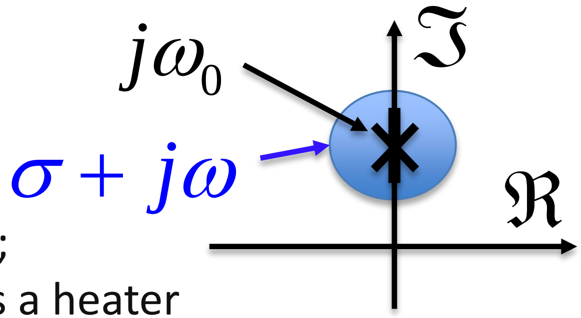

<u>Better way:</u>
Coefficients are kept real, in line with formal circuit theory;
However, positive realness does not hold unless the load is a heater

$$Y_L \approx A(V_L)\times(j\omega)^\alpha + B(V_L)\times(j\omega)^\beta \xrightarrow{\text{extension}} A(V_L)s^\alpha + B(V_L)s^\beta$$

where $A(.)$ and $B(.)$ are real valued.

Can we replace *s* by $\frac{d}{dt}$???

Yes, but subject to correct interpretation:

- Caputo, D_* (initial conditions in terms of integer derivatives)
- Riemann-Liouville, D (initial conditions in terms of fractional derivatives)
- Grunwald-Leitnikov, $\mathbb{D}$ (close to ARFIMA model)

related (Riemann-Liouville, Grunwald-Leitnikov)

$$\underbrace{\begin{pmatrix} a_1 D_{(*)}^{\alpha_1} + b_1 D_{(*)}^{\beta_1} & \cdots & 0 \\ \vdots & \ddots & \vdots \\ 0 & \cdots & a_n D_{(*)}^{\alpha_n} + b_n D_{(*)}^{\beta_n} \end{pmatrix}}_{\text{Distribution network}} \underbrace{\begin{pmatrix} V_1 \\ \vdots \\ V_n \end{pmatrix}}_{\substack{\text{State} \\ \text{(load voltages)}}} = \underbrace{A(Y_{\text{Line}})}_{\text{Transmission network}} \begin{pmatrix} V_1 \\ \vdots \\ V_n \end{pmatrix} + B(Y_{\text{Line}}) \underbrace{\begin{pmatrix} V_{G_1} \\ \vdots \\ V_{G_m} \end{pmatrix}}_{\text{Generation}}$$

Part I: Summary

Empirical

Single Exponent

DFA

ARIMA

$$\left(1-\sum_{i=1}^{p}\phi_i B^i\right)(1-B)^d X_t = \left(1+\sum_{i=1}^{q}\theta_i B^i\right)\varepsilon_t$$

ARFIMA

Berg Model

$$I_L(t) = AD_*^{\alpha}V_L(t) - BD_*^{\beta}V_L(t)$$

Mathematics

Grünwald-Letnikov

$$\mathbb{D}^d = \lim_{|B|\to 0}\frac{(I-|B|)^d}{|B|^d}$$

Riemann-Liouville

$$\begin{aligned} D^{\alpha}f(x) &= D^m J^{m-\alpha}f(x) \\ &= D^m\left(\frac{1}{\Gamma(m-\alpha)}\int_0^t (t-\tau)^{m-\alpha-1}f(\tau)d\tau\right) \end{aligned}$$

Feedback Model of Power System

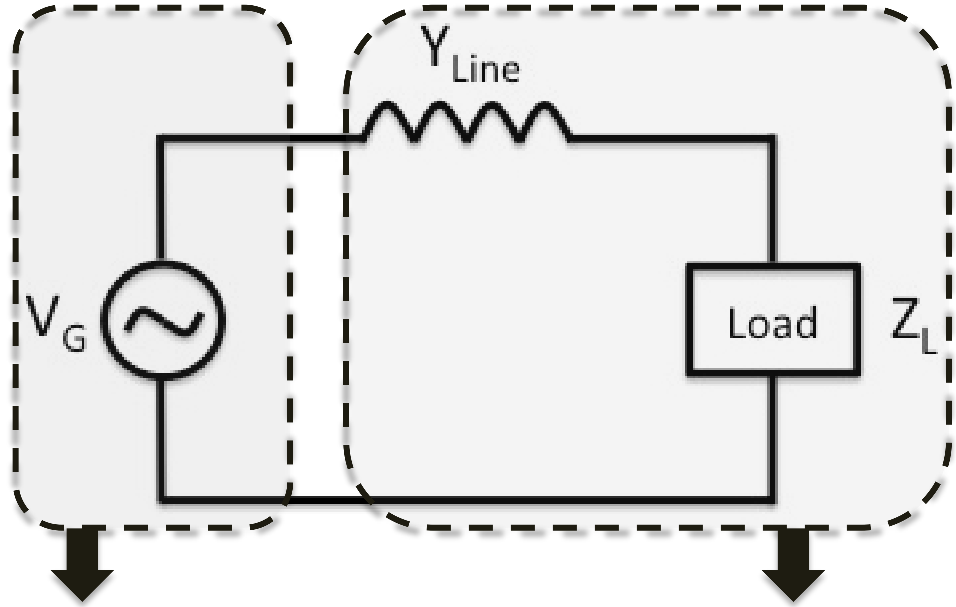

Deliberately simplified model of the generator…

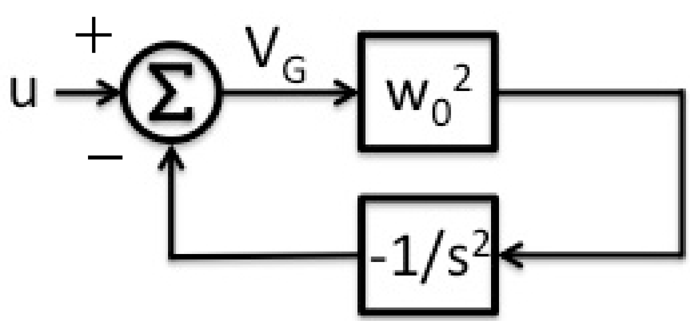

to put the load in the spotlight.

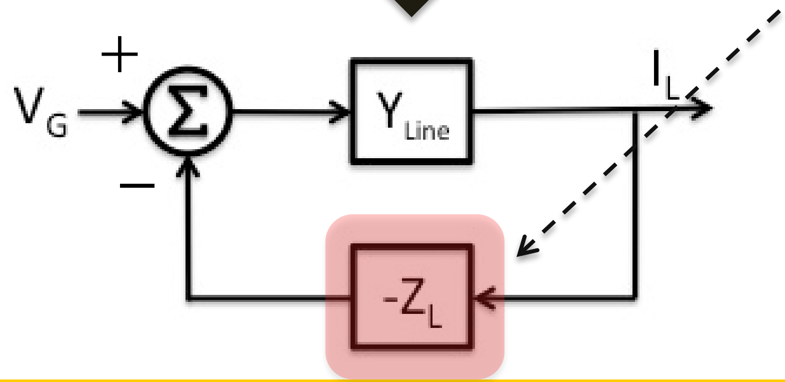

Feedback Model of Power System

$$y = (I - GF)^{-1} Gu$$

$$u = [u_1 \quad u_2]^t$$

$$y = [y_1 \quad y_2]^t$$

$$G = \begin{bmatrix} Y_{Line} & Y_{Line} \\ 0 & \omega_0^{\ 2} \end{bmatrix}$$

$$F = \begin{bmatrix} -Z_L & 0 \\ 0 & -s^{-2} \end{bmatrix}$$

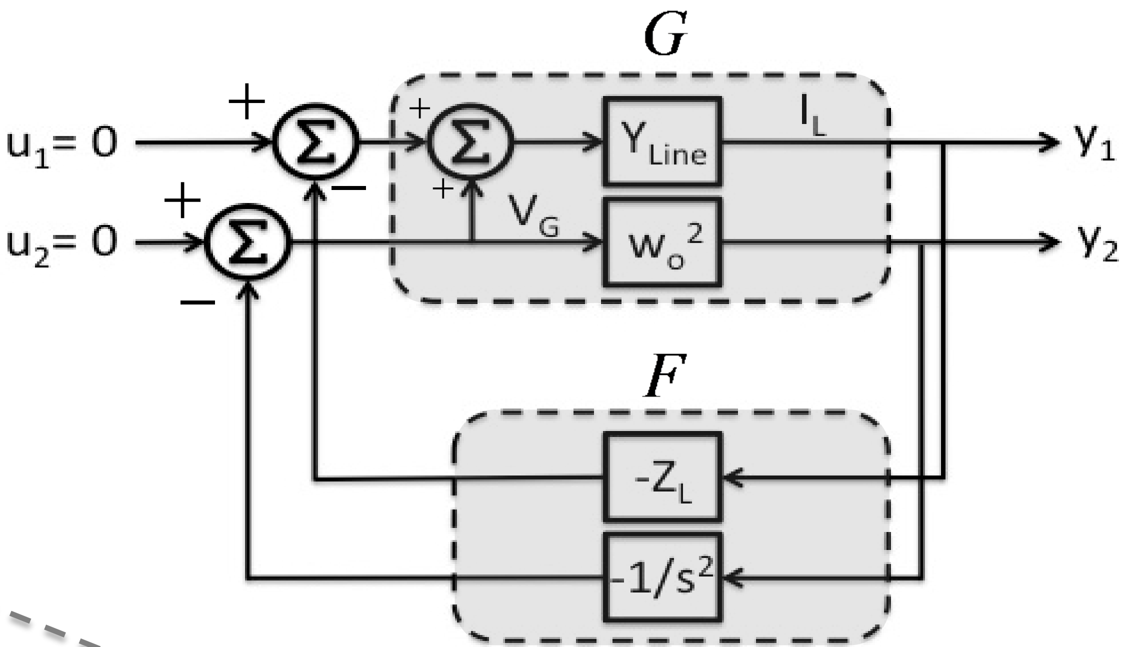

Simplification:
No back-action of the load to the generator

Voltage Collapse Solution

- Power system represented by the feedback model has a solution if

$$\left|(I-GF)^{-1}G\right| = \left(1+Z_L Y_{Line}\right)\left(1+\omega_0{}^2/s^2\right) = 0$$

  - $\left(1+\omega_0{}^2/s^2\right)=0$ ➡ Purely harmonic solution $V_L cos(\omega_0 t)$
  - $\left(1+Z_L Y_{Line}\right)=0$ ➡ Voltage collapsing solution $V_L e^{\sigma t} cos(\omega t)$

- The voltage collapsing solution exists if
  - ➢ $1+Z_L Y_{Line} = 0$
  - ➢ $Y_L\left(V_L, \omega - j\sigma\right) + Y_{Line}\left(\omega - j\sigma\right) = 0$
  - ➢ $K_p V_L{}^{p_v-2}\left((\omega - j\sigma)/\omega_0\right)_{p\omega} - jK_q V_L{}^{q_v-2}\left((\omega - j\sigma)/\omega_0\right)_{q\omega} + K_{Line}/(\sigma + j\omega) = 0$
  - ➢ $K_p(-j/\omega_0)^{p_\omega} V_L{}^{p_v-2} s^{p_\omega+1} - jK_q(-j/\omega_0)^{q_\omega} V_L{}^{q_v-2} s^{q_\omega+1} + K_{Line} = 0$

Voltage Collapse Solution - Special Case

- The voltage collapse solution exists in case of special loads (p_v=q_v and p_ω=q_ω) if

$$s = \sigma + j\omega = \alpha V_L^{\ \beta}$$

$$\alpha = (-K_{Line} / ((-j/\omega_0)^{p_\omega} (K_p - jK_q)))$$

$$\beta = (2 - p_v)/(p_\omega - 1)$$

- Voltage collapse conditions:

1) $\Re(\alpha) < 0$ and $\Im(\alpha) > 0$

2) $\beta < 0$

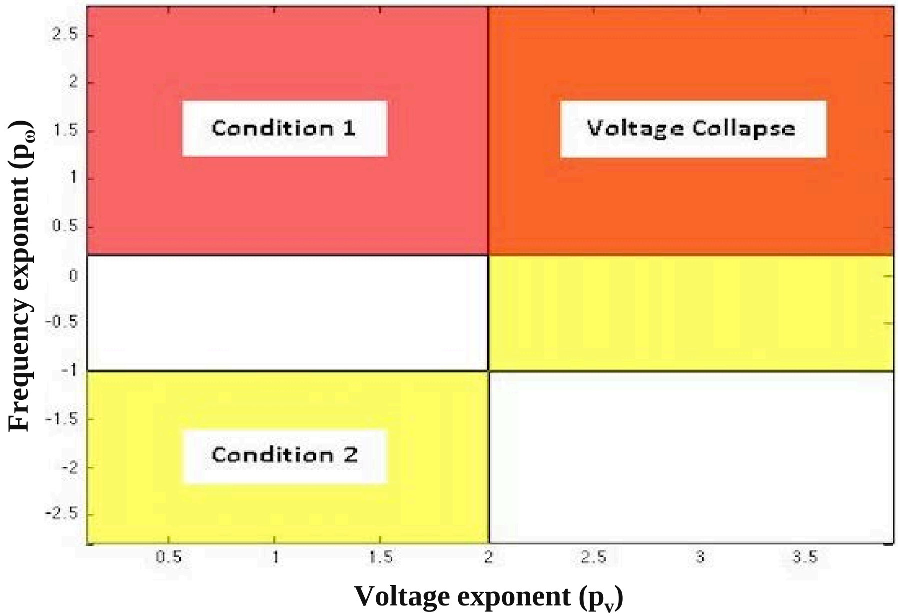

Sigma (σ) and Frequency (ω) for Different Special Loads ($s=\sigma+j\omega$)

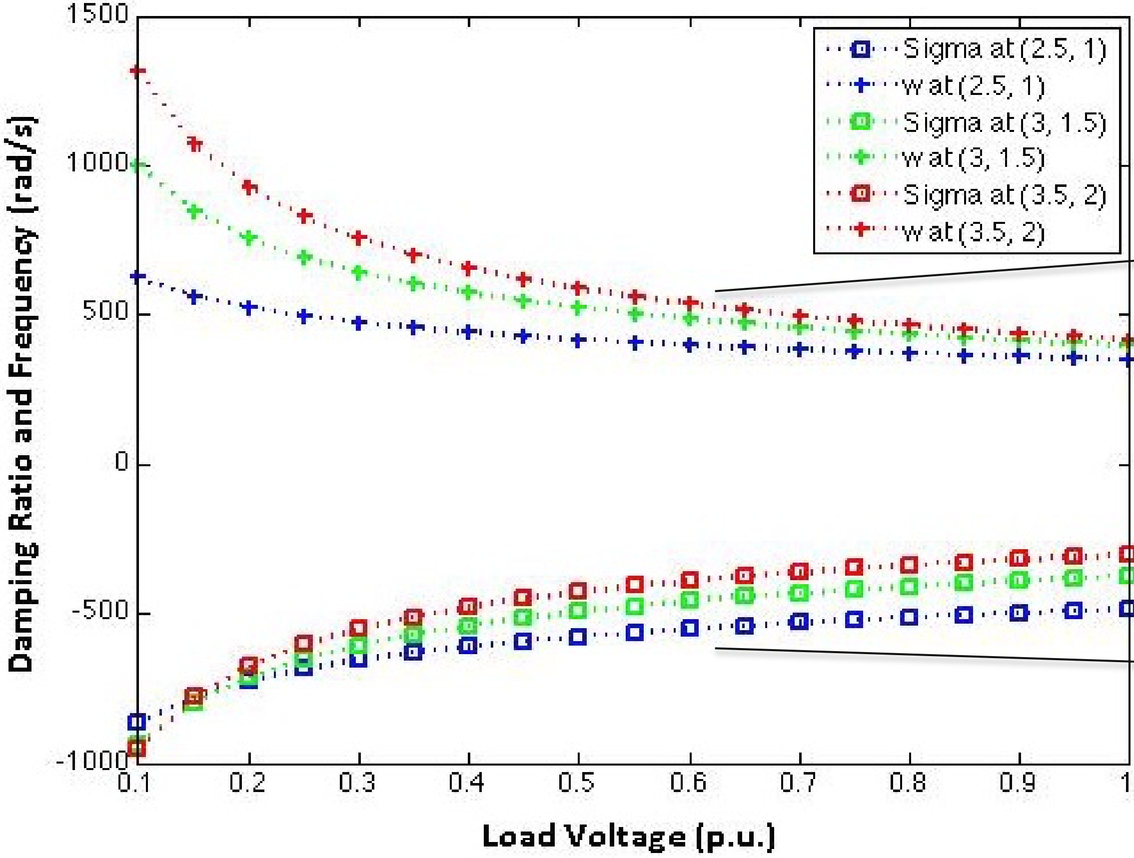

Frequency is disrupted as well

Voltage decreases and damping increases

Sigma (σ) and Frequency (ω) for Induction Motor (Stable)

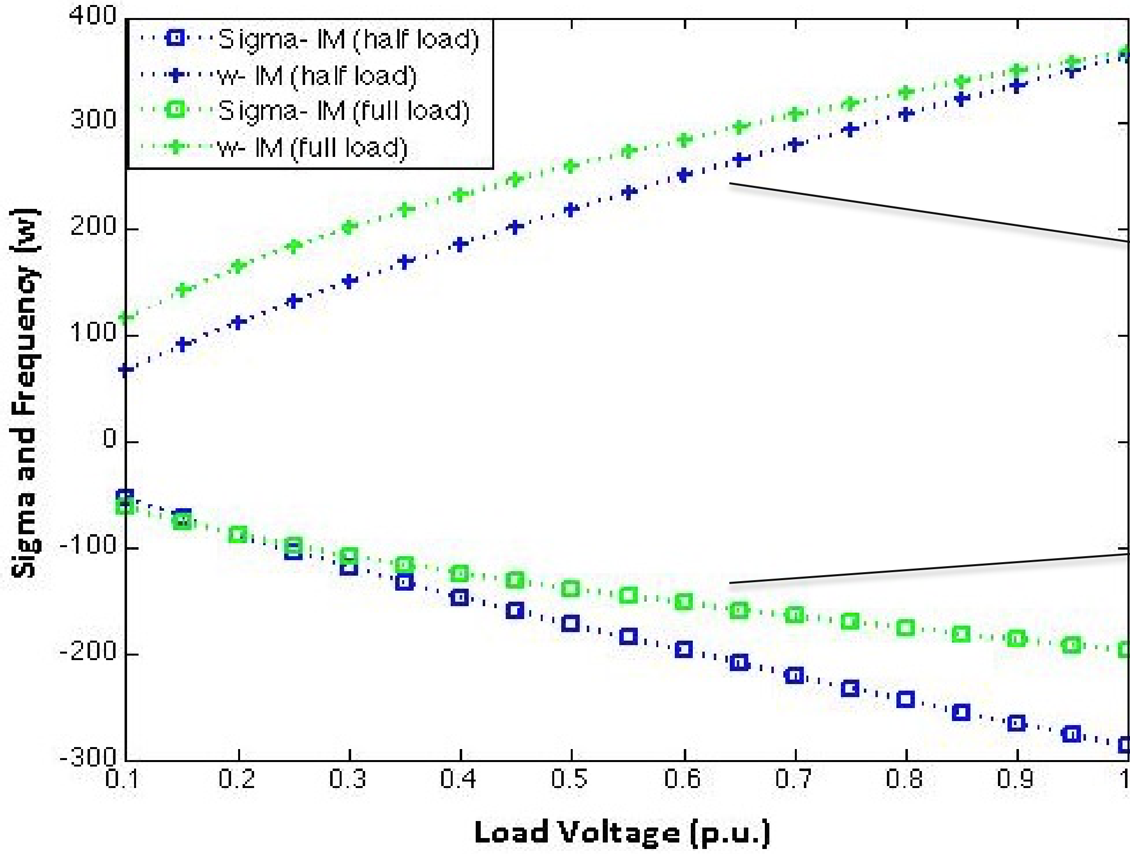

Frequency is disrupted as well

Voltage decreases and damping decreases

Sigma (σ) and Frequency (ω) for Regulated Aluminum Plant (Unstable)

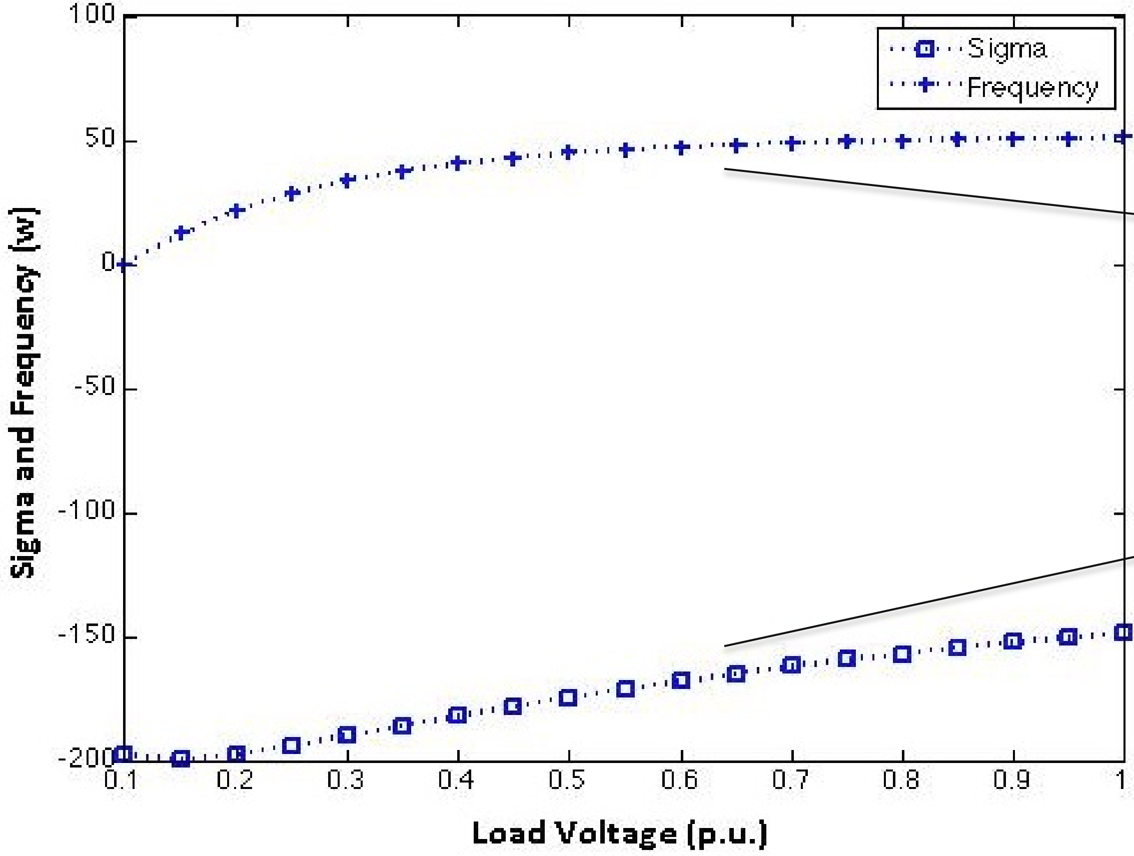

Frequency is disrupted as well

Voltage decreases and damping increases

The Relationship Between Transmission Line Coefficient (K_{Line}) and Sigma (σ)

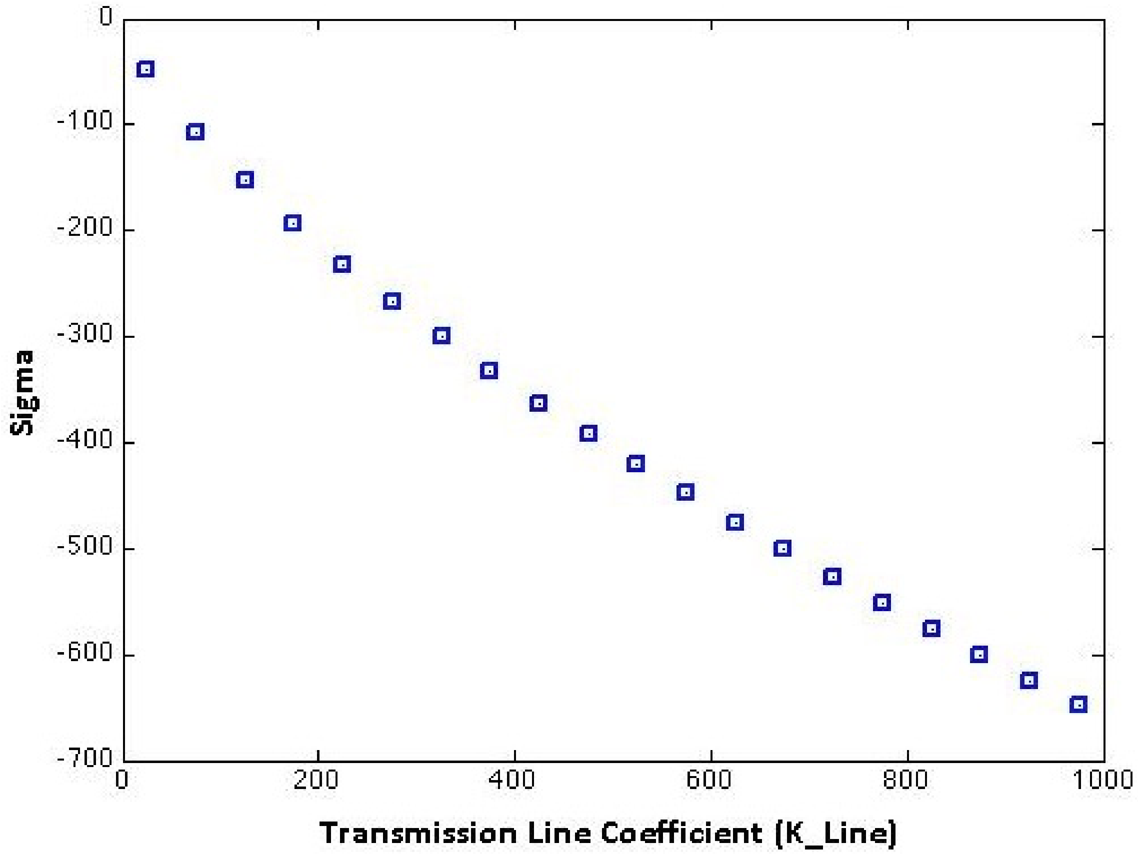

K_{line} is directly proportional to maximum power transfer

The Relationship Between Active Power Coefficient (K_p) and Sigma (σ)

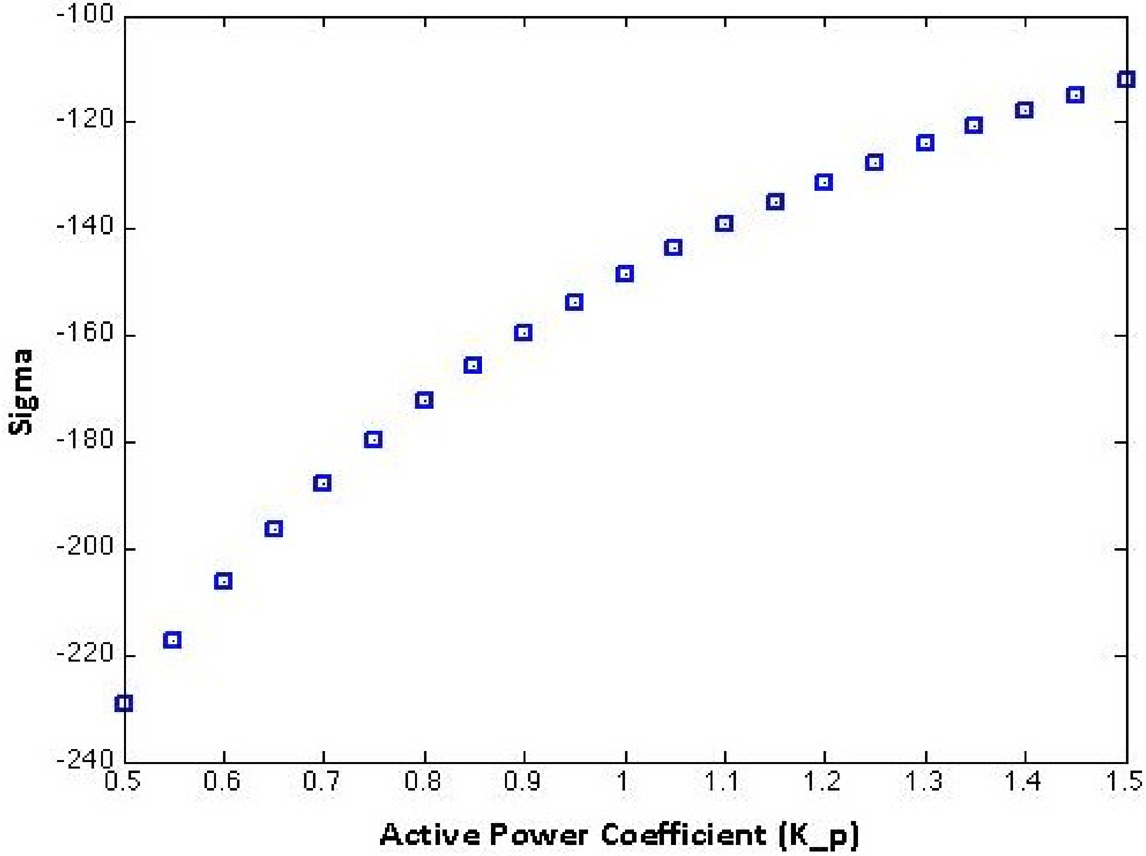

The Relationship Between Reactive Power Coefficient(K_q) and Sigma (σ)

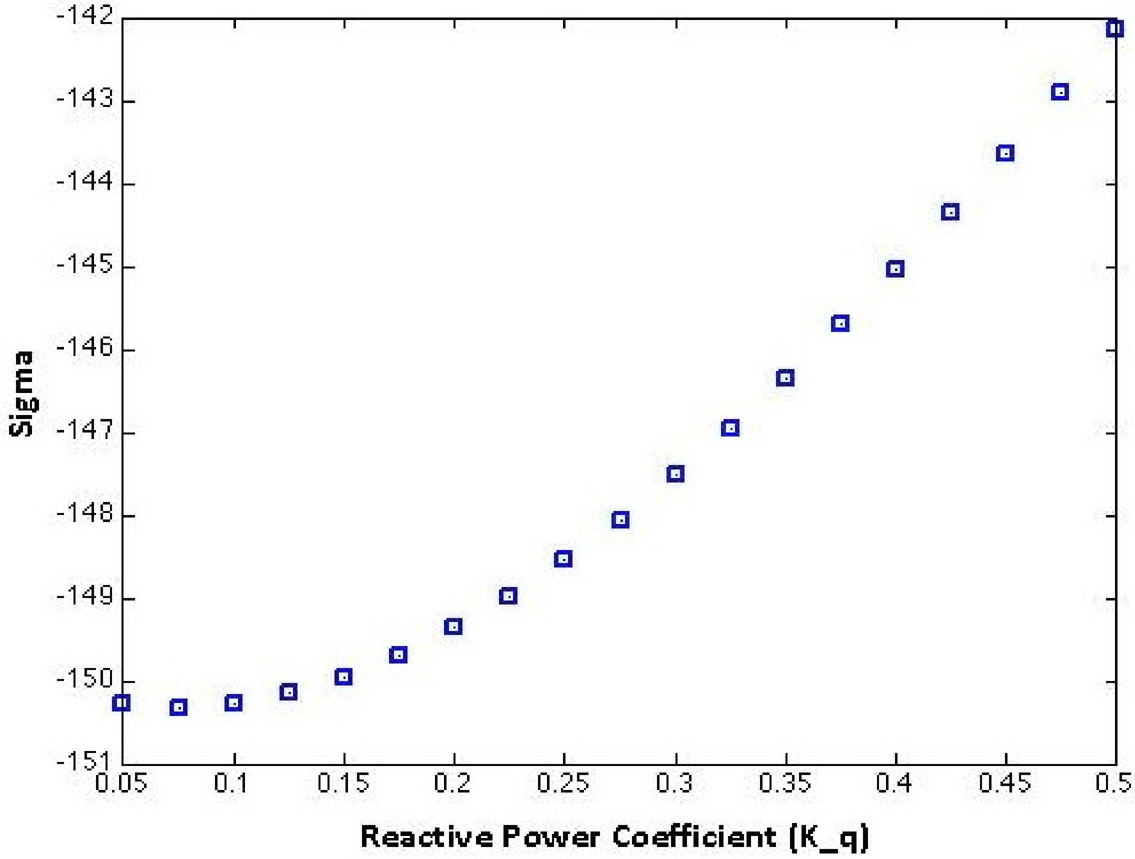

Plan of Action: Part 1A – Modeling

- Data driven modeling
  - Detrended Fluctuation Analysis (DFA)
  - Auto-Regressive Fractionally Integrated (ARFIMA) modeling
  - Berg model (Scandinavian grid)
- *"First principles"* modeling
  - Load aggregation
  - Falsification of swing equation by PMU data

Hidden Feedback in Power Systems

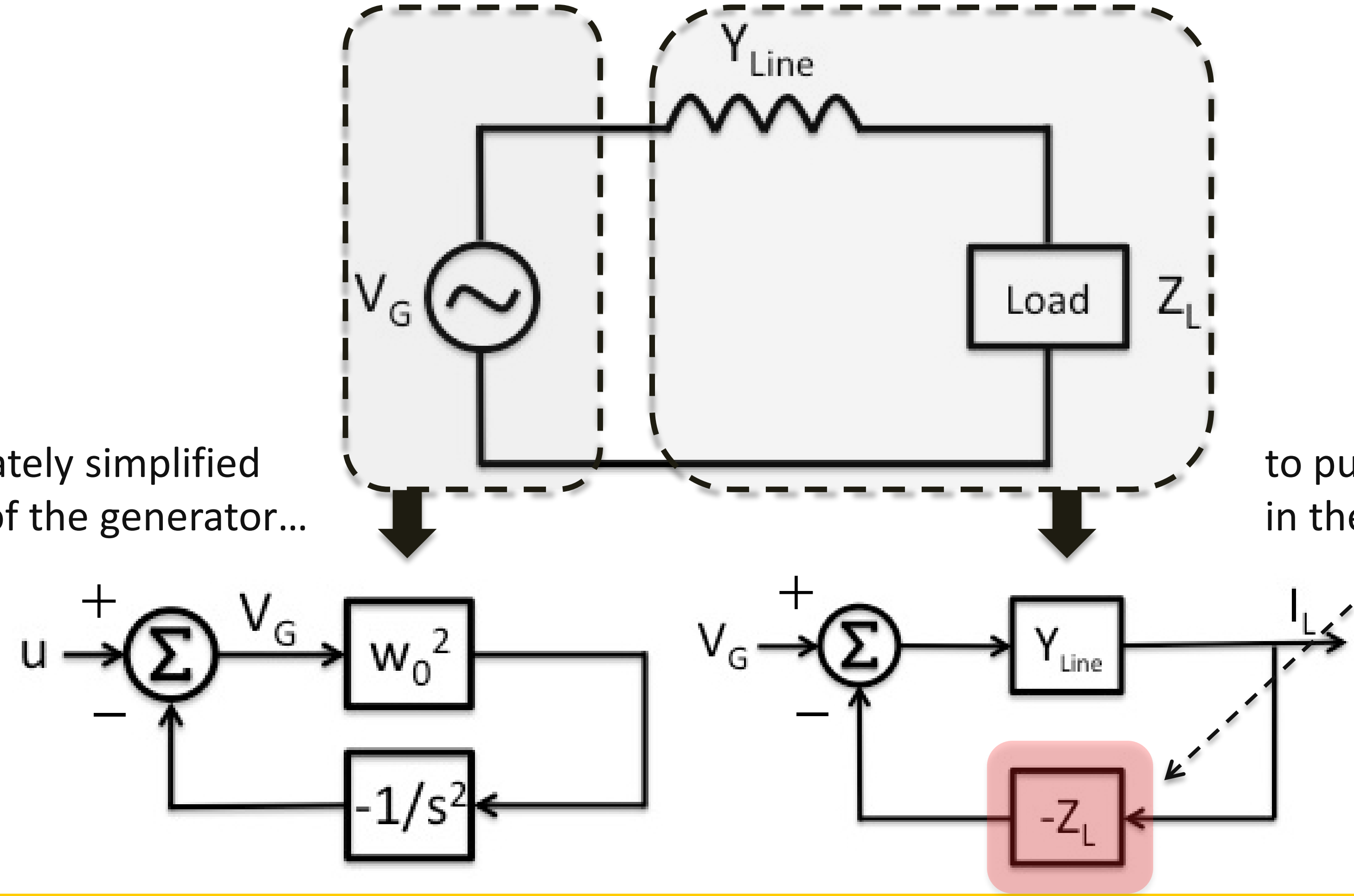

Deliberately simplified model of the generator…

to put the load in the spotlight.

Feedback Model of Power System

$$y = (I - GF)^{-1} Gu$$

$$u = \begin{bmatrix} u_1 & u_2 \end{bmatrix}^t$$

$$y = \begin{bmatrix} y_1 & y_2 \end{bmatrix}^t$$

$$G = \begin{bmatrix} Y_{Line} & Y_{Line} \\ 0 & \omega_0^{\ 2} \end{bmatrix}$$

$$F = \begin{bmatrix} -Z_L & 0 \\ 0 & -s^{-2} \end{bmatrix}$$

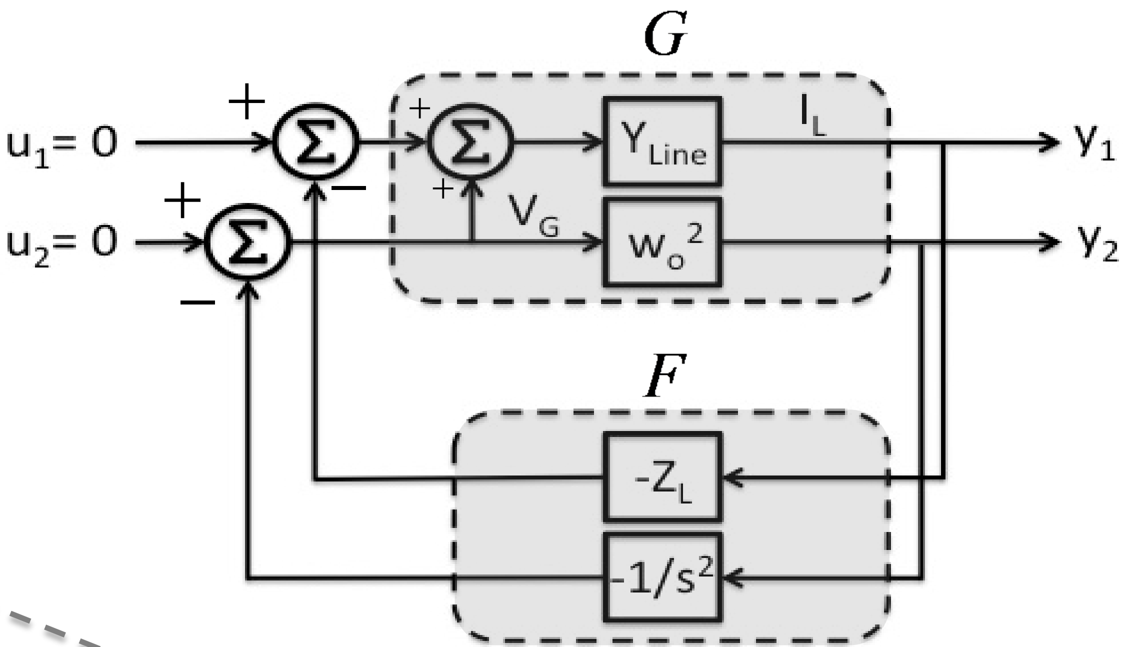

Simplification:
No back-action of the load to the generator

Towards more Complicated Feedback Models of Power System

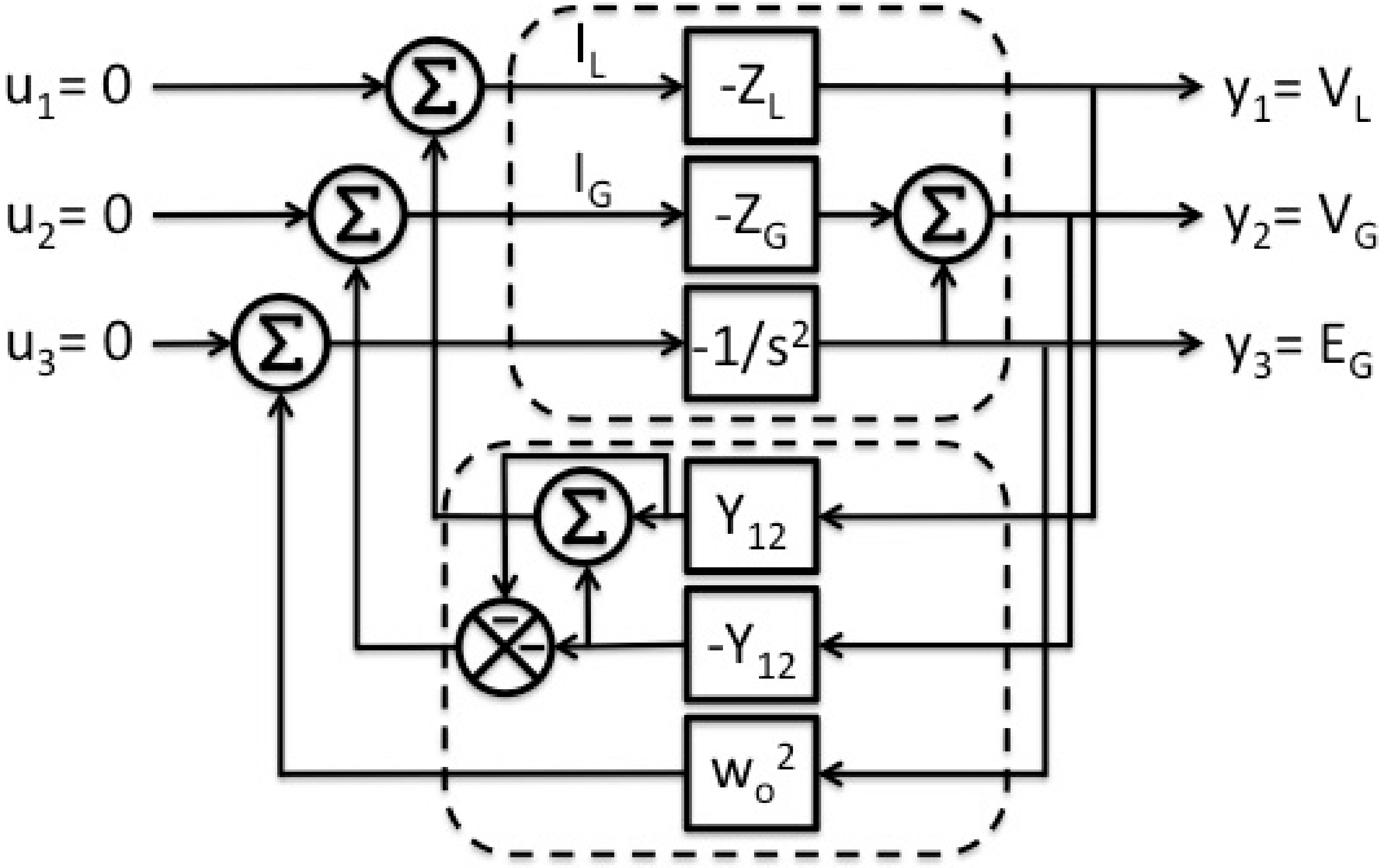

Time to Conceptualize

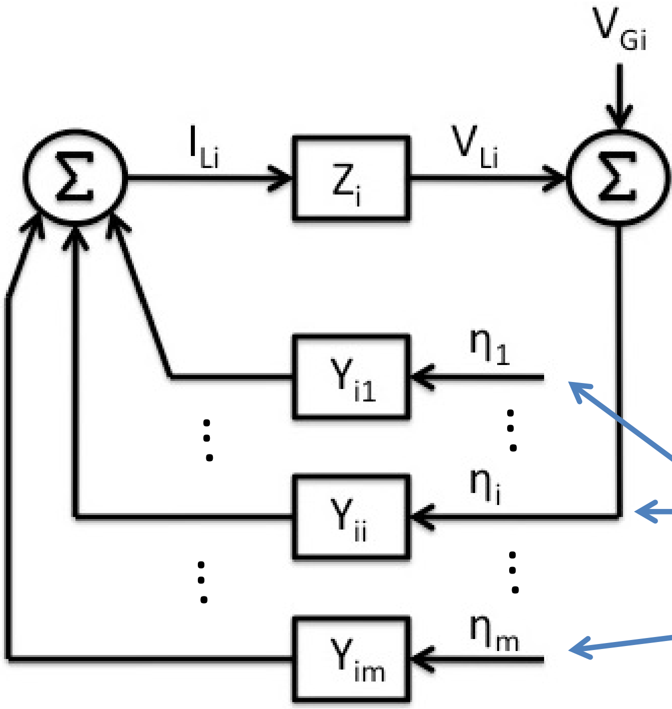

714 IEEE TRANSACTIONS ON CIRCUITS AND SYSTEMS, VOL. CAS-23, NO. 12, DECEMBER 1976

Input–Output Stability Theory of Interconnected Systems Using Decomposition Techniques

FRANK M. CALLIER, MEMBER, IEEE, WAN S. CHAN, STUDENT MEMBER, IEEE, AND CHARLES A. DESOER, FELLOW, IEEE

Nominal impedance, line Z_i, Y_{ii}

Connecting lines 1, 2, …, $\neq$i, …, m

Lump everything

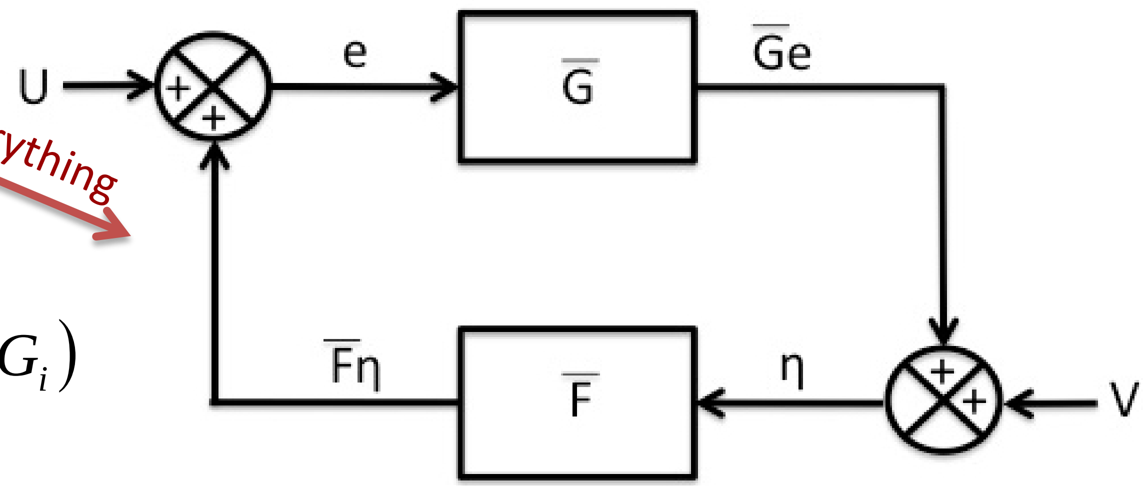

Are we sure that

$$\det\left(I - \overline{F}\overline{G}\right) \neq \Pi_i \det\left(I - F_i G_i\right)$$

Decomposition of Digraph into Strongly Connected Components $D(U_i)$

Feedback connections, if any, are lumped into strongly connected subsets

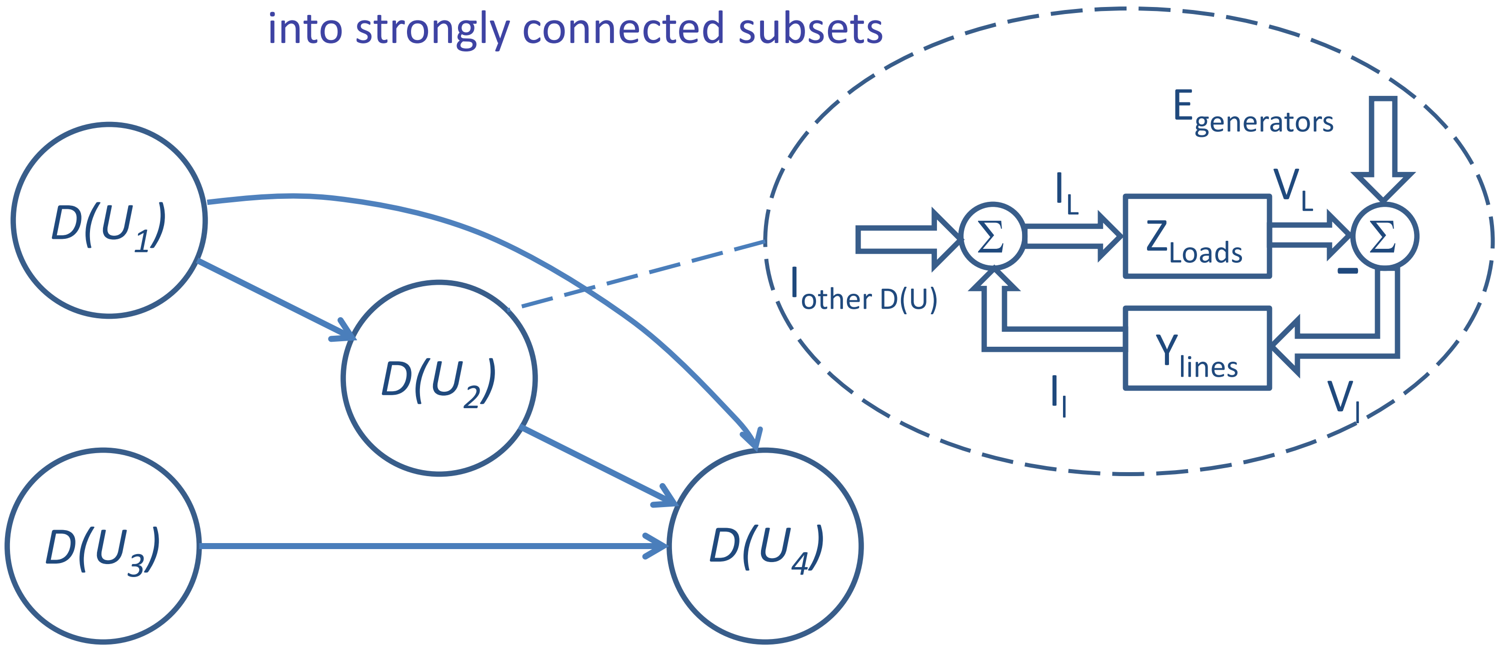

No large scale feedback connections
at the large scale of the structure graph

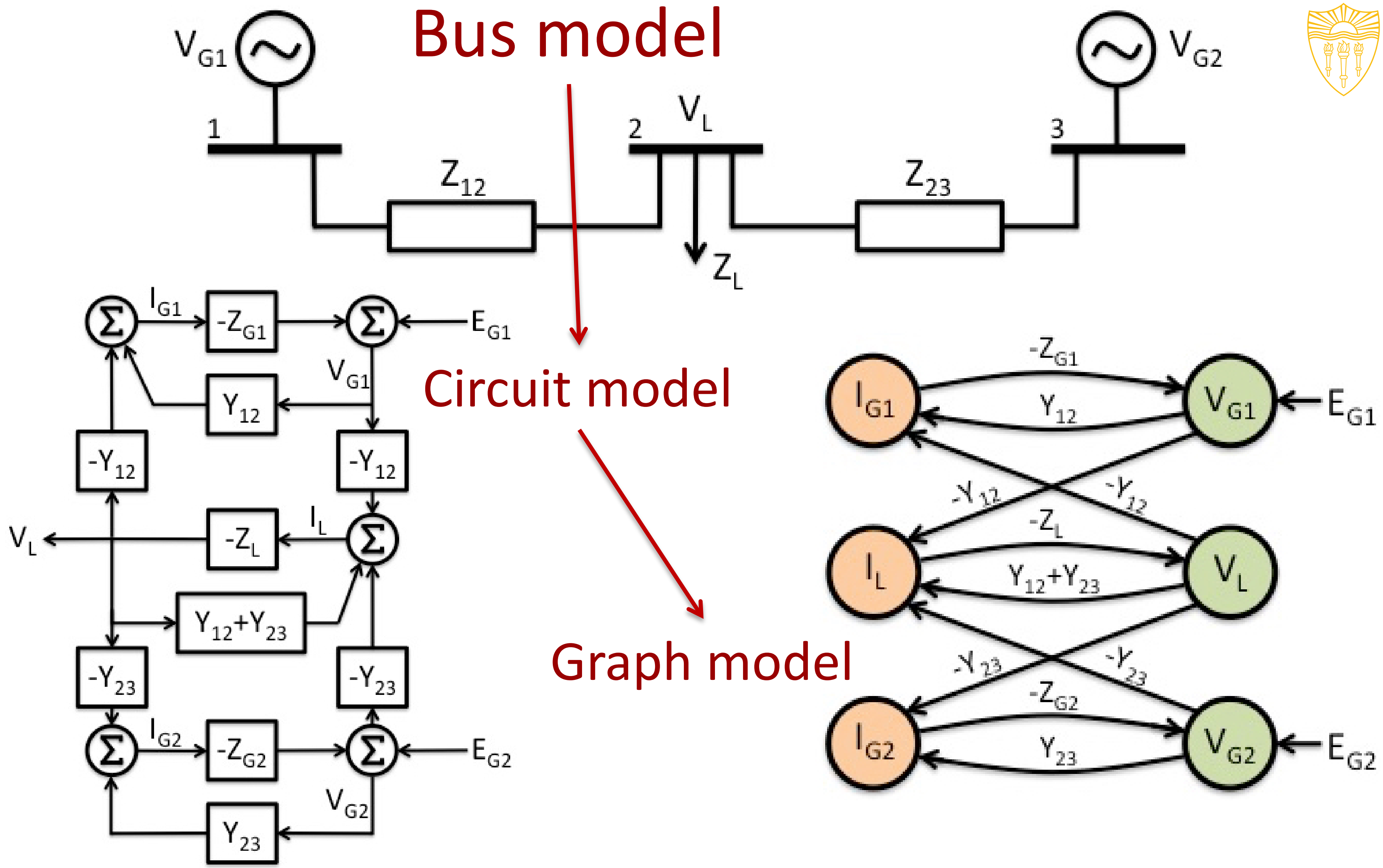

Bus model
Circuit model
Graph model
V_{G1}
V_{G2}
1
2
3
V_L
Z_{12}
Z_{23}
Z_L
I_{G1}
$-Z_{G1}$
E_{G1}
V_{G1}
Y_{12}
$-Y_{12}$
I_L
$-Z_L$
V_L
$Y_{12}+Y_{23}$
$-Y_{23}$
I_{G2}
$-Z_{G2}$
E_{G2}
V_{G2}
Y_{23}
I_{G1}
V_{G1}
I_{L}
V_{L}
I_{G2}
V_{G2}

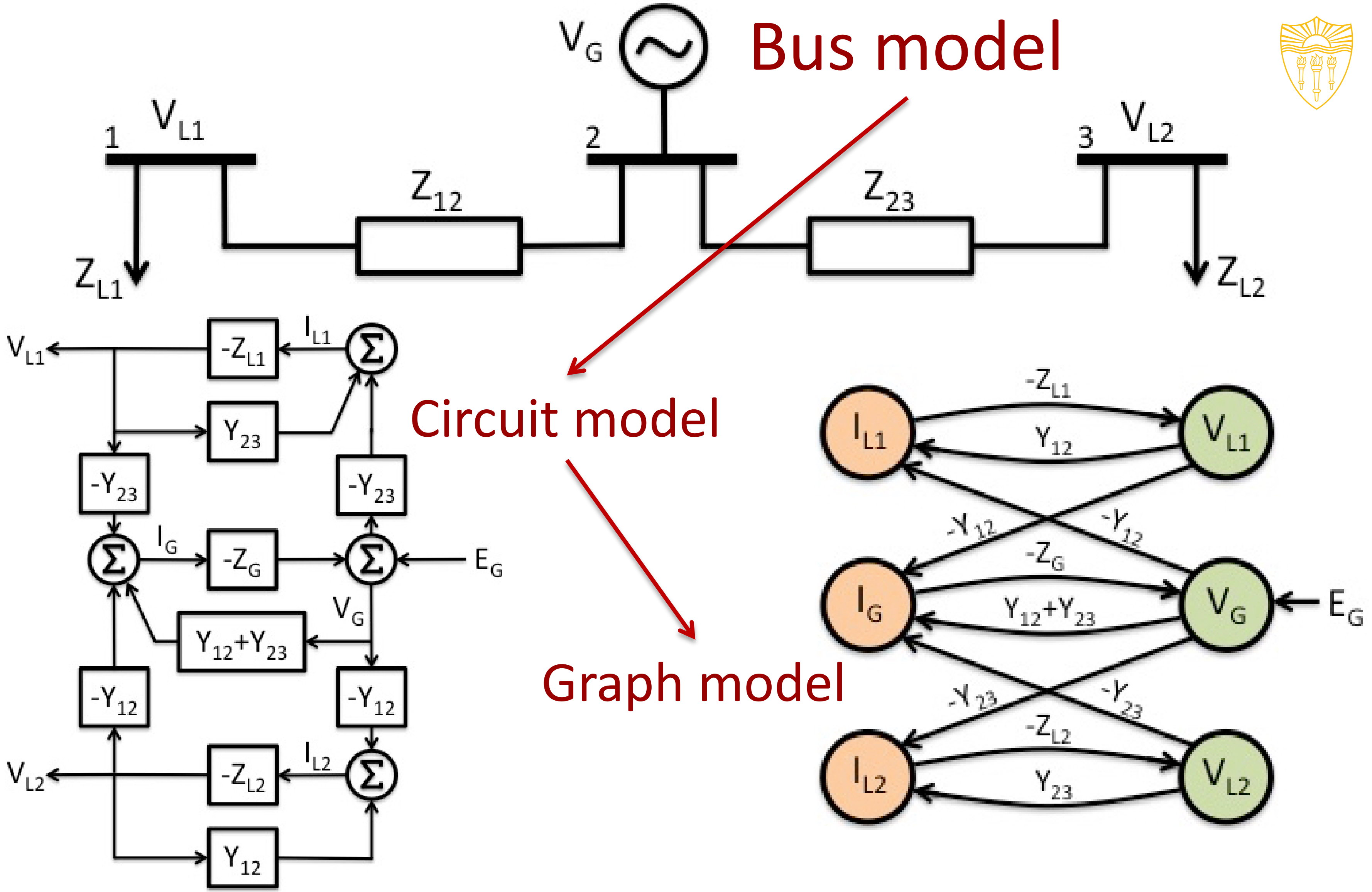

Bus model
Circuit model
Graph model
V_G
1
V_{L1}
2
3
V_{L2}
Z_{12}
Z_{23}
Z_{L1}
Z_{L2}
V_{L1}
$-Z_{L1}$
I_{L1}
Y_{23}
$-Y_{23}$
$-Y_{23}$
I_G
$-Z_G$
E_G
V_G
$Y_{12}+Y_{23}$
$-Y_{12}$
$-Y_{12}$
V_{L2}
$-Z_{L2}$
I_{L2}
Y_{12}
I_{L1}
V_{L1}
$-Z_{L1}$
Y_{12}
$-Y_{12}$
$-Y_{12}$
I_G
V_G
$-Z_G$
$Y_{12}+Y_{23}$
E_G
$-Y_{23}$
$-Y_{23}$
I_{L2}
V_{L2}
$-Z_{L2}$
Y_{23}

Bus model

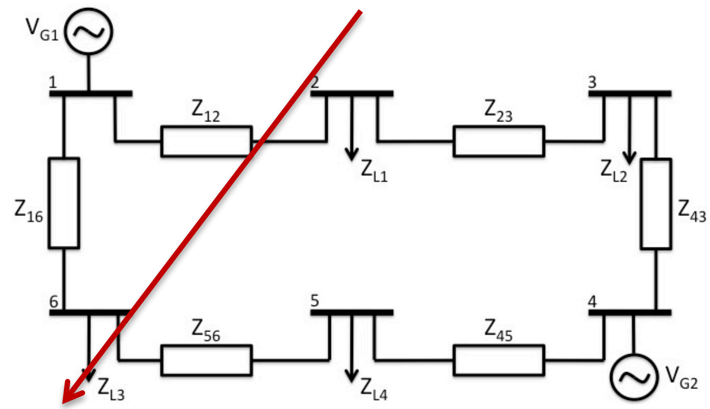

Circuit model

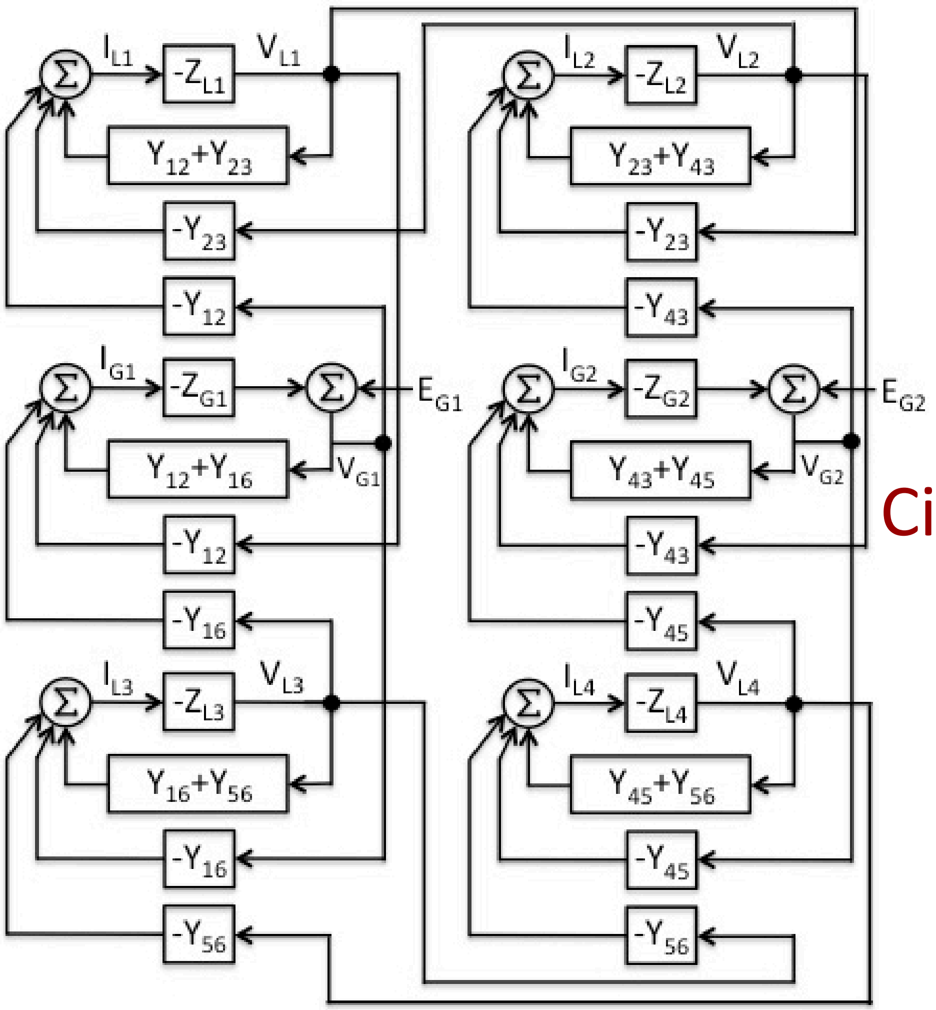

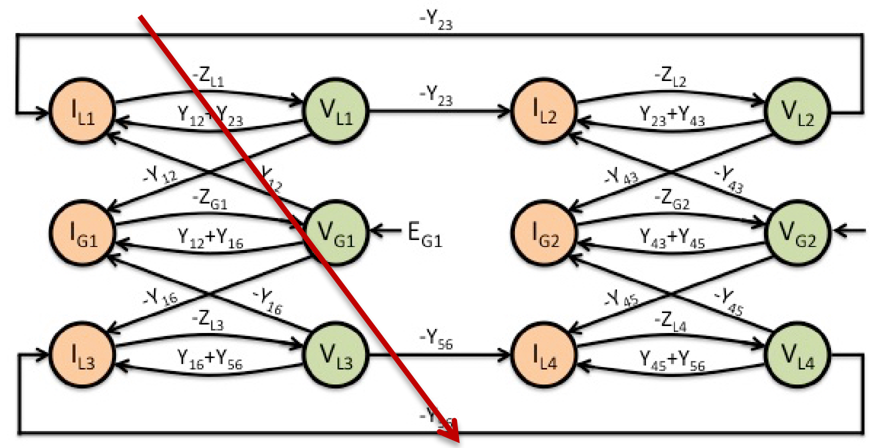

Graph model

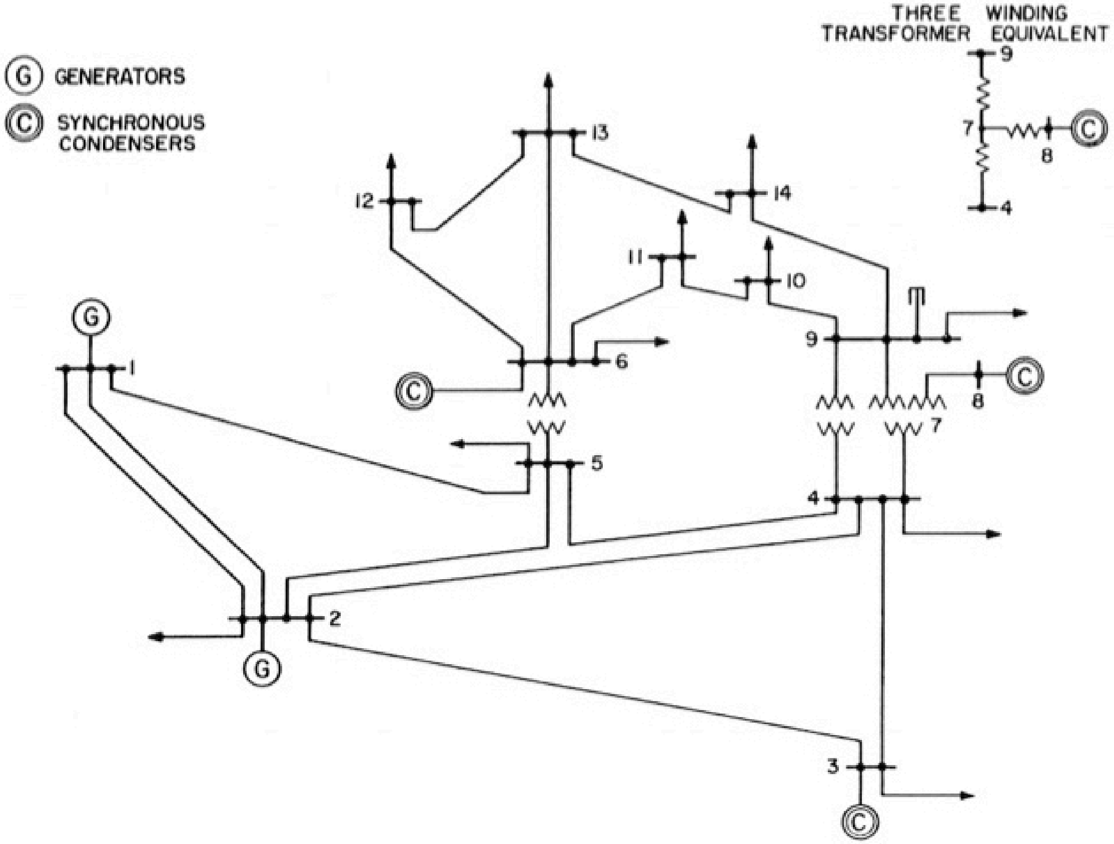
G GENERATORS
C SYNCHRONOUS CONDENSERS
THREE WINDING TRANSFORMER EQUIVALENT
1
2
3
4
5
6
7
8
9
10
11
12
13
14

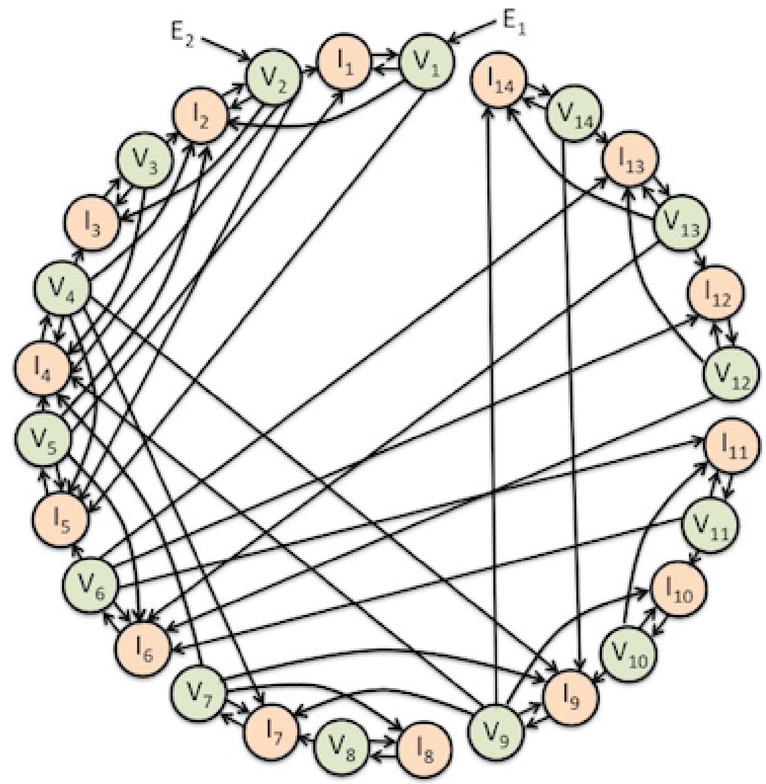
E1
E2
V1
I1
V2
I2
V3
I3
V4
I4
V5
I5
V6
I6
V7
I7
V8
I8
V9
I9
V10
I10
V11
I11
V12
I12
V13
I13
V14
I14

Effect of Single Contingency

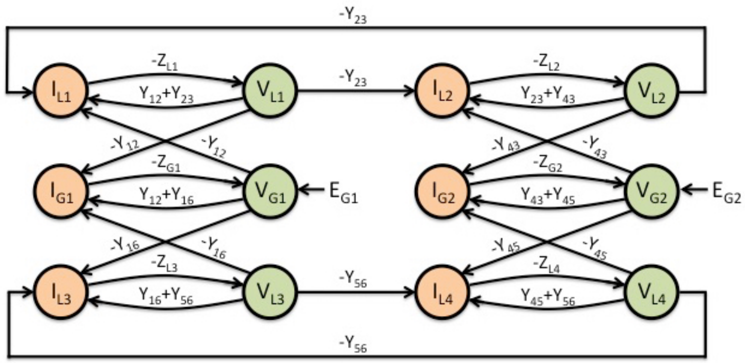

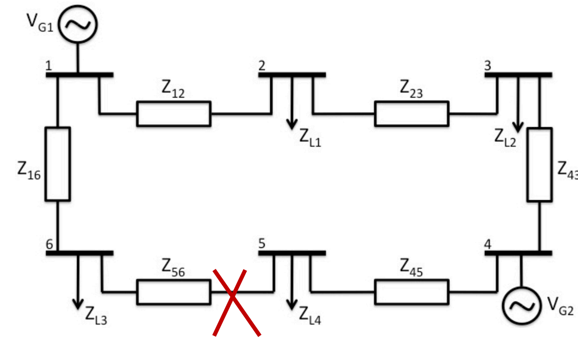

Single transmission line 5-6 tripping:

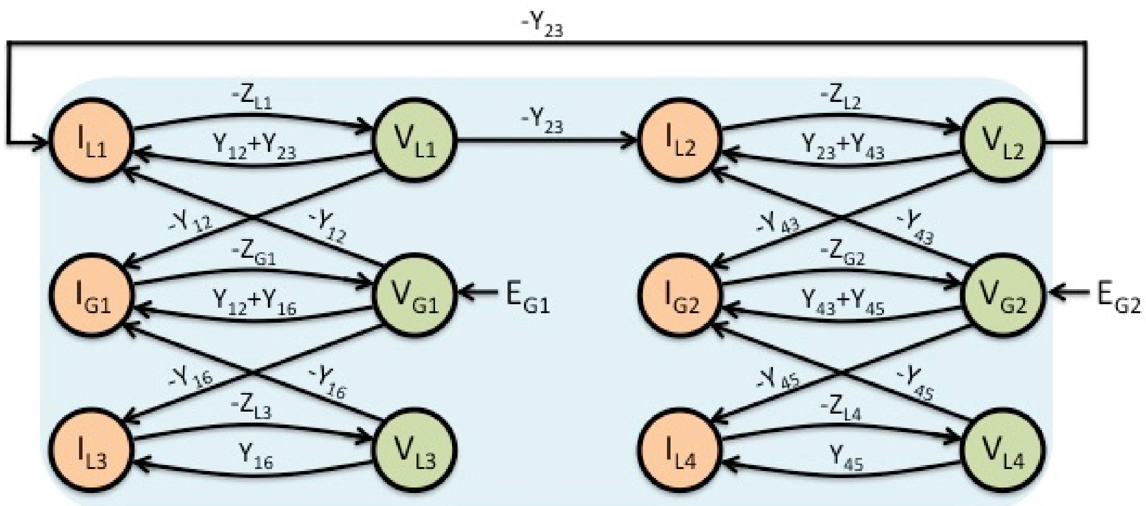

No loss of strong connectivity!

Effect of Single Contingency

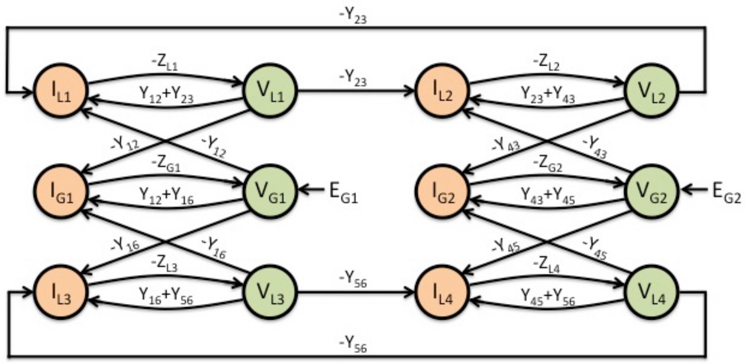

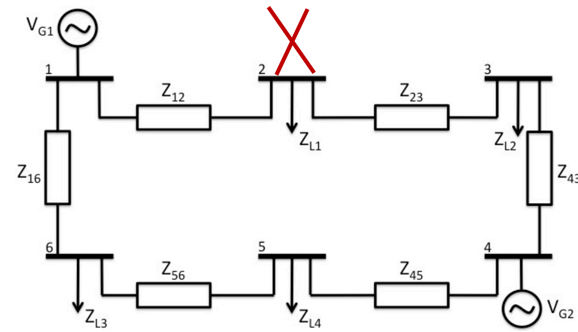

Three-phase fault at Load 1:

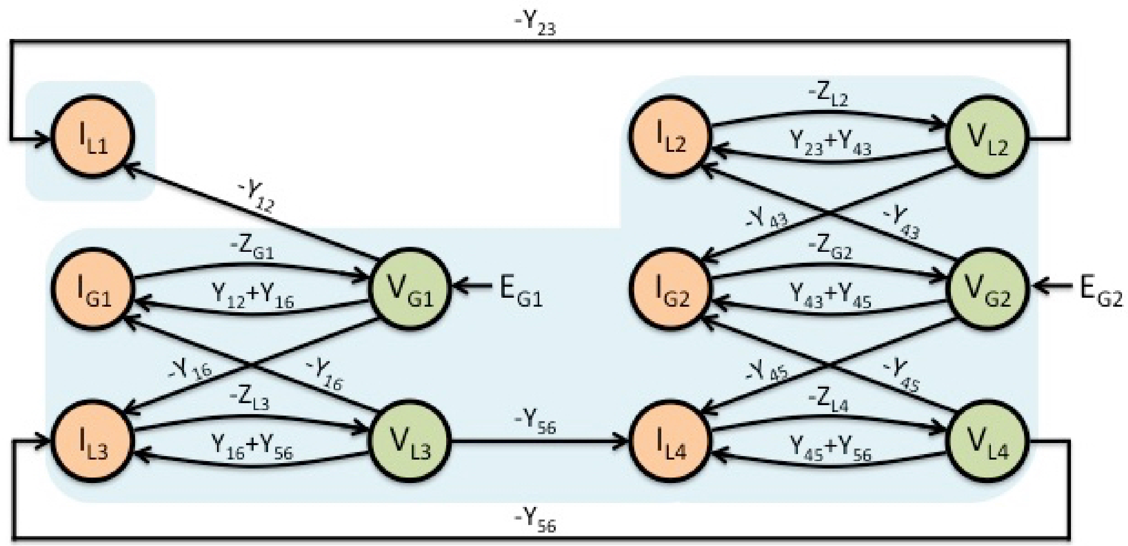

Loss of strong connectivity: two strongly connected components!

Effect of Double Contingency

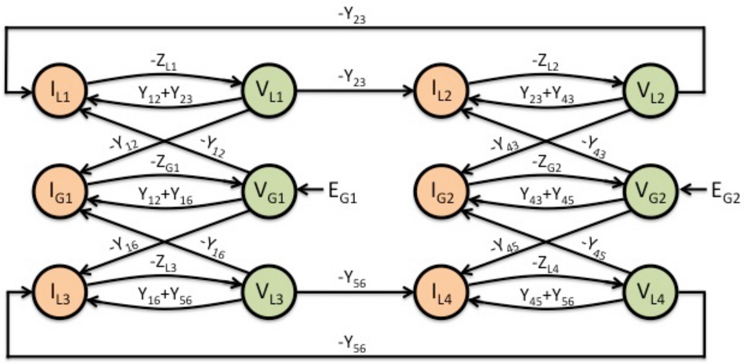

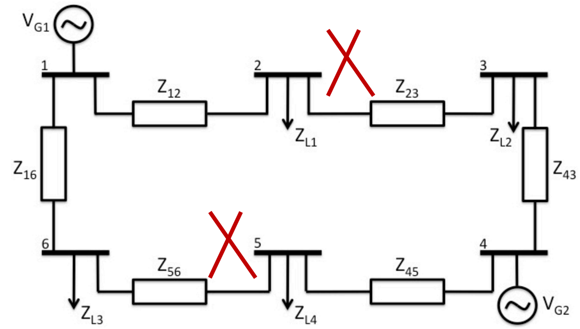

Double transmission line 5-6, 2-3 tripping:

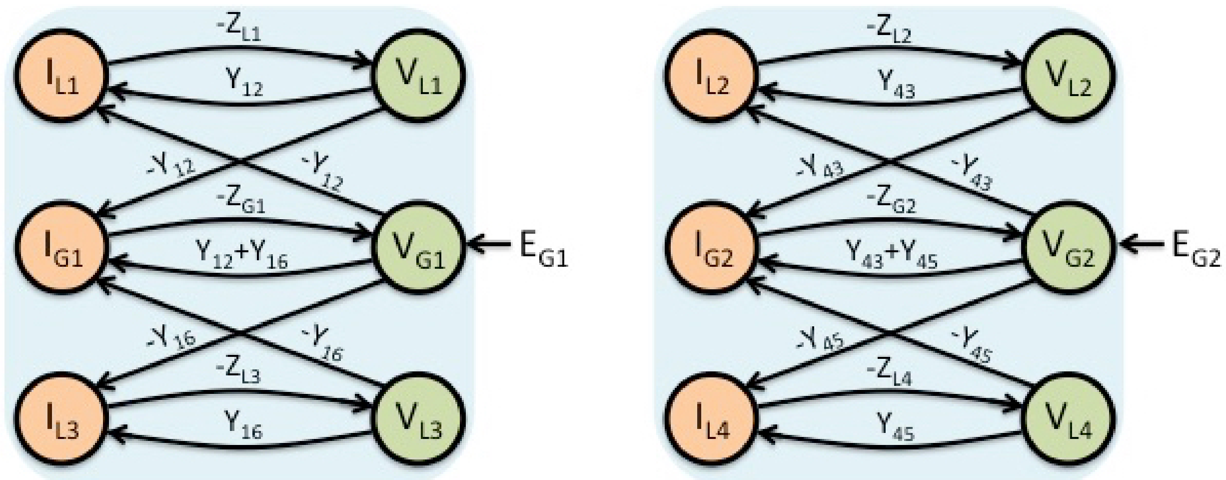

Loss of connectivity: two connected components!

Effect of Double Contingency

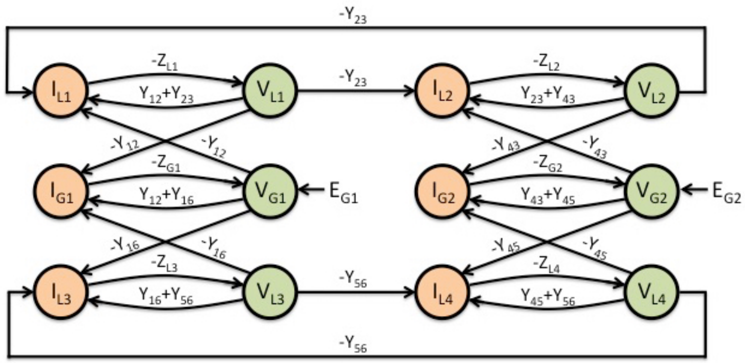

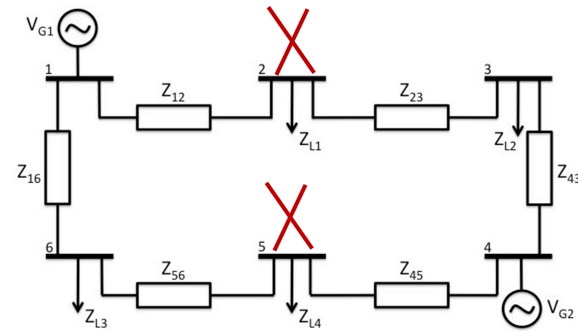

Two three-phase faults at Loads 1 and 4:

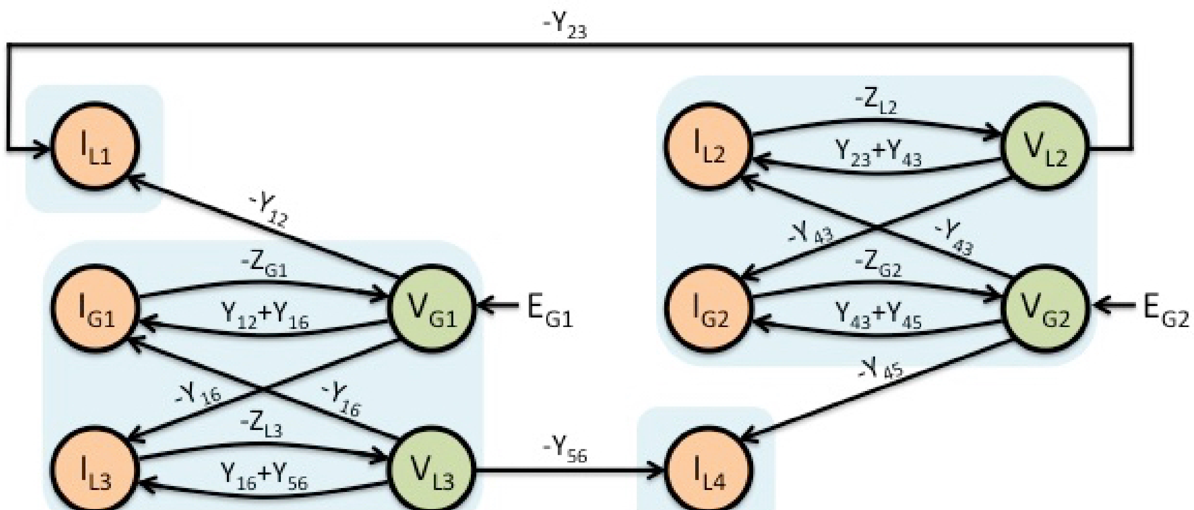

Loss of strong connectivity: four strongly connected components!

Main Theorem

Theorem: Under the conditions that

- the bus system is connected,
- all generators have non-vanishing internal impedance,

and the contingencies are restricted to

- single transmission line tripping,

the graph model is strongly connected.

Conclusion

- The power grid is a complicated system…
  - Fractional dynamics…
  - Strongly connected feedback structure…
- *Are "classical" methods (differential equations, feedback theory) appropriate?*
  - Or would we have to aim for another approach?
    - The large-scale property of the grid calls for *statistical mechanics* approach.

Plan of Action: Part 1A – Modeling

- Data driven modeling
  - Detrended Fluctuation Analysis (DFA)
  - Auto-Regressive Fractionally Integrated (ARFIMA) modeling
  - Berg model (Scandinavian grid)
- *"First principles"* modeling
  - Load aggregation
  - Falsification of swing equation by PMU data

$1,000,000 Question

- What grid model reproduces the fractal behavior of the PMU signals???
- There is a tendency to forget that a signal is generated by a dynamics, which might be very "complicated," e.g., chaotic, transitive, Axiom A, …
- We develop an approach firmly rooted in the tradition of the great Russian dynamicists: Krylov, Bogoliubov, Kolmogorov, Sinai, …
- The popular swing model is unable to reproduce this behavior.

Krylov-Bogoliubov Invariant Measure

Consider an *abstract dynamical system,*

$$\big((X, \mathcal{B}, \mu), F^t\big)$$

where

$F^{-t}(A)$

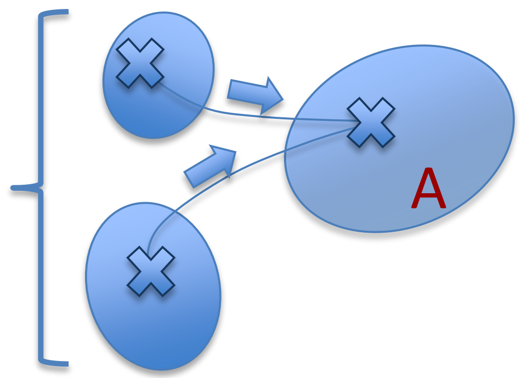

- $(X, \mathcal{B}, \mu)$ is a probability space:
  - X is a sample space or state-space
  - $\mathcal{B}$ is a Borel field of subsets of X
  - $\mu: \mathcal{B} \longrightarrow \mathbb{R}_{\geq 0}$ is a measure
- $F^t: X \longrightarrow X$ is a one-parameter family of measurable transformations of X; it could be
  - $F^t: x(0) \longmapsto x(t)$ in case of continuous dynamics $\frac{dx(t)}{dt} = f\big(x(t)\big)$
  - $F^{k\in\mathbb{N}}: x(0) \longmapsto x(k)$ in case of discrete dynamics $x(k+1) = f\big(x(k)\big)$
  - the Doob stochastic shift in case of stochastic dynamics
- The measure is invariant relative to the dynamics

$$\mu(F^{-t\leq 0}(A)) = \mu(A), \quad \forall A \in \mathcal{B}$$

Krylov-Bogoliubov Construction

An invariant measure always exists, as proved constructively by Krylov and Bogoliubov:
Idea:

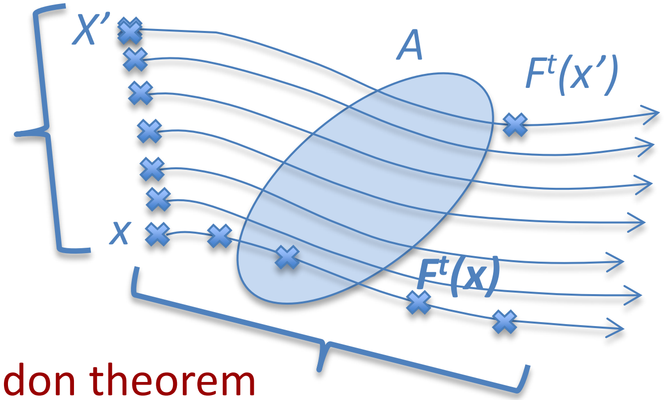

- Start with an arbitrary measure μ
- Iterate in both
  - space $\int_X \, dx$
  - time $\frac{1}{T}\int_0^T dt$

  to make the measure invariant
- Precisely, given μ, construct μ_T invoking Riesz-Radon theorem

$$\frac{1}{T}\int_0^T d\tau \int_X \varphi(F^\tau(x))\mu(dx) = \int_X \varphi(x)\mu_T(dx), \qquad \varphi(x) = I_A(x)$$

- Repeat for an increasing unbounded sequence of *T* to get the invariant measure:

$$T_1 \leq T_2 \leq \cdots \implies \lim_{i\longrightarrow\infty} \mu_{T_i} = \mu^*$$

Krylov-Bogoliubov construction
μ^* is invariant

$$\lim_{i\to\infty}\frac{1}{T_i}\int_0^{T_i} d\tau \int_X \varphi(F^\tau(x))\mu(dx) = \int_X \varphi(x)\mu^*(dx), \qquad \varphi(x) = I_A(x)$$

$$\lim_{i\to\infty}\frac{1}{T_i}\int_0^{T_i} d\tau \int_X \varphi(F^{\tau+t}(x))\mu(dx) = \int_X \varphi(F^t x)\mu^*(dx), \qquad \varphi(x) = I_A(x)$$

=

$$\mu^*(A) = \int_X I_A(F^t(x))\,\mu^*(dx) = \int_A \mu^*(F^{-t}dy) = \mu^*(F^{-t}(A))$$

Kolmogorov–Sinai Entropy from Invariant Measure

$$H_{KS}(T) = -\sup_A \lim_{N\to\infty}$$

$$\sum_{i,j,\ldots,k=1}^{N} \mu\left(A_i \cap T^{-1}A_j \cap \cdots \cap T^{-N+1}A_k\right) \log \mu\left(A_i \cap T^{-1}A_j \cap \cdots \cap T^{-N+1}A_k\right)$$

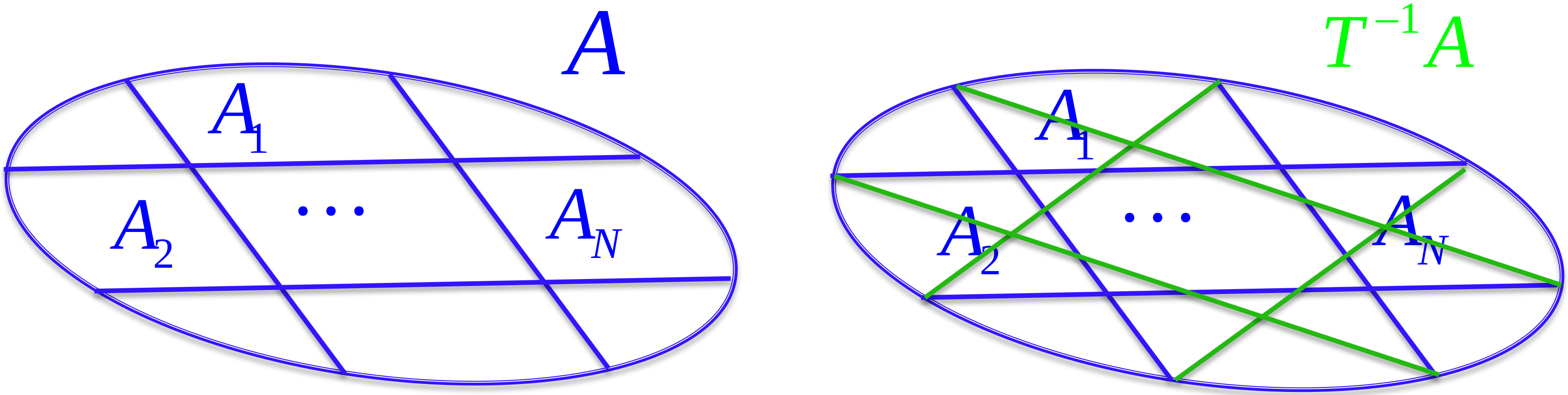

Invariant Measure Beyond Classical Measure Theory

- The invariant measure could be singular (relative to the Lebesgue measure), it could be fractal, multi-fractal, etc.
- It is argued that such properties beyond measure theory reveal qualitative properties of the dynamics
  - Multi-fractality ⇔ lack of ergodicity
- Practically, we proceed with a counting measure in the ball $B_c(\varepsilon)$

$$\frac{1}{K}\sum_{k=1}^{K}\frac{1}{N}\sum_{n=1}^{N} I_{B_c(\varepsilon)}\left(F^k\left(x_{0_n}\right)\right) = \mu_{K,N}(B_c(\varepsilon))$$

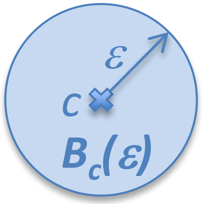

- Then proceed as

$$\lim_{\varepsilon \downarrow 0}\frac{\log \mu_{K,N}(B_c(\varepsilon))}{\log \varepsilon} = \alpha_c \Longrightarrow \quad \mu(B_c(\varepsilon)) = \varepsilon^{\alpha_c}$$

Part I: Summary

Ergodic Theory

Krylov-Bogoliubov

Empirical

Single Exponent

DFA

ARIMA

ARFIMA

$$\left(1-\sum_{i=1}^{p}\phi_i B^i\right)(1-B)^d X_t = \left(1+\sum_{i=1}^{q}\theta_i B^i\right)\varepsilon_t$$

Berg Model

$$I_L(t) = A D_*^{\alpha} V_L(t) - B D_*^{\beta} V_L(t)$$

Mathematics

Grünwald-Letnikov ⟷ Riemann-Liouville

$$\mathbb{D}^d = \lim_{|B|\to 0}\frac{(I-|B|)^d}{|B|^d}$$

$$\begin{aligned} D^{\alpha} f(x) &= D^m J^{m-\alpha} f(x) \\ &= D^m\left(\frac{1}{\Gamma(m-\alpha)}\int_0^t (t-\tau)^{m-\alpha-1} f(\tau)\,d\tau\right)\end{aligned}$$

Fractal Dimension

- Capacity (Box Counting)

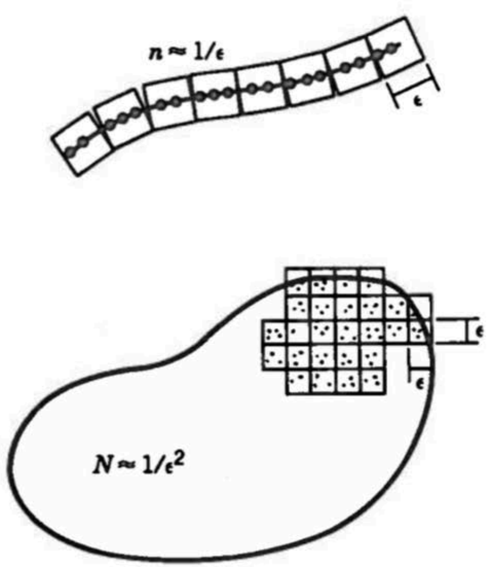

Figure 6-4 Covering procedure for linear and planar distributions of points.

$$d_C = \lim_{\epsilon \to 0} \frac{\log N(\epsilon)}{\log(1/\epsilon)}$$

where $N(\epsilon)$ - number of cubes to cover a set embedded in a line or a surface

ϵ - cubes with sides of length ϵ

Said to be fractal for non-integer dimension d_C

Moon, F. C. Chaotic and Fractal Dynamics: An Introduction to Applied Scientist and Engineers. 1992.

Measures of Fractal Dimension

- **Pointwise Dimension**
  - Time-sample the trajectory to set of N points
  - Place a sphere of radius r at some point and count the number of points N(r) within sphere
  - Probability of finding a point in sphere of radius r

$$P(r) = \frac{N(r)}{N_0} \approx a r^{d_P}$$

Pointwise dimension

$$d_P = \lim_{r \to 0} \frac{\log P(r; x_i)}{\log r}$$

Averaged pointwise dimension

$$\hat{d}_P = \frac{1}{M} \sum_{i=1}^{M} d_P(x_i)$$

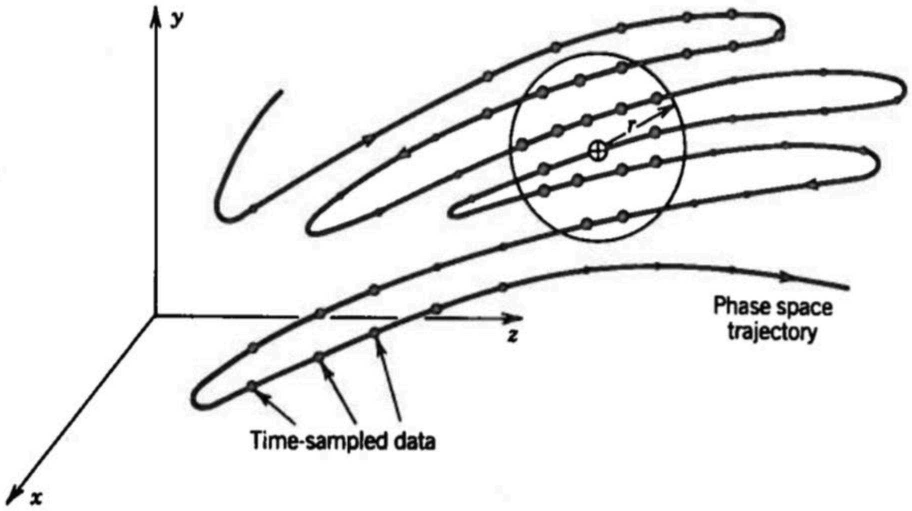

Moon, F. C. Chaotic and Fractal Dynamics: An Introduction to Applied Scientist and Engineers. 1992.

Measures of Fractal Dimension

- **Correlation dimension (Grassberger and Proccacia, 1983)**
  - Discretizes trajectory to set of N points
    - One can also create a pseudo-phase-space
  - Calculates distances between pairs of points x_i and x_j $\rho(x_i, x_j) = |x_i - x_j|$

Correlation function:

$$C(r) = \lim_{N\to\infty} \frac{1}{N^2} \binom{\text{number of pairs } (i,j)}{\text{with distances } s_{ij}<r}$$

Power law dependence on r

$$\lim_{r\to 0} C(r) = ar^d$$

Fractal dimension:

$$d_G = \lim_{r\to 0} \frac{\log C(r)}{\log r}$$

*slope of the log C(R) vs log r curve

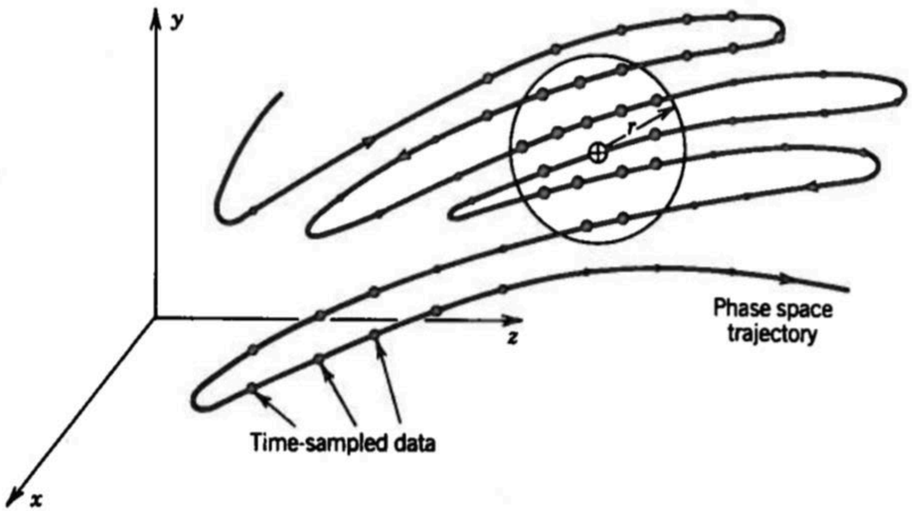

Moon, F. C. Chaotic and Fractal Dynamics: An Introduction to Applied Scientist and Engineers. 1992.

Measures of Fractal Dimension

- **Effective implementation**

$$C(r) = \lim_{N\to\infty} \frac{1}{N^2} \binom{\text{number of pairs } (i,j)}{\text{with distances } s_{ij}<r}$$

$$C(r) = \lim_{N\to\infty} \frac{\sum_{i=1}^{N} \sum_{j>i}^{N} H\left(r - \rho(x_i - x_j)\right)}{\frac{1}{2}N(N-1)}$$

Where:

Heaviside function: $$H(s) = \begin{cases} 1, & s \geq 0 \\ 0, & s < 0 \end{cases}$$

Distance: $$\rho(x_i, x_j) = |x_i - x_j|$$

Bounds:

$$r_{max} = \max_{i,j} \rho(x_i, x_j) \qquad r_{min} = \max_{i,j} \rho(x_i, x_j)$$

Only consider computations for C(r) within bounds $r_{min} \leq r \leq r_{max}$

Strange Attractor Example

- **Duffing Strange Attractor**
  - **Two-well potential strange attractor**

$$\ddot{y} + \gamma \dot{y} - \frac{1}{2}\left(1 - x^2\right) x = A_0 \cos \Omega t$$

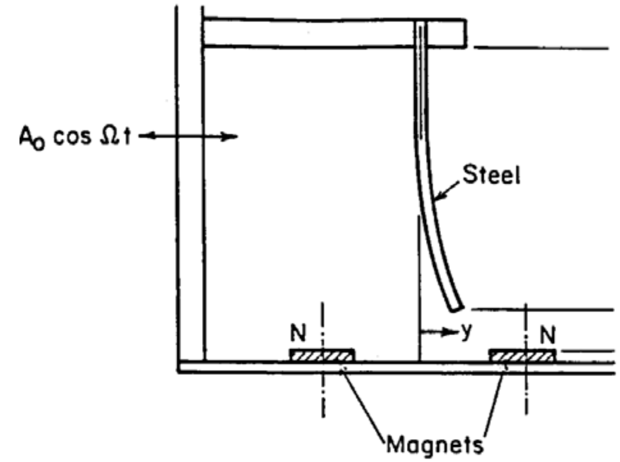

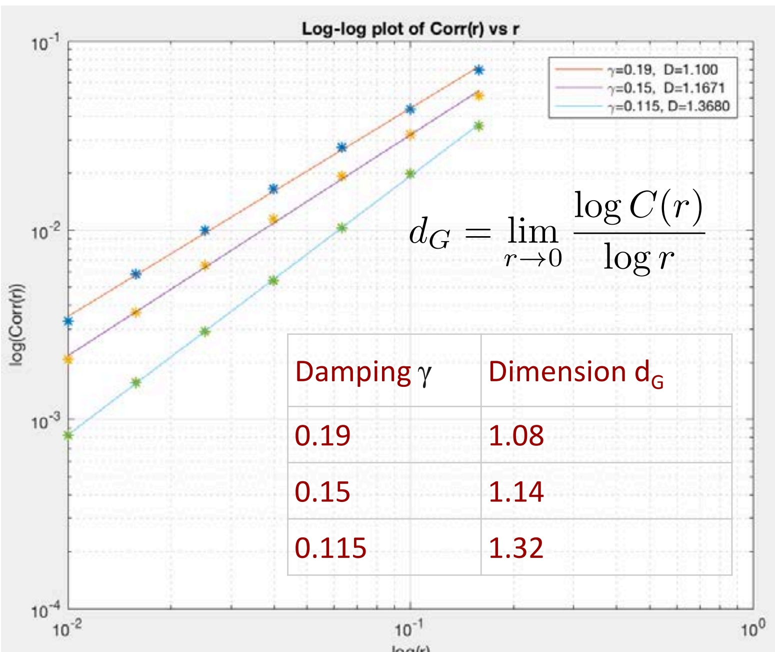

$$d_G = \lim_{r \to 0} \frac{\log C(r)}{\log r}$$

Damping γ	Dimension d_G
0.19	1.08
0.15	1.14
0.115	1.32

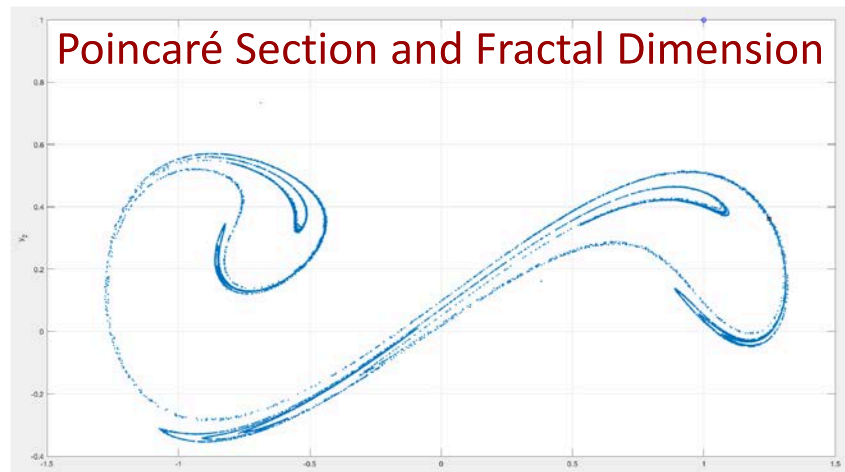

Moon, F. C. Chaotic and Fractal Dynamics: An Introduction to Applied Scientist and Engineers. 1992.

Swing Equation Model

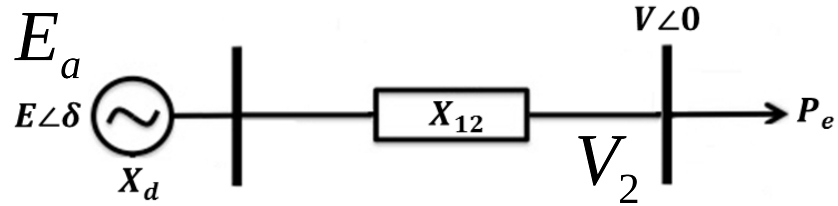

$$P_m(t) = P_e(t) + D\left(1 + \dot{\delta}(t)\right) + M\ddot{\delta}(t)$$

$$P_e(t) = \frac{E_a V_2(t)}{X_d + X_{12}} \sin(\delta(t)), \quad V_2(t) = 1 + \mathcal{N}(0, \sigma_v)$$

Noise perturbation at V_2

What is usually done! Is this correct???

where

- P_m - Mechanical power
- P_e - Electrical power
- D - Damping coefficient
- M - Moment of inertia of the rotor
- δ - Phase angle of the rotor with respect to the rotating frame
- E_a - Generator voltage
- X_d - Internal resistance of generator
- X_{12} - Reactance of transmission line
- V_2 - Load bus voltage magnitude

Swing Equation Simulation Results

Noise added at V_2: $V_2(t) = 1 + N(0, \sigma_v)$, $\sigma_v = 0.01$

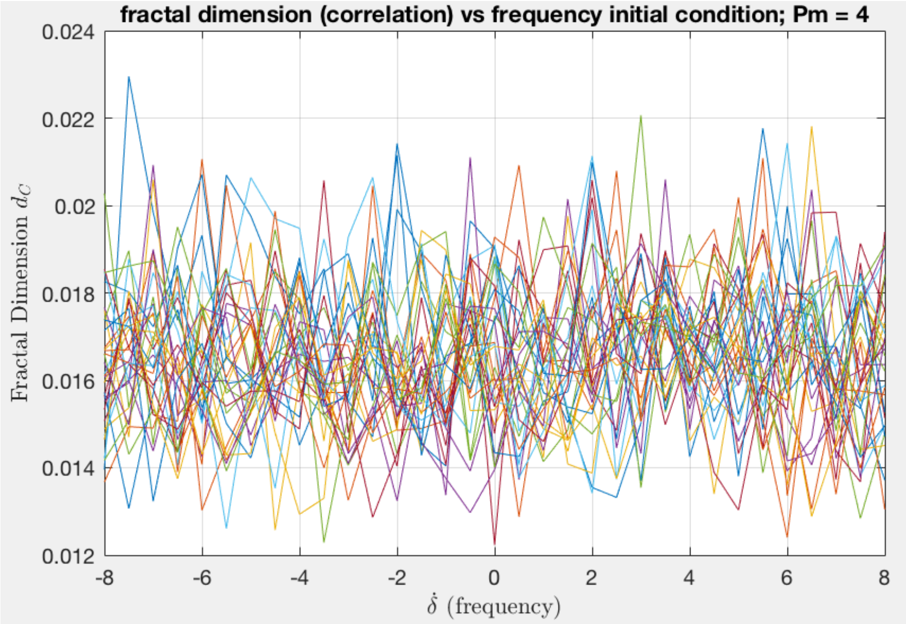

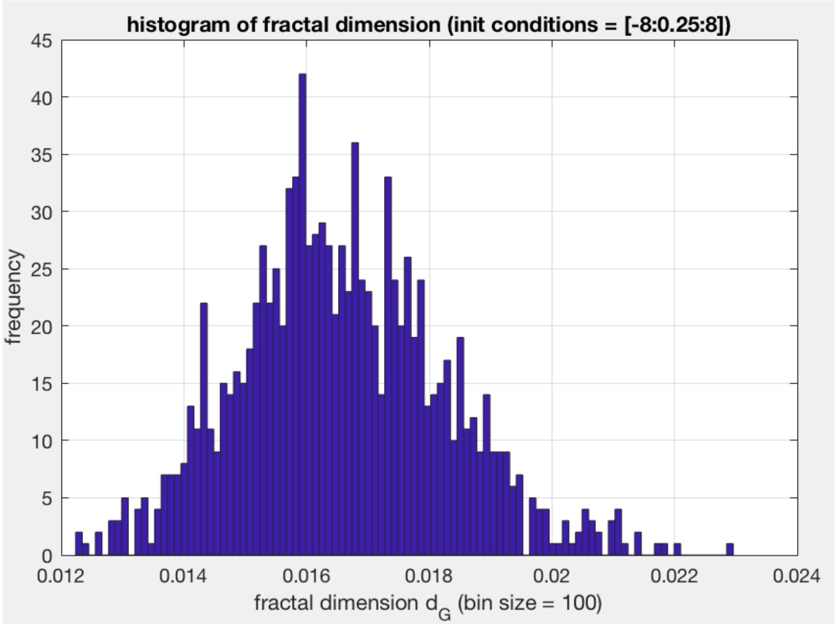

initial conditions	[-0.8:0.25:0.8]
N	10001
size(alpha)	1089
mean(d)	0.016572
std(d)	0.001675

Indian Blackout PMU Time Series Data

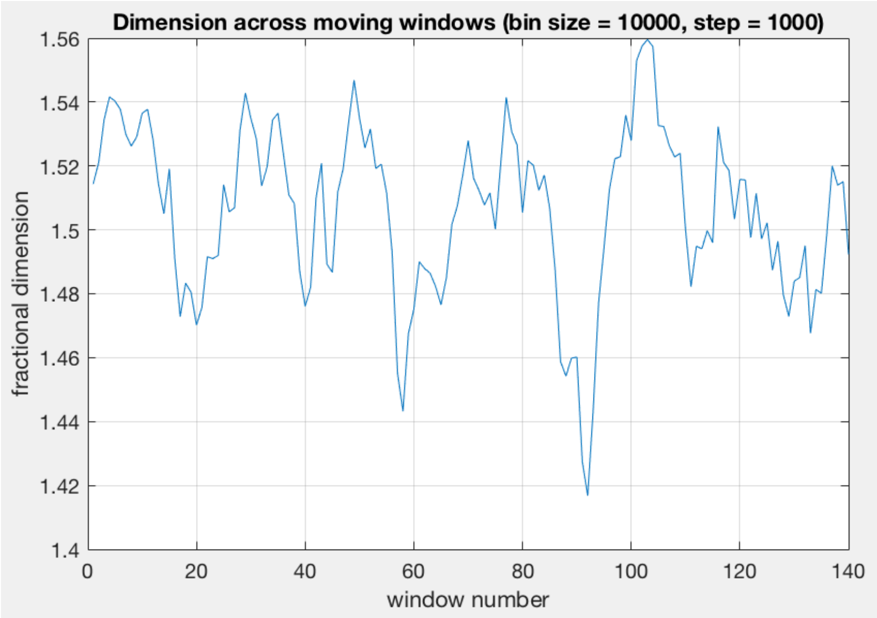

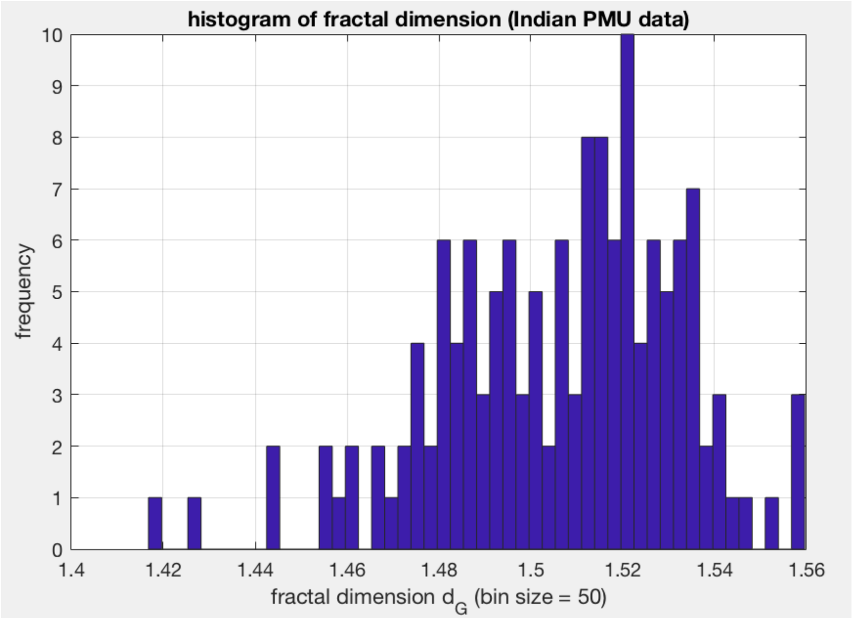

N	10000
size(alpha)	140
mean(d)	1.506059
std(d)	0.026241

Indian Blackout PMU Time Series Data

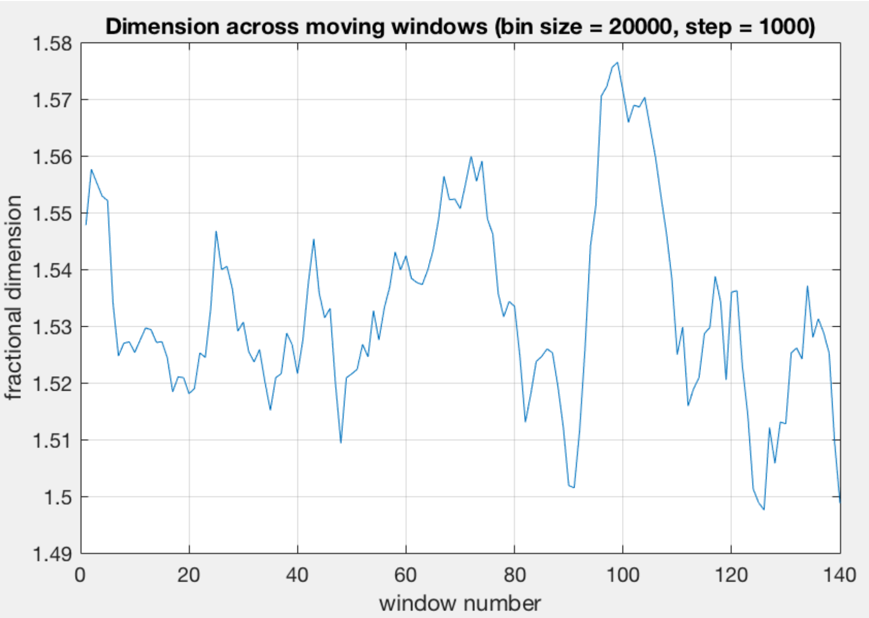

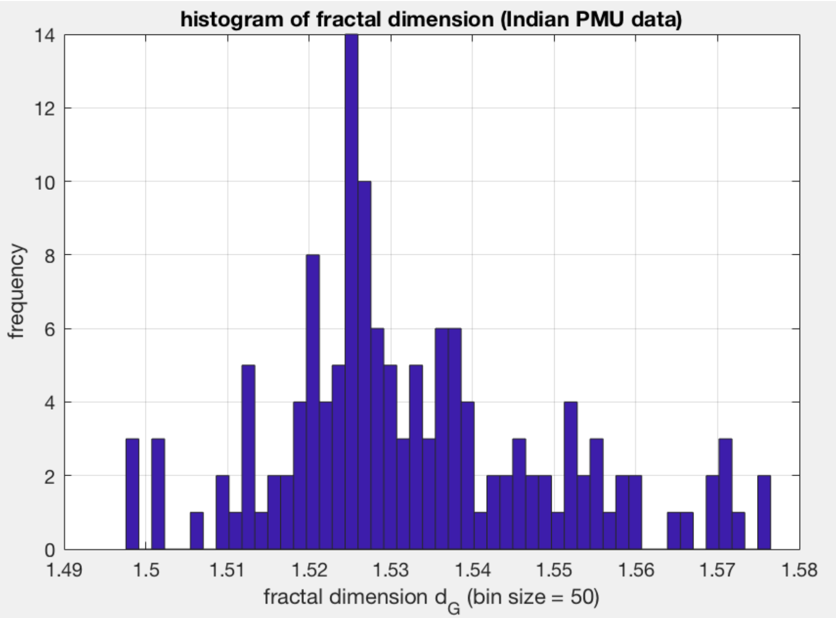

N	20000
size(alpha)	140
mean(d)	1.532877
std(d)	0.017066

Texas (Station 1) PMU Time Series Data

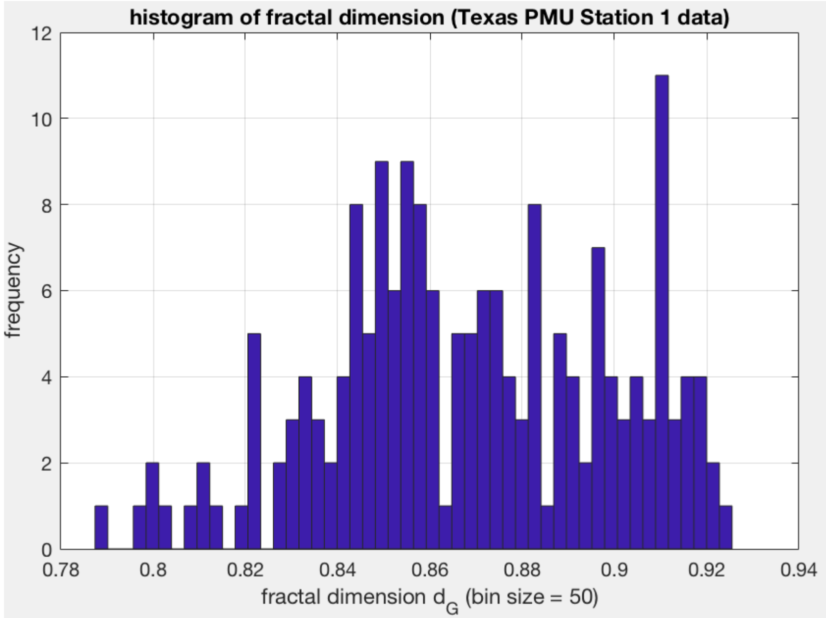

N	10000
size(alpha)	180
mean(d)	0.868504
std(d)	0.030948

Texas (Station 1) PMU Time Series Data

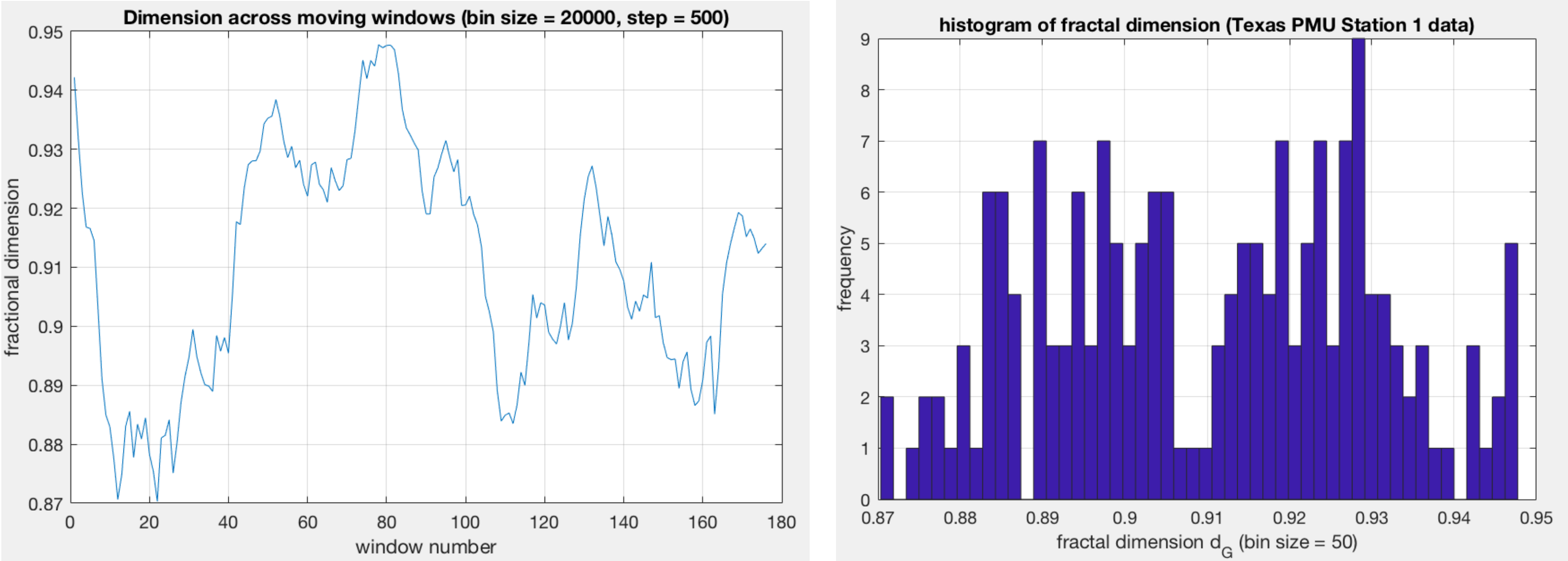

N	20000
size(alpha)	176
mean(d)	0.910081
std(d)	0.019405

Kolmogorov-Smirnov Test (Two-Sampled)

- tries to determine if two datasets differ significantly
- has the advantage of making no assumption about the distribution of data.

$$D_{n,m} = \sup_x |F_{1,n}(x) - F_{1,m}(x)|$$

where: $F_{1,n}$, $F_{2,m}$ - empirical distributions
with n and m sizes for the
and second samples, respectively

Null hypothesis is rejected at level α

$$D_{n,m} > c(\alpha)\sqrt{\frac{(n+m)}{nm}}$$

$$c(\alpha) = \sqrt{-\frac{1}{2}\ln\left(\frac{\alpha}{2}\right)}$$

- The K-S test was performed on the simulated swing equation data (with Gaussian noise (sigma = 0.01) vs. the PMU data (for both Indian blackout and Texas station 1)
- Both tests **reject** the null hypothesis (that the two sample sets are from the same distribution) at the 5% significance level

Part I: Summary

Ergodic Theory

Krylov-Bogoliubov

Empirical

Single Exponent

↓

DFA

ARIMA

$$\left(1-\sum_{i=1}^{p}\phi_i B^i\right)(1-B)^d X_t = \left(1+\sum_{i=1}^{q}\theta_i B^i\right)\varepsilon_t$$

ARFIMA

Berg Model

$$I_L(t) = A D_*^{\alpha} V_L(t) - B D_*^{\beta} V_L(t)$$

Mathematics

Grünwald-Letnikov ↔ Riemann-Liouville

$$\mathbb{D}^d = \lim_{|B|\to 0} \frac{(I-|B|)^d}{|B|^d}$$

$$\begin{aligned} D^{\alpha} f(x) &= D^m J^{m-\alpha} f(x) \\ &= D^m \left(\frac{1}{\Gamma(m-\alpha)} \int_0^t (t-\tau)^{m-\alpha-1} f(\tau)\, d\tau\right) \end{aligned}$$

Plan of Action

Part 1B – General Introduction to Fractality

- Mono versus multi-fractal analysis
- Multi-fractal space-time modeling

Fractals

- Fractal: *infinite*, *iterated*, *self-similar* mathematical constructs
- Geometric fractals
  - Self-similarity implies that a motif is (almost) preserved at all scales
- Non-smooth, more complex:
  - In the sense of space-filling capacity
  - Characterized by *fractal dimension*
  - Measure of complexity

Andrei Nikolaevich Kolmogorov (1941-1965) – *Universal Laws of Turbulence*

Benoit B. Mandelbrot (1975) - *Theory of roughness* (3 pages of algebra that changed our understanding of Nature)

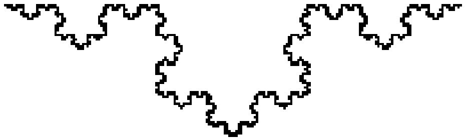

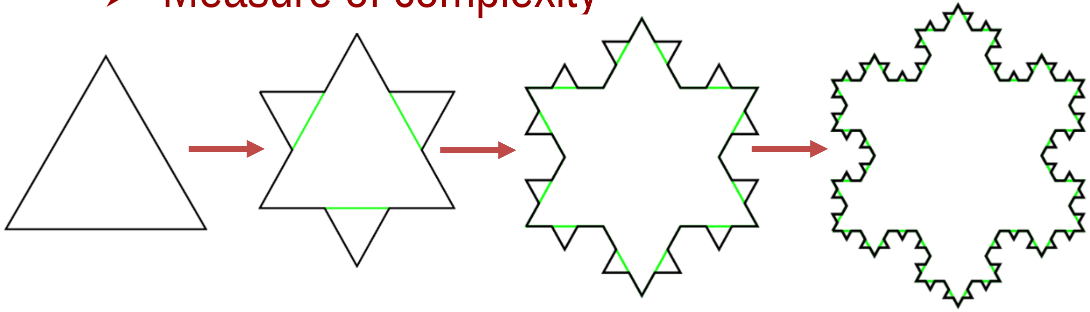

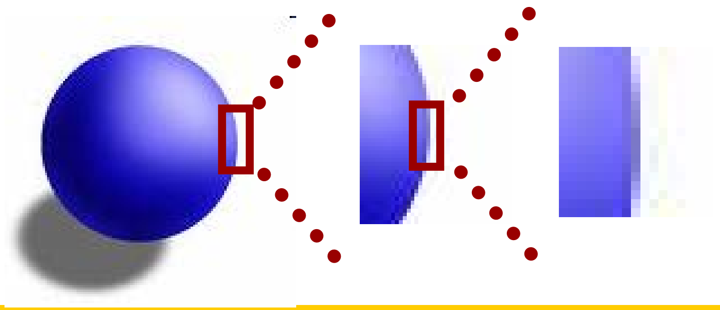

Fractal Dimension

$$fractal\ dimension = \frac{\log(number\ of\ self\text{-}similar\ pieces)}{\log(magnification\ factor)}$$

Full length segment

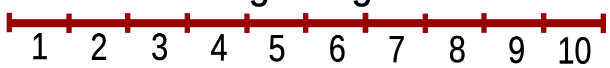

Self-similar unit

η = 1/10

$$f = \frac{\log(10)}{\log(1/\eta)} = 1$$

Cantor set

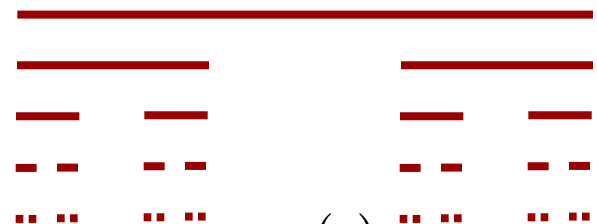

$$f = \frac{\log(2)}{\log(3)} = 0.6309$$

***f* = 2**

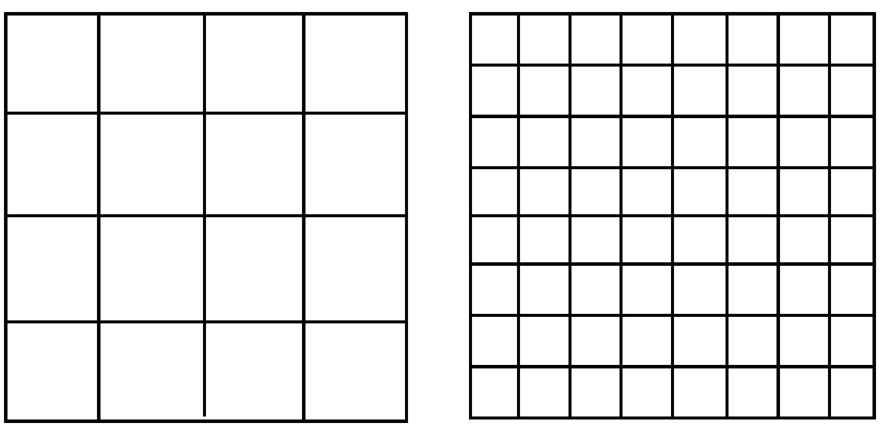

***f* = 1.81**

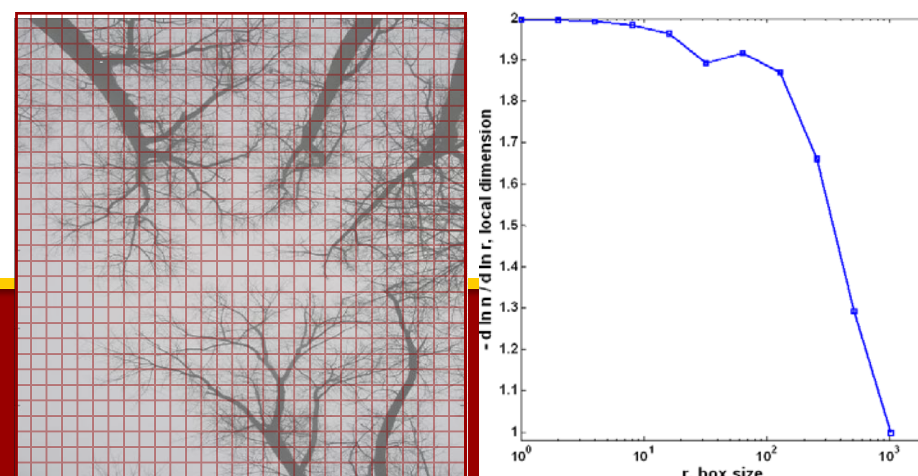

Mono-Fractal Analysis

- Box-counting method
  - Partition the data set with *minimal number* $N(r)$ of boxes of size r
  - *Fractal dimension* d is determined by

$$d = -\lim_{r\to 0} \frac{\log\left[N(r)\right]}{\log\left[r/R\right]}$$

  - Fractal: *power-law* scaling dependence

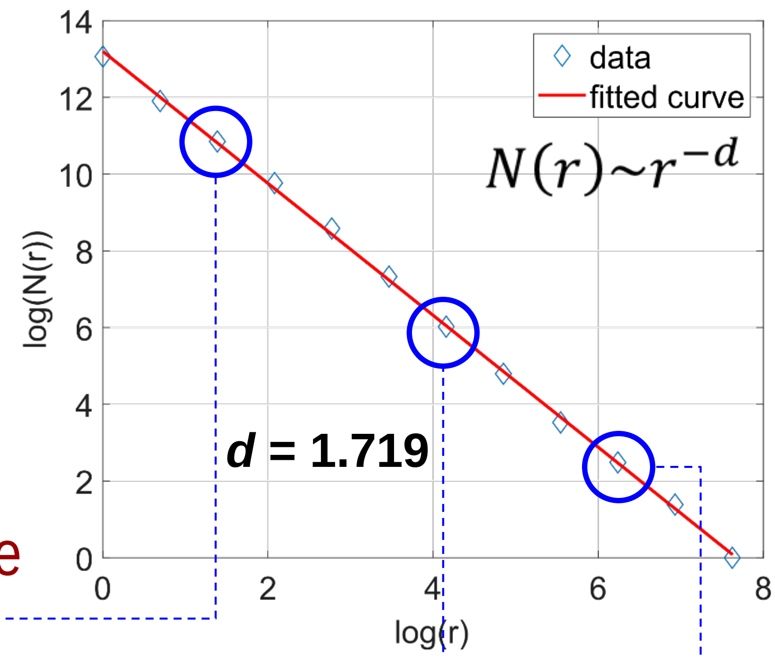

Multi-Fractal Analysis

- Investigate scaling behavior via *distortion factor q*
  - Partition by box $B(r)$ of size r
  - Assign a probability measure

$$p_i = \mu\left[B_i(r)\right]$$

  - Define a partition function

$$Z_q(r) = \sum_{i=1}^{n} p_i^q$$

- Generalized fractal dimension

$$D(q) = \lim_{r\to 0} \frac{1}{q-1} \frac{\log\left[Z_q(r)\right]}{\log\left[r/R\right]}$$

Multi-fractal scaling behavior

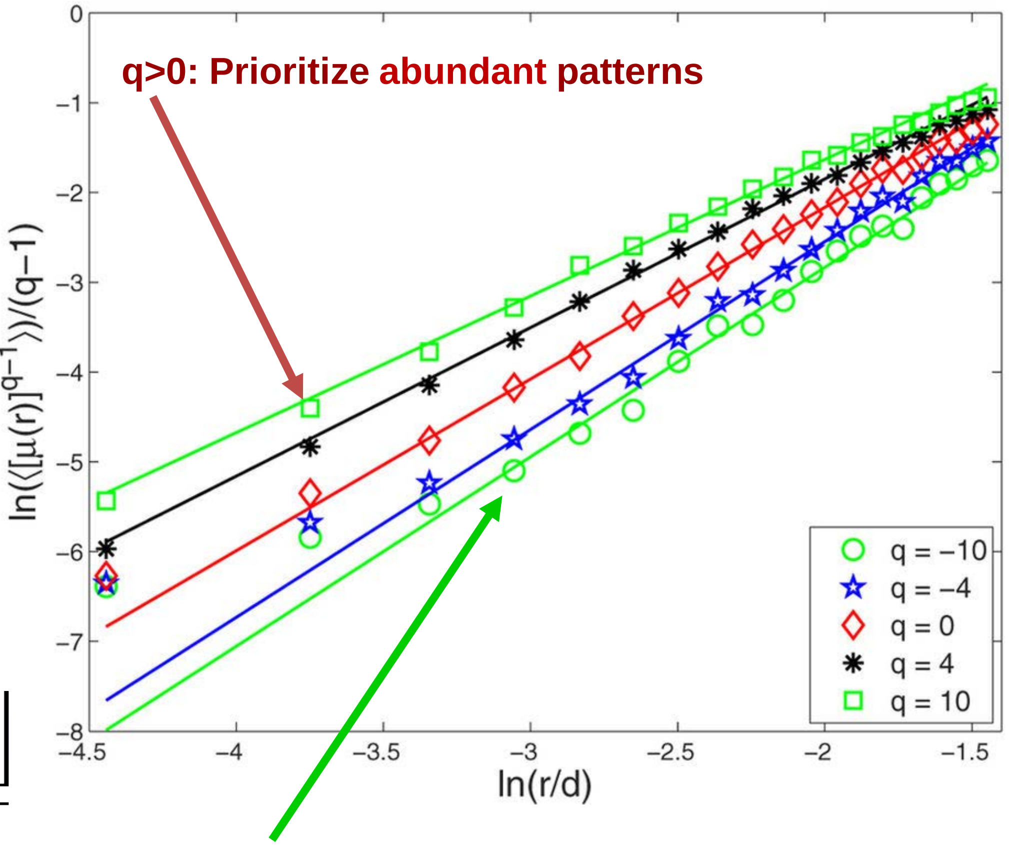

Mono-fractality vs. Multi-fractality

- The q-th order moment exhibits a time power law relationship with
  - A linear mass exponent function $\tau(q)$ with respect to q for a mono-fractal
  - A complex nonlinear mass exponent function $\tau(q)$ with respect to q for a multi-fractal

$$Z_q(t) = \sum_x x^q P(x,t) \approx g(q)\ t^{\tau(q)}$$

  - Applying the Legendre transform to the mass exponent $\tau(q)$

$$\tau(q) = \alpha(q) - h(\alpha), \quad \alpha = \frac{d\tau(q)}{dq}$$

  - Leads to a narrow delta-like function for mono-fractals
  - Leads to a wider bell-like shape function for multi-fractals

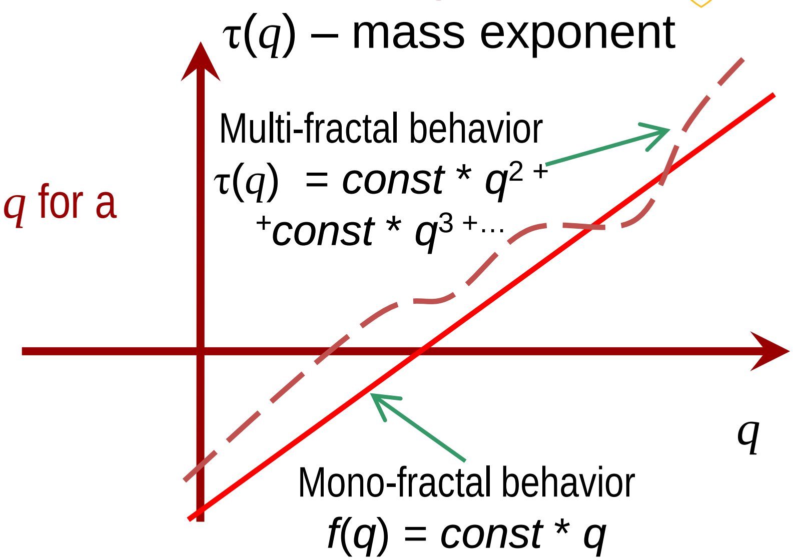

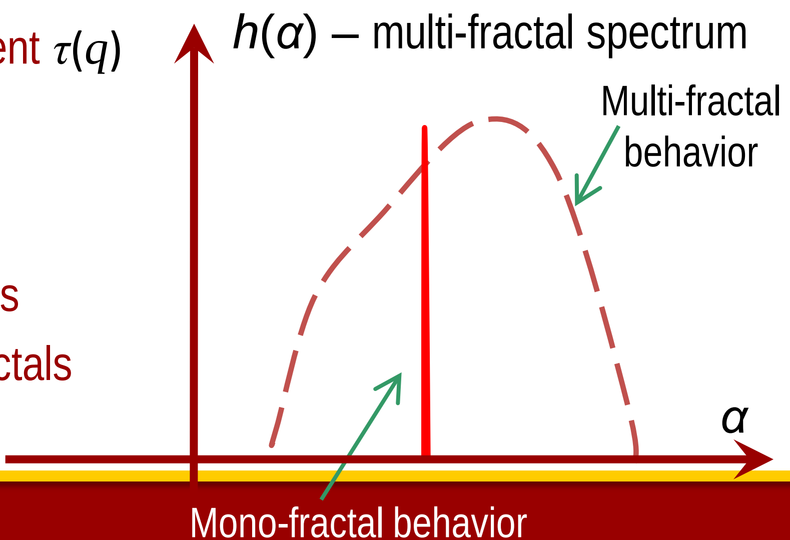

Part I: Summary

Multi-fractals ↔ Ergodic Theory

Krylov-Bogoliubov

Empirical

Single Exponent

DFA

ARIMA

ARFIMA

$$\left(1-\sum_{i=1}^{p}\phi_i B^i\right)(1-B)^d X_t = \left(1+\sum_{i=1}^{q}\theta_i B^i\right)\varepsilon_t$$

Bi-Exponent

Berg Model

$$I_L(t) = A D_*^{\alpha} V_L(t) - B D_*^{\beta} V_L(t)$$

Mathematics

Grünwald-Letnikov ↔ Riemann-Liouville

$$\mathbb{D}^d = \lim_{|B|\to 0} \frac{(I-|B|)^d}{|B|^d}$$

$$\begin{aligned} D^\alpha f(x) &= D^m J^{m-\alpha} f(x) \\ &= D^m \left(\frac{1}{\Gamma(m-\alpha)} \int_0^t (t-\tau)^{m-\alpha-1} f(\tau) d\tau \right) \end{aligned}$$

Plan of Action

Part 1B – General Introduction to Fractality

- Mono versus multi-fractal analysis
- Multi-fractal space-time modeling

Magnitude and Inter-Event Times

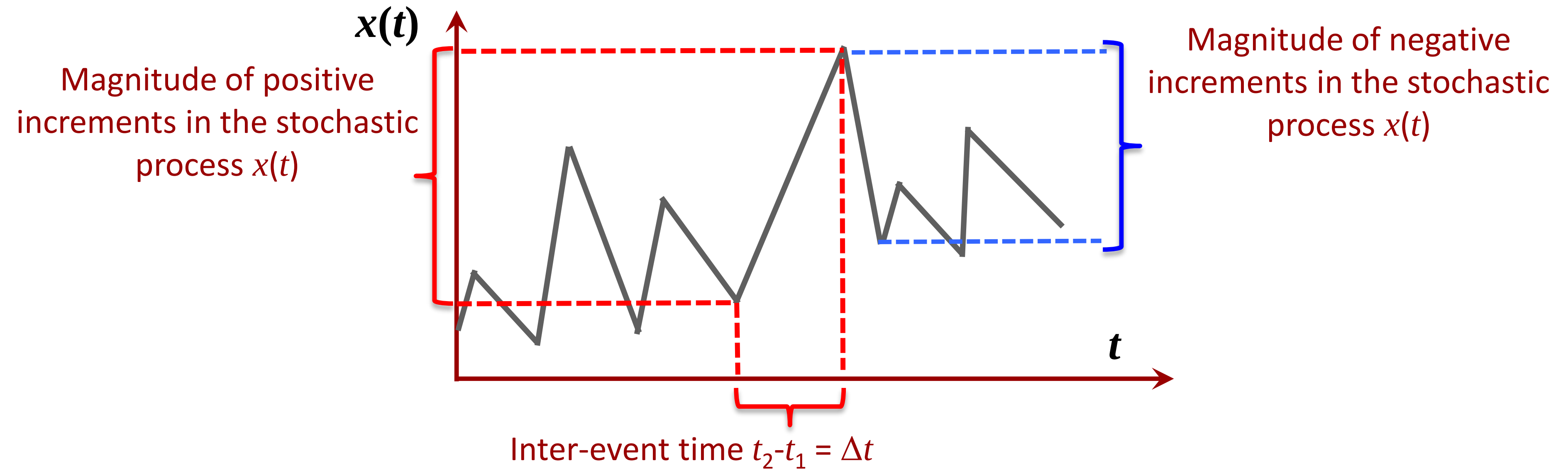

- Analysis of the magnitude of positive and negative increments in the stochastic process
  - dictates the degree of nonlinearity / confidence in linearity assumption
- Analysis of inter-event times distribution
  - dictates whether the stochastic process has short-range or long-range memory

Data-Driven Modeling – Learning From Data

- Statistical properties of increments determine the degree of linearity / nonlinearity
  - Exponentially distributed increments indicate an almost linear behavior
- Stochastic processes can display an asymmetric dynamics
  - Statistical properties of positive and negative magnitude increments can be different leading to a radically new dynamic equation

➢ Quantify probability $P(x,t|\alpha,\beta)$ of process $x(t)$ (workload)

  ➢ to attain value x at time t whose magnitude increments and inter-event times are characterized by fractal dimensions α and β

$$P(x,t|\alpha,\beta) = \underbrace{P(x_0,0)}_{\text{Initial condition}} + \int_0^t d\tau \int_{-\infty}^{x} \underbrace{w_+(x-y,t-\tau)}_{\text{Coupling between negative increments and their inter-event times}} P(y,\tau|\alpha,\beta)\,dy + \int_0^t d\tau \int_x^{\infty} \underbrace{w_-(x-y,t-\tau)}_{\text{Coupling between positive increments and their inter-event times}} P(y,\tau|\alpha,\beta)\,dy$$

Initial condition

Coupling between **negative increments** and their inter-event times

Coupling between **positive increments** and their inter-event times

Multi-Fractal Space-Time Modeling
(MFST)

- Employing fractional calculus concepts
  - Riemann-Liouville fractional order integral and derivative

$$\left.\begin{aligned} {}_0I_t^{\beta} P(x,t) &= \frac{1}{\Gamma(\beta)} \int_0^t (t-\tau)^{\beta-1} P(x,\tau)\, d\tau \\ {}_0D_t^{\alpha} \circ {}_0I_t^{\alpha} P(x,t) &= P(x,t) \end{aligned}\right\} \quad P(x,t\,|\,\alpha,\beta) = {}_0I_t^{\beta}\left[\int_{-\infty}^{\infty} w(x-y) P(y,t\,|\,\alpha,\beta)\, dy\right]$$

- Allows to describe the evolution of the probability $P(x,t)$ via a multi-fractional space-time Fokker-Planck equation:

$$\int_{\beta_{\min}}^{\beta_{\max}} h(\beta) \frac{\partial^{\beta} P(x,t)}{\partial t^{\beta}} d\beta = \int_{\alpha_{\min}}^{\alpha_{\max}} g(\alpha) \left\{ c_{dr}^{+} \frac{\partial^{\alpha} P(x,t)}{\partial x^{\alpha}} + c_{dr}^{-} \frac{\partial^{\alpha} P(x,t)}{\partial (-x)^{\alpha}} + c_{diff}^{+} \frac{\partial^{2\alpha} P(x,t)}{\partial x^{2\alpha}} + c_{diff}^{-} \frac{\partial^{2\alpha} P(x,t)}{\partial (-x)^{2\alpha}} \right\} d\alpha$$

  - $h(\beta)$ – distribution of fractal exponents characterizing the inter-event times
  - $g(\alpha)$ – distribution of fractal exponents characterizing the magnitudes

Example: Bi-Exponent Case

- Multi-fractional space-time Fokker-Planck Equation:

$$\int_{\beta_{\min}}^{\beta_{\max}} h(\beta)\frac{\partial^{\beta}P(x,t)}{\partial t^{\beta}}d\beta=\int_{\alpha_{\min}}^{\alpha_{\max}} g(\alpha)\left\{c_{dr}^{+}\frac{\partial^{\alpha}P(x,t)}{\partial x^{\alpha}}+c_{dr}^{-}\frac{\partial^{\alpha}P(x,t)}{\partial(-x)^{\alpha}}+c_{diff}^{+}\frac{\partial^{2\alpha}P(x,t)}{\partial x^{2\alpha}}+c_{diff}^{-}\frac{\partial^{2\alpha}P(x,t)}{\partial(-x)^{2\alpha}}\right\}d\alpha$$

- Bi-exponent form: $h(\beta) = A\delta(\beta-\beta_0) + B\delta(\beta-\beta_0)$

$$\int_{\beta_{min}}^{\beta_{max}} h(\beta)\frac{\partial^{\beta}P(x,t)}{\partial t^{\beta}}d\beta = A\frac{\partial^{\beta_0}P(x,t)}{\partial t^{\beta_0}} + B\frac{\partial^{\beta_1}P(x,t)}{\partial t^{\beta_1}}$$

- Berg Model:

$$I_L(t) = AD_*^{\alpha}V_L(t) - BD_*^{\beta}V_L(t)$$

Part I: Summary

Multi-fractals ⟷ Ergodic Theory

Krylov-Bogoliubov

Empirical

Single Exponent

DFA

ARIMA

ARFIMA

$$\left(1-\sum_{i=1}^{p}\phi_i B^i\right)(1-B)^d X_t = \left(1+\sum_{i=1}^{q}\theta_i B^i\right)\varepsilon_t$$

Bi-Exponent

Berg Model

$$I_L(t) = A D_*^{\alpha} V_L(t) - B D_*^{\beta} V_L(t)$$

Mathematics

Grünwald-Letnikov ⟷ Riemann-Liouville

$$\mathbb{D}^d = \lim_{|B|\to 0} \frac{(I-|B|)^d}{|B|^d}$$

$$\begin{aligned} D^{\alpha} f(x) &= D^m J^{m-\alpha} f(x) \\ &= D^m \left(\frac{1}{\Gamma(m-\alpha)} \int_0^t (t-\tau)^{m-\alpha-1} f(\tau) d\tau\right) \end{aligned}$$

Part I: Summary

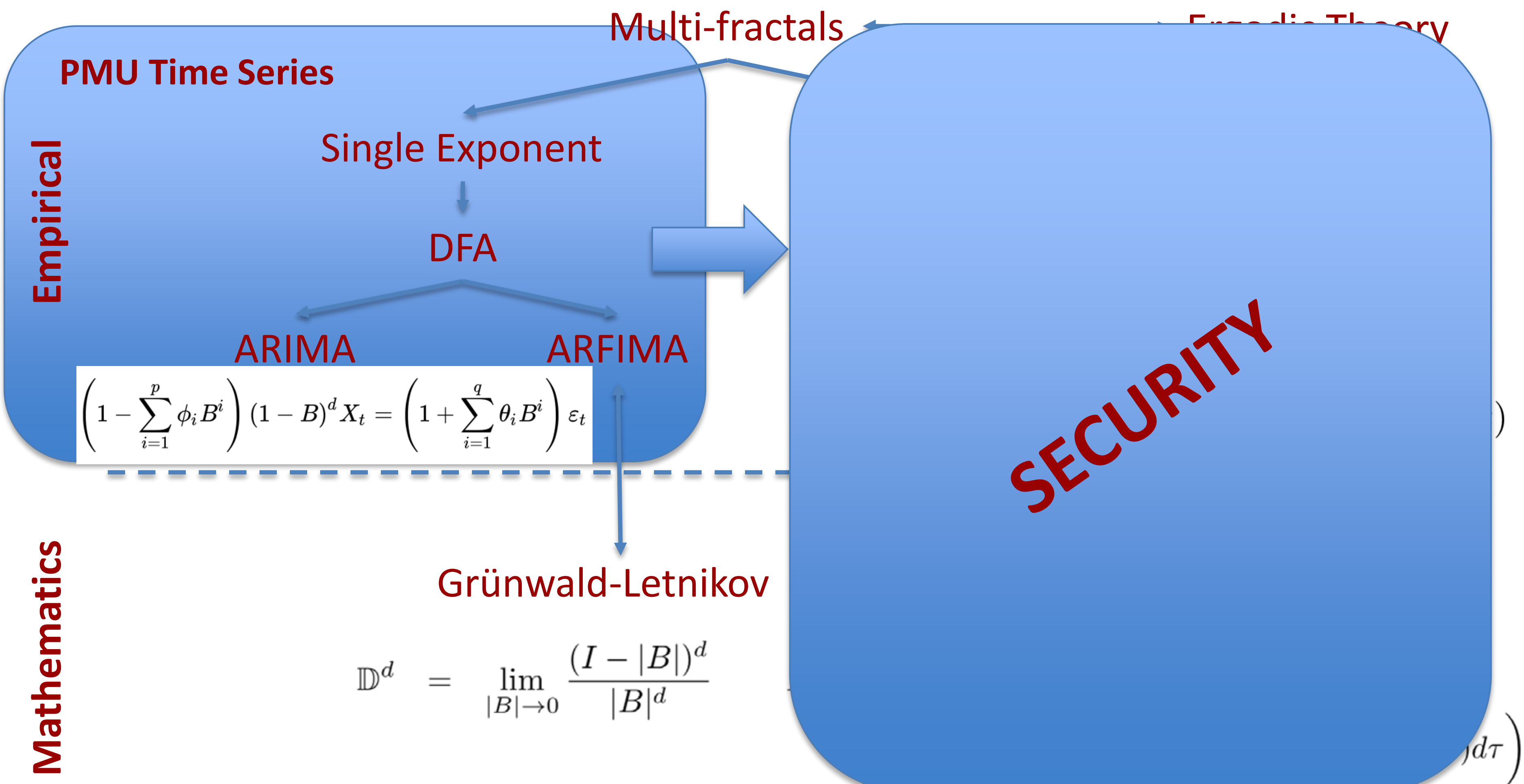

Voltage Collapse

<u>Definition:</u>

Voltage collapse is critical phenomena that threatens the power infrastructure, and that manifests itself by a sudden and fast collapse of the system voltage.

<u>Source of problem:</u>

Traditionally, it is blamed on a supply-demand imbalance…

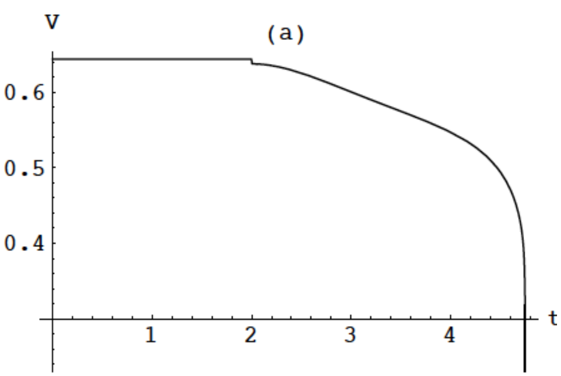

Voltage collapses

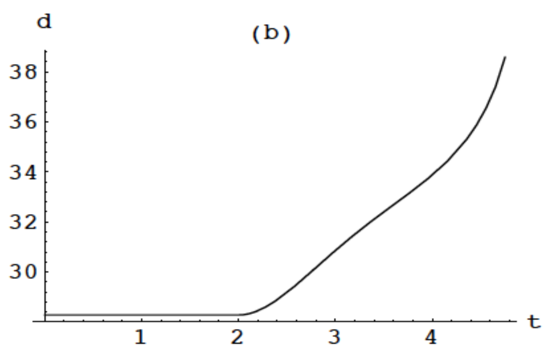

Damping increases

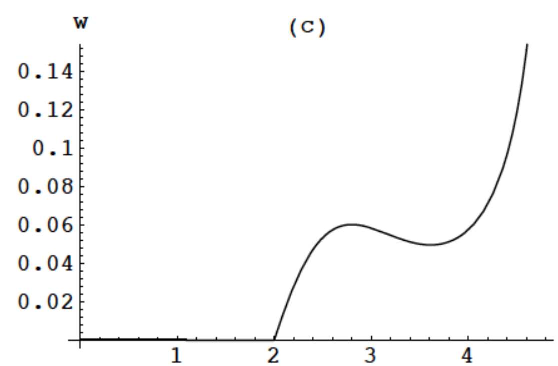

Frequency is disrupted!!!

The Frequency Dependence Debate

''The differences in time constants have led many researchers to only consider voltage dynamics for the analysis of bifurcations problems, ignoring frequency dynamics. However, the previous example clearly shows that this assumption is not completely justifiable''

Prof. Claudio Cañizares

''This model was motivated by voltage stability studies; frequency dependence of the load has not been considered''

Prof. David Hill

"Wehenkel stated that better modeling of loads and demand is also needed; specifically, better dynamic models that respond to voltage/frequency variations over shorter time periods (seconds and minutes) are needed for stability analysis"

Government Report

Plan of Action: Part II – Security

- Increase of Hurst exponent towards black-out
  - Kendall tau as statistical confirmation
- AR(1) versus Hurst exponent sample distribution for abnormality detection
- Falsification of swing equation by Hurst exponent
- Change Point Detection
  - Historic precedent: UDP flooding attack
  - Detection and simultaneous detection & identification
  - Threshold for False Alarm Rate
  - Indian blackout

Critical Transition in Harvested Population

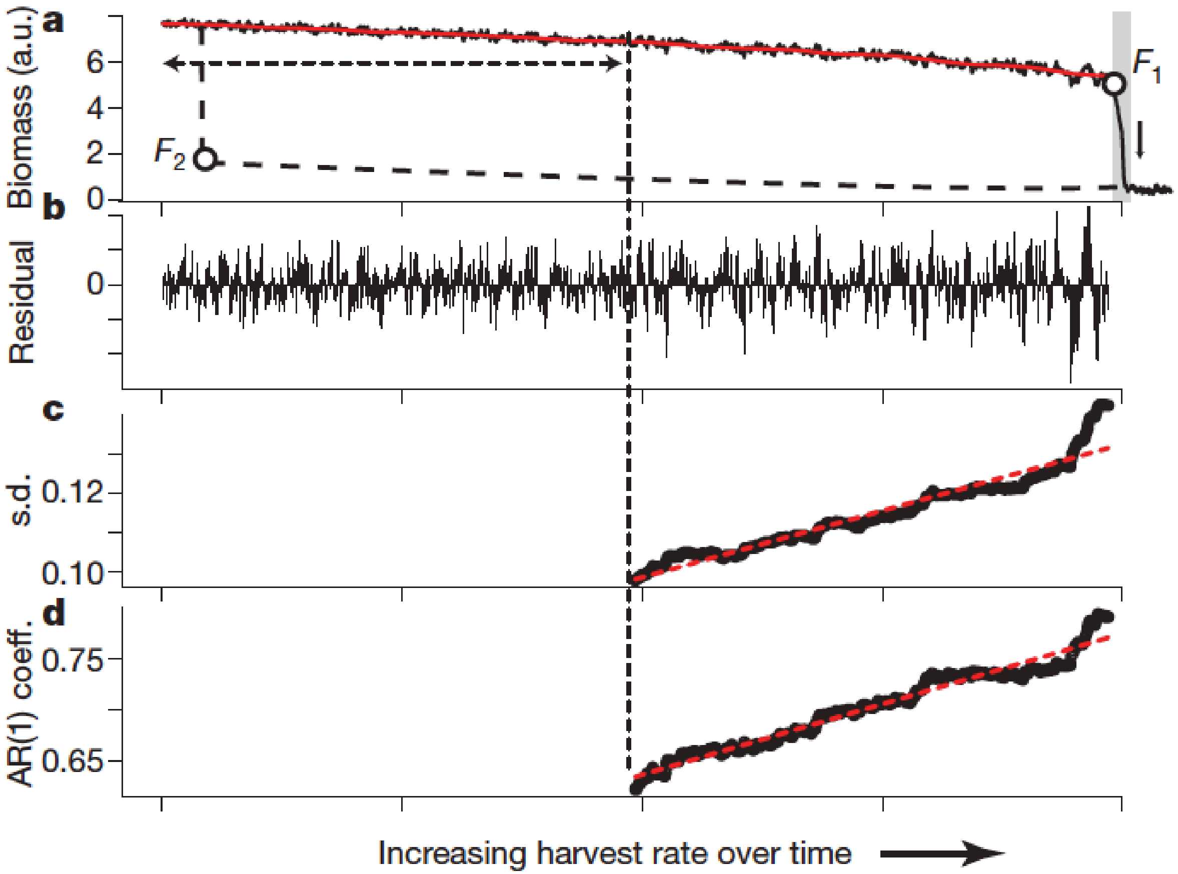

Early warning signals for a critical transition in a time series generated by a model of a harvested population driven slowly across a bifurcation

M. Scheffer, et.al, "Early- warning signals for critical transitions," Nature, vol. 461, pp. 53–59, 2009.

2012 Indian Blackout

➢ The blackout occurred on July 30, 2012 and affected more than 300 million people living in Northern India.

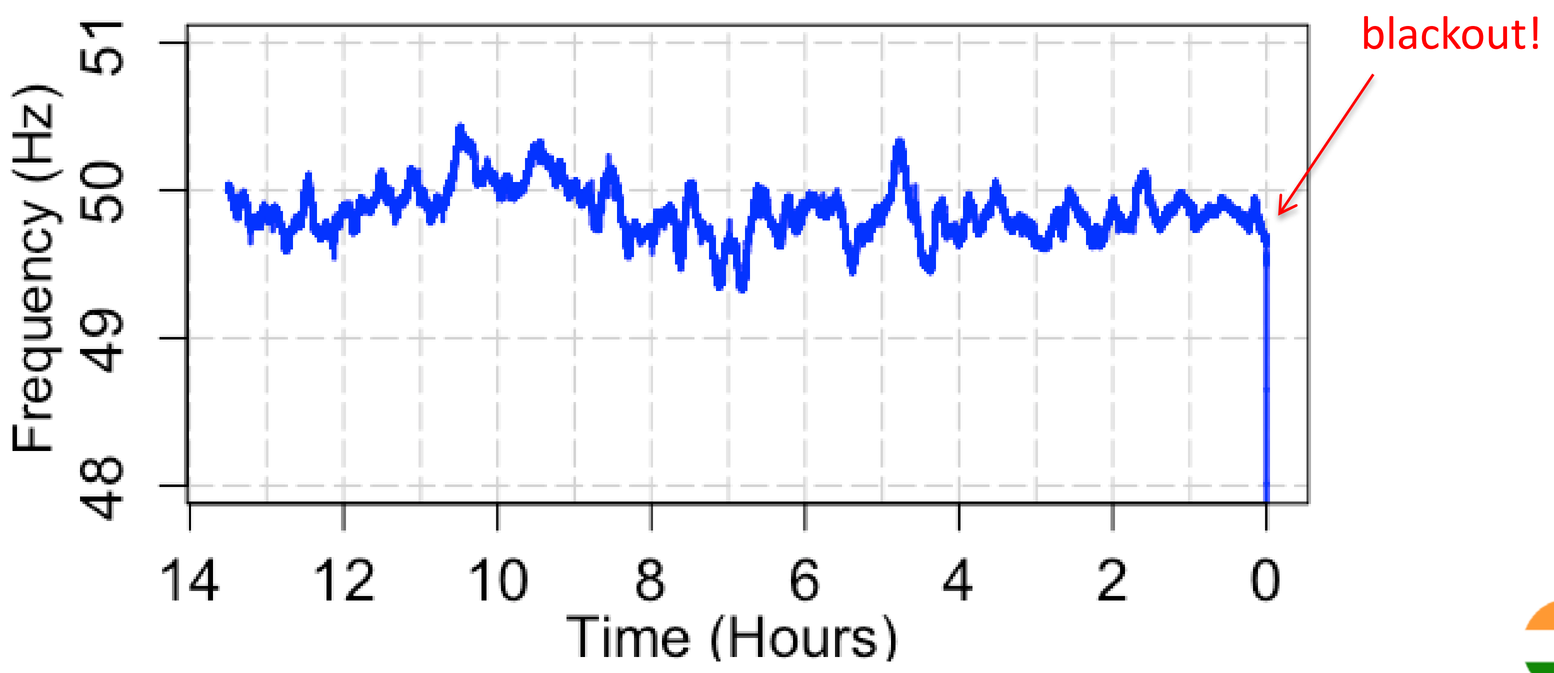

Increase in Autoregressive Coefficient before Blackout

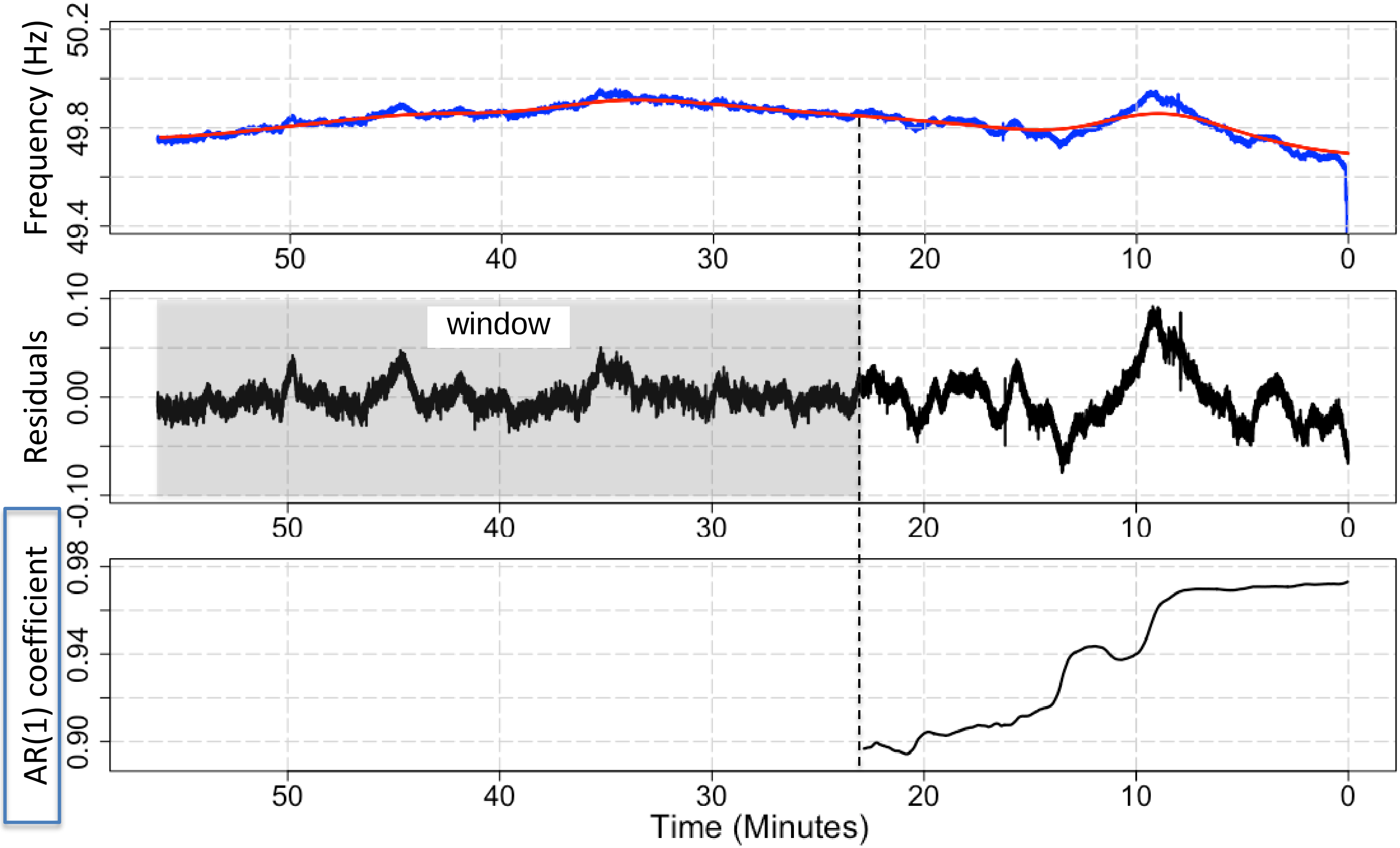

Increase in Hurst Exponent before Blackout

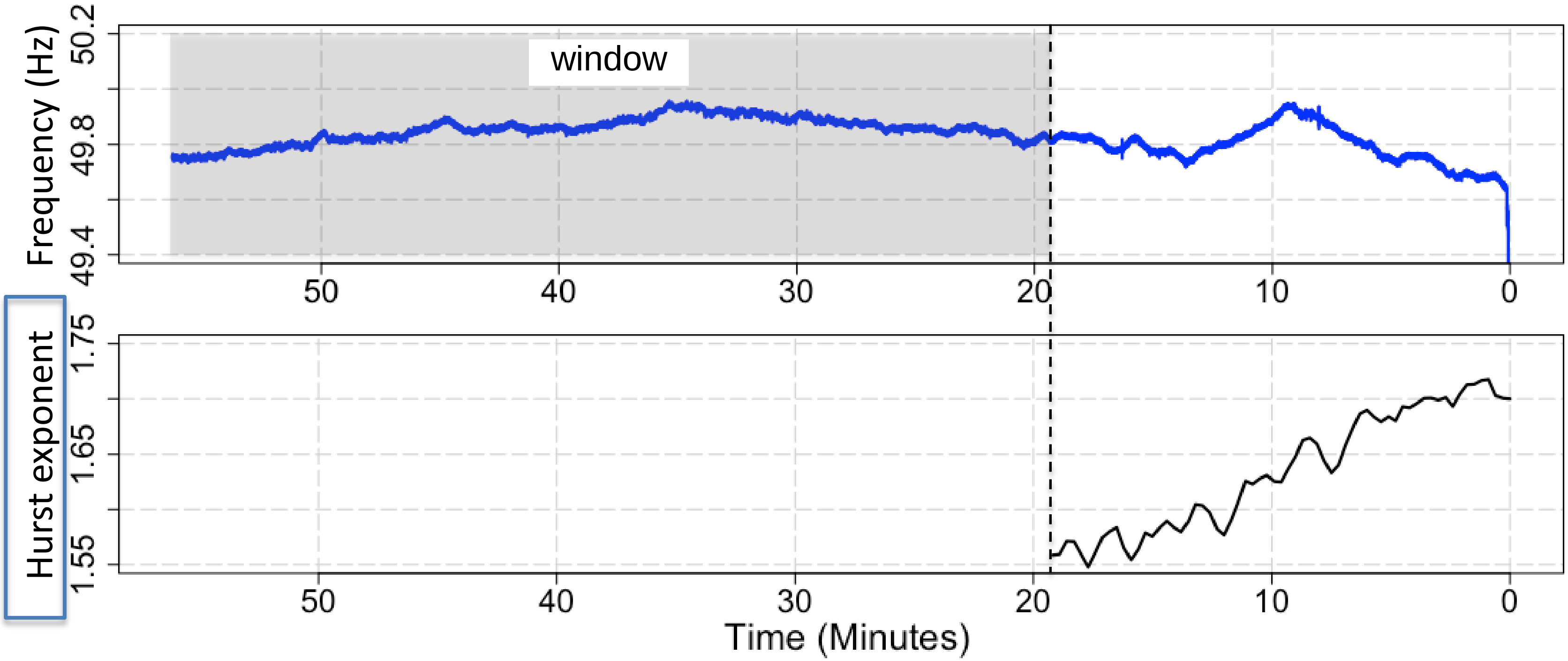

Kendall's tau

- Kendall's tau is a rank correlation coefficient that is used to measure—*in a statistically meaningful sense*—the ordinal association between two datasets, $\{(t_i,\alpha_i)\}$.
- Assuming that we have n pairs of x and y data
  - $((x_1,y_1); (x_2,y_2); \ldots; (x_n,y_n))$,
  - Kendall's tau is defined as

$$\tau = \frac{\text{\# of concordant pairs} - \text{\# of discordant pairs}}{n(n-1)/2}$$

- Concordant pair ➡ $x_i > x_j$ & $y_i > y_j$ or $x_i < x_j$ & $y_i < y_j$
- Discordant pair ➡ $x_i > x_j$ & $y_i < y_j$ or $x_i < x_j$ & $y_i > y_j$

Plan of Action: Part II – Security

- Increase of Hurst exponent towards black-out
  - Kendall tau as statistical confirmation
- AR(1) versus Hurst exponent sample distribution for abnormality detection
- Falsification of swing equation by Hurst exponent
- Change Point Detection
  - Historic precedent: UDP flooding attack
  - Detection and simultaneous detection & identification
  - Threshold for False Alarm Rate
  - Indian blackout

Kendall's Tau of AR(1) Coefficient versus Hurst Exponent

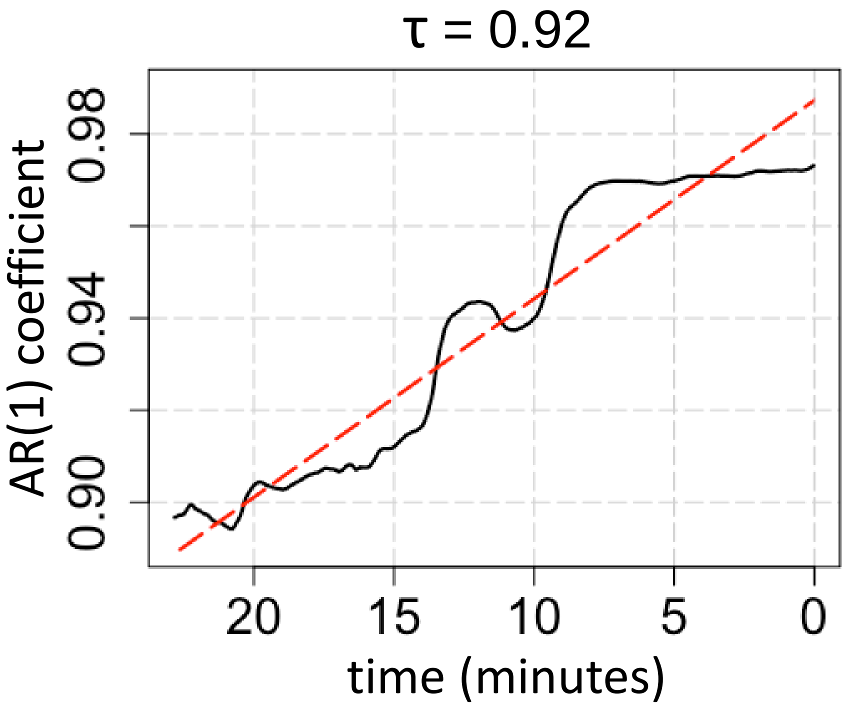

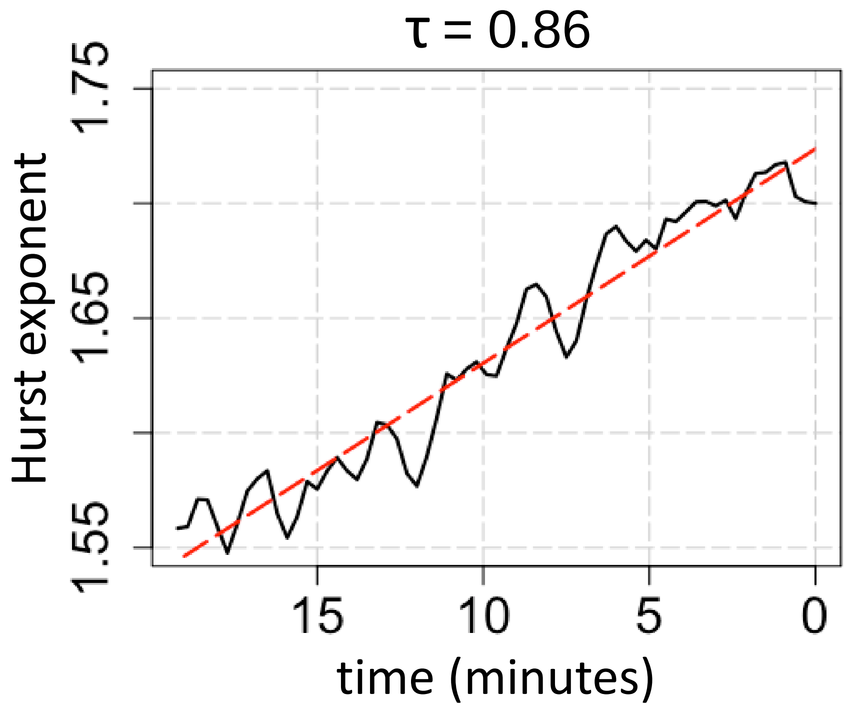

Laith Shalalfe, Paul Bogdan and Edmond Jonckheere, Kendall's Tau of Frequency Hurst Exponent as Blackout Proximity Margin, IEEE International Conference on Smart Grid Communications (SmartGridComm), 2016.

AR(1) versus Hurst Exponent Sample Distributions

Normal frequency data   Frequency data before blackout

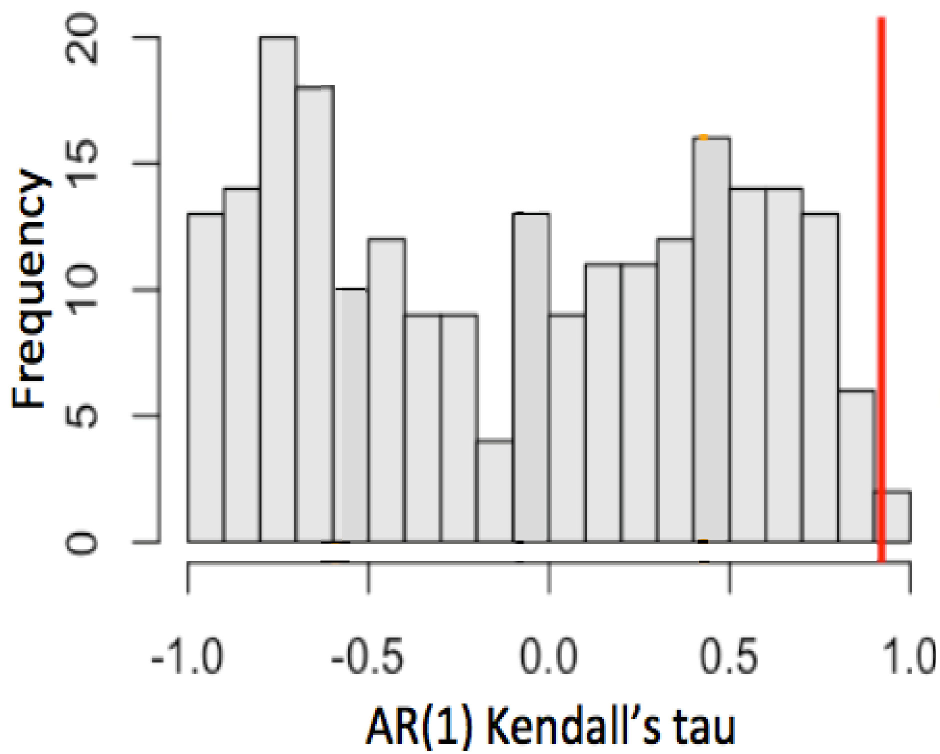

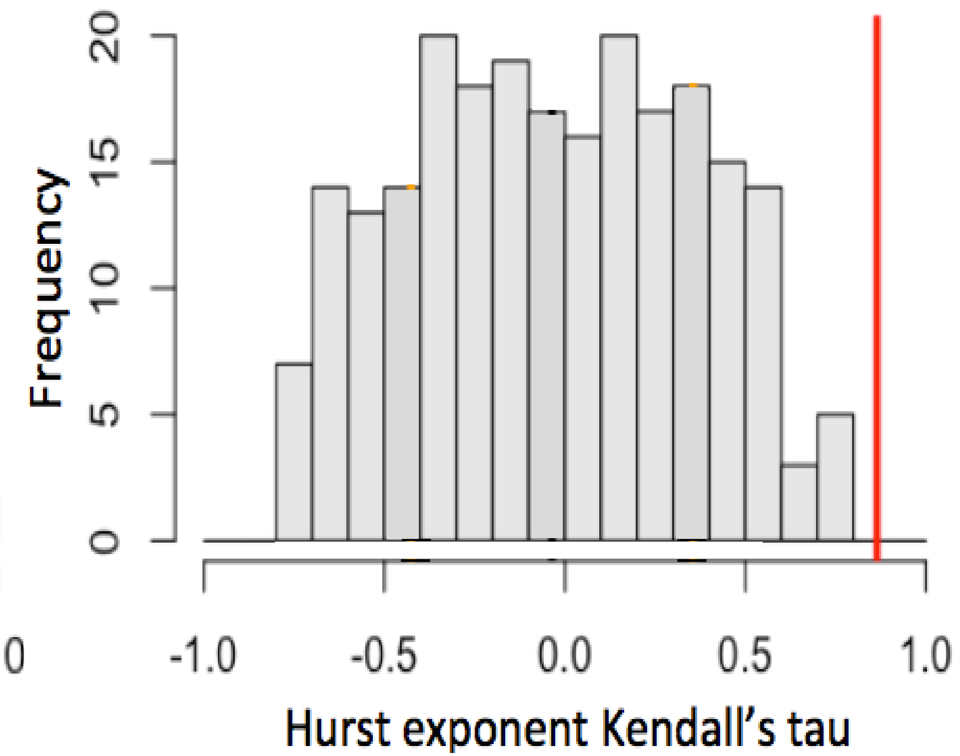

Early Observation

➢ Early investigation with more blackout data points (San Diego blackout) indicates that the empirical distributions of the normal and blackout Hurst frequency data *are random draws from different distributions.*

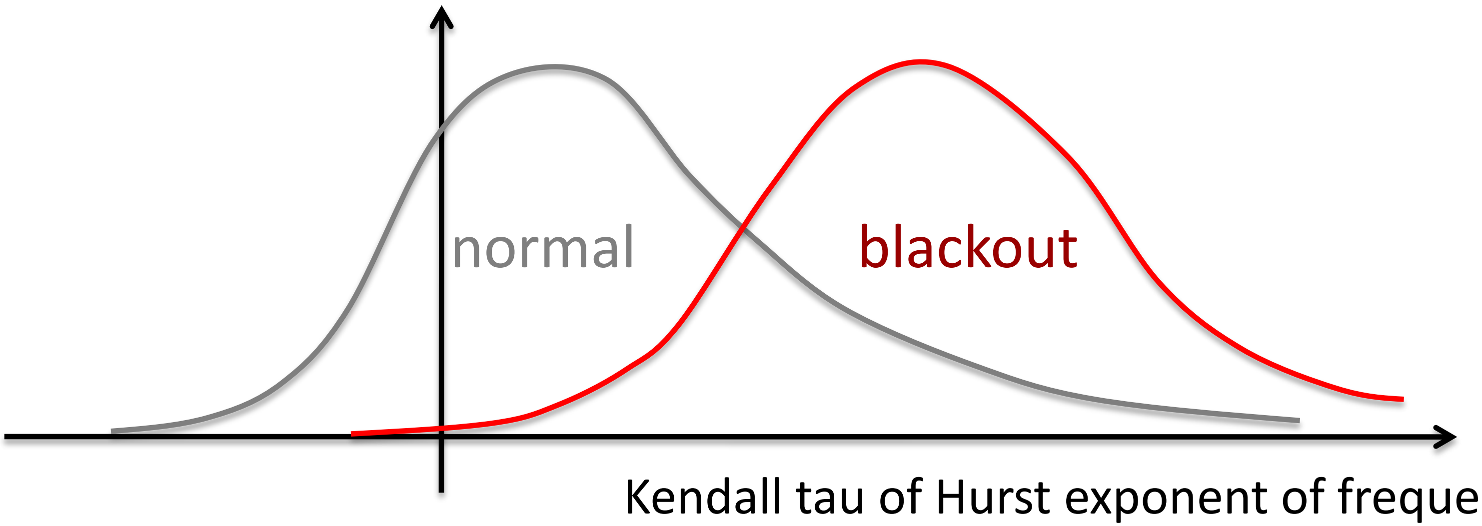

Plan of Action: Part II – Security

- Increase of Hurst exponent towards black-out
  - Kendall tau as statistical confirmation
- AR(1) versus Hurst exponent sample distribution for abnormality detection
- Falsification of swing equation by Hurst exponent
- Change Point Detection
  - Historic precedent: UDP flooding attack
  - Detection and simultaneous detection & identification
  - Threshold for False Alarm Rate
  - Indian blackout

Hurst Exponent Analysis of the Swing Equation

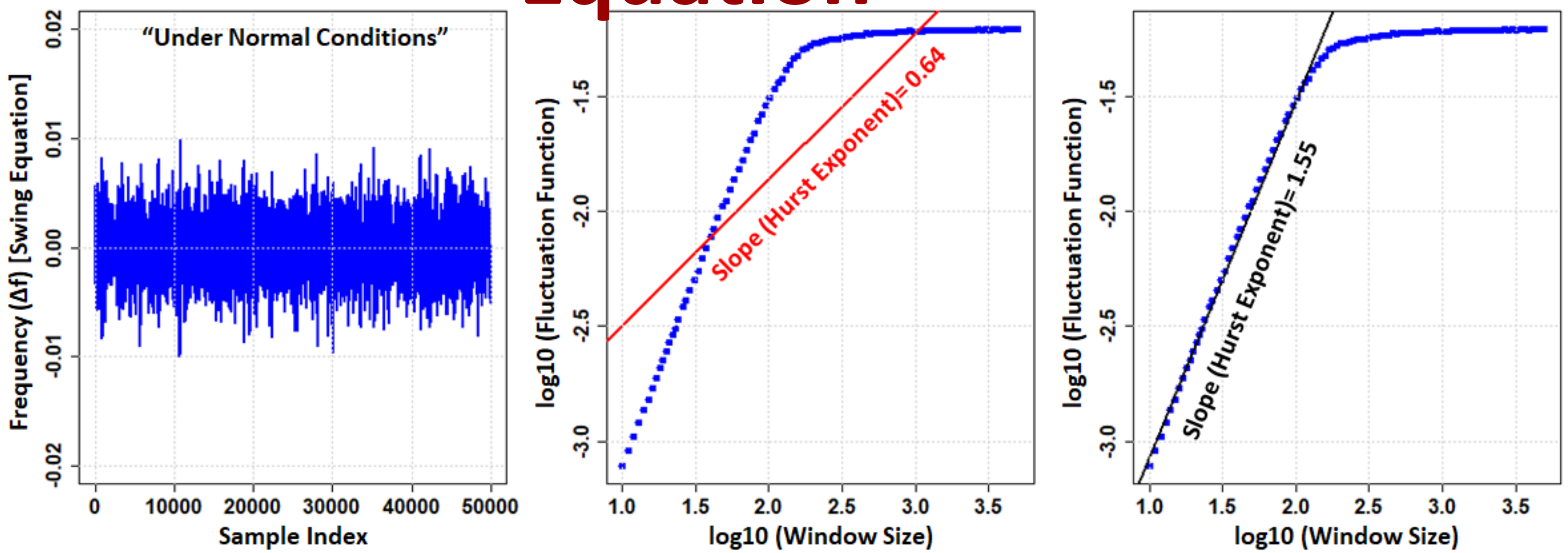

Note that the Hurst exponent of the frequency (under normal conditions) is around 1.55. This Hurst exponent is higher than the previous analysis because we considered the slope of the linear region only to calculate the Hurst exponent, as shown in the middle picture.

Discrepancy

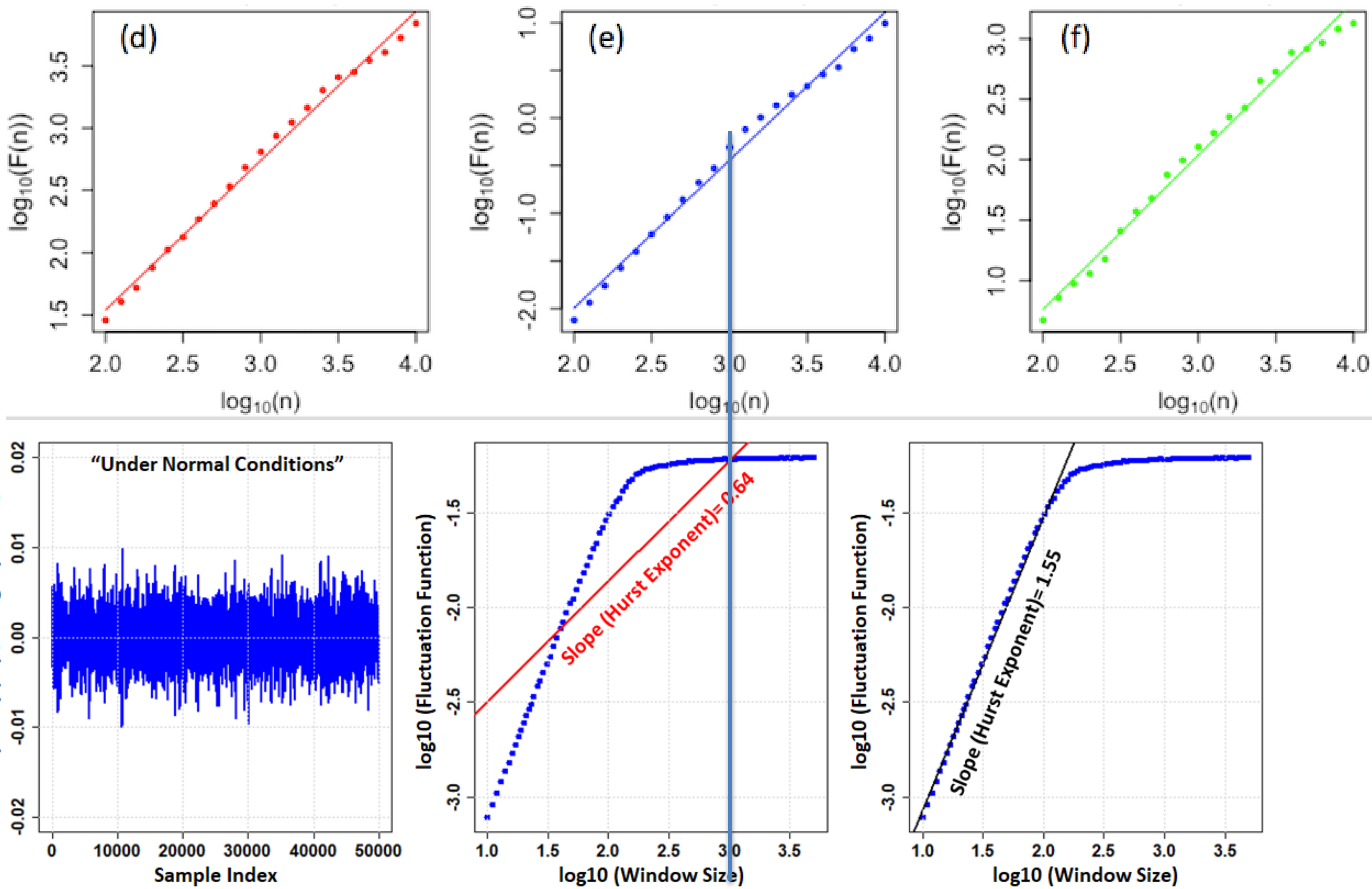

Hurst Exponent Analysis of the Swing Equation

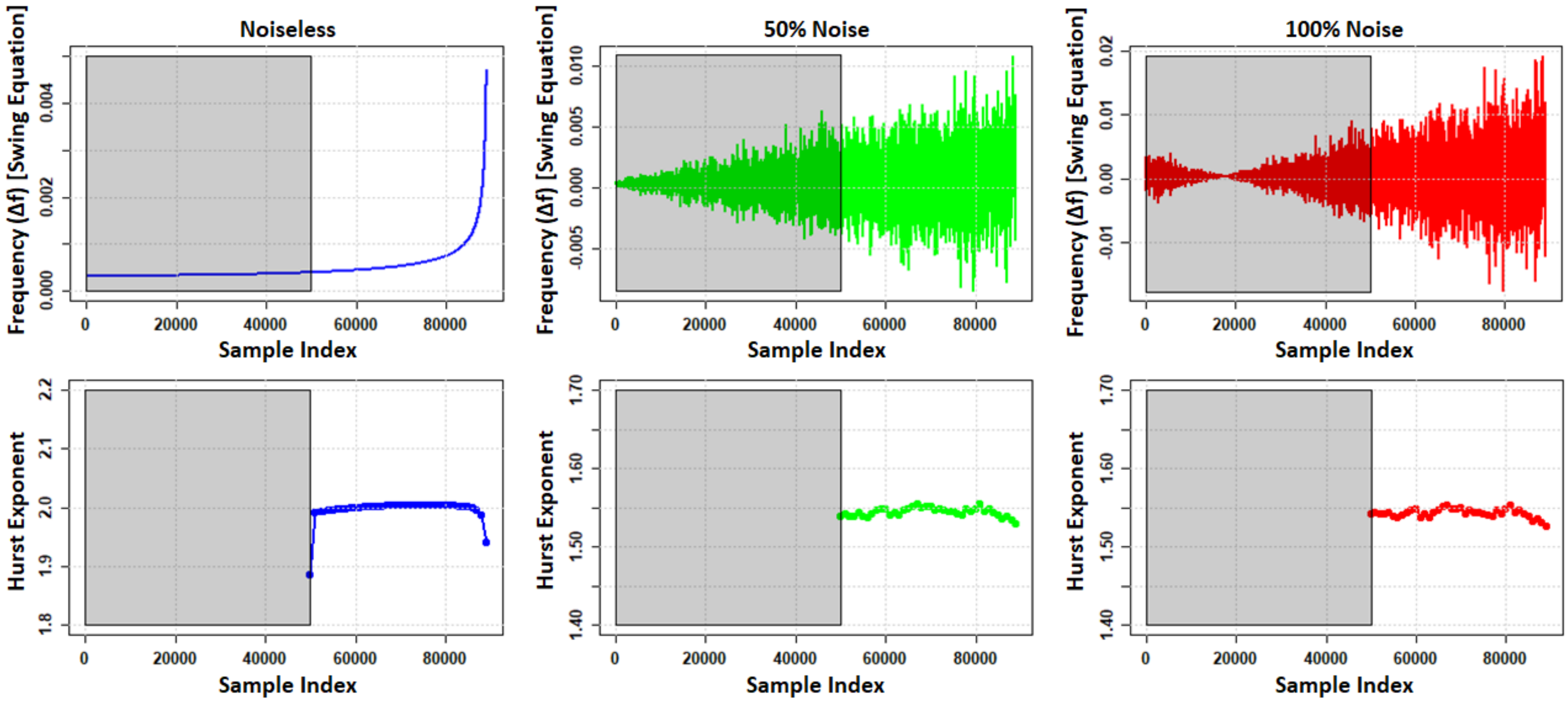

- Hurst exponent of the frequency remains almost constant near the bifurcation.
- The Hurst exponent is equal to 2 for the noiseless frequency and approximately 1.55 for the frequency time series with 50% and 100% noise in the middle image.
- These results show that driving the swing equation to the unstable region by increasing Pm does not reproduce the increasing trend in Hurst exponent as in the 2012 Indian blackout.

Hurst Exponent Analysis of the Swing Equation

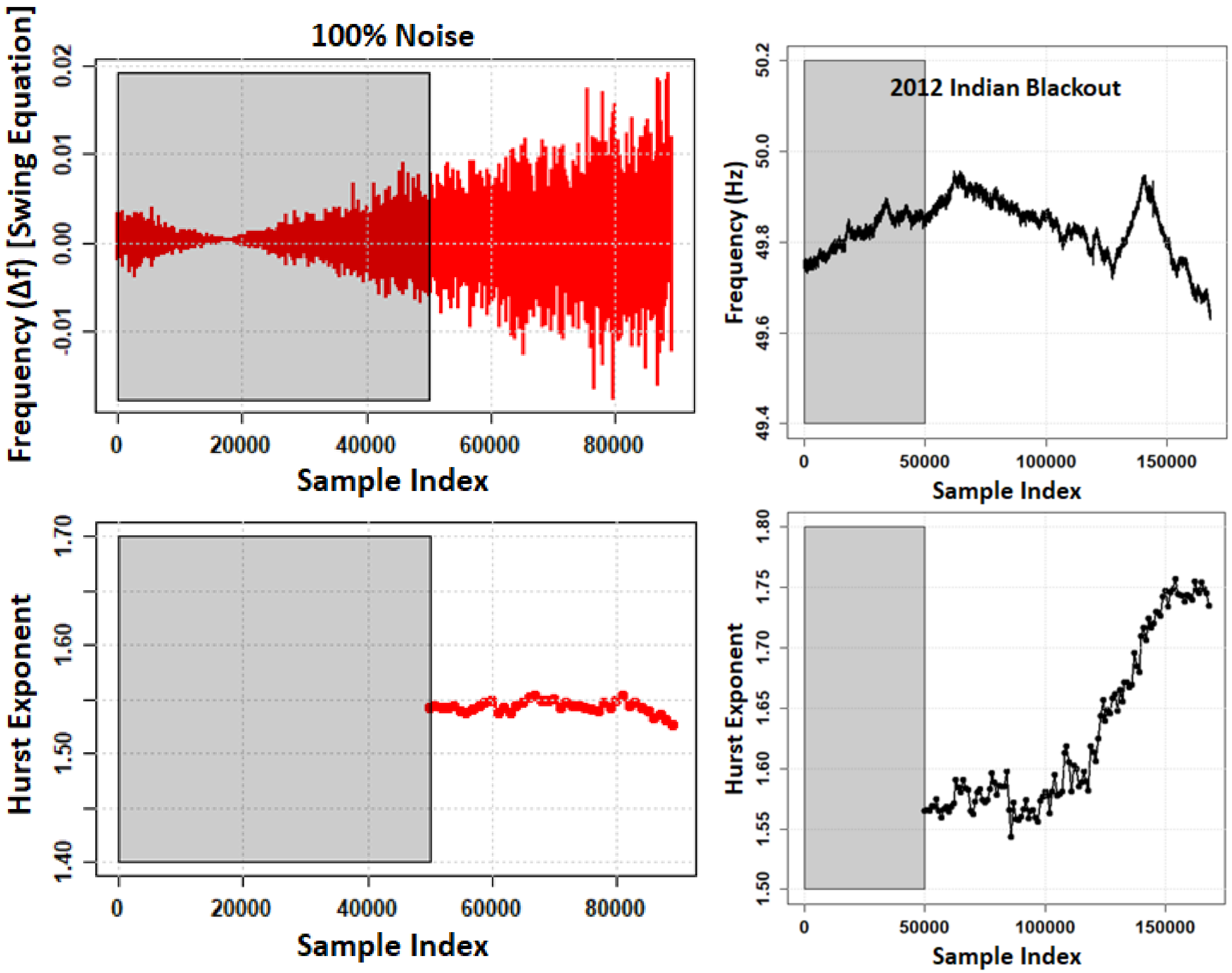

- These results show that driving the swing equation to the unstable region by increasing Pm does not reproduce the increasing trend in Hurst exponent as in the 2012 Indian blackout
- The swing equation with added noise does not show an increase in the Hurst exponent like the one in the Indian blackout.

Plan of Action: Part II – Security

- Increase of Hurst exponent towards black-out
  - Kendall tau as statistical confirmation
- AR(1) versus Hurst exponent sample distribution for abnormality detection
- Falsification of swing equation by Hurst exponent
- Change Point Detection
  - Historic precedent: UDP flooding attack
  - Detection and simultaneous detection & identification
  - Threshold for False Alarm Rate
  - Indian blackout

Part II: Summary

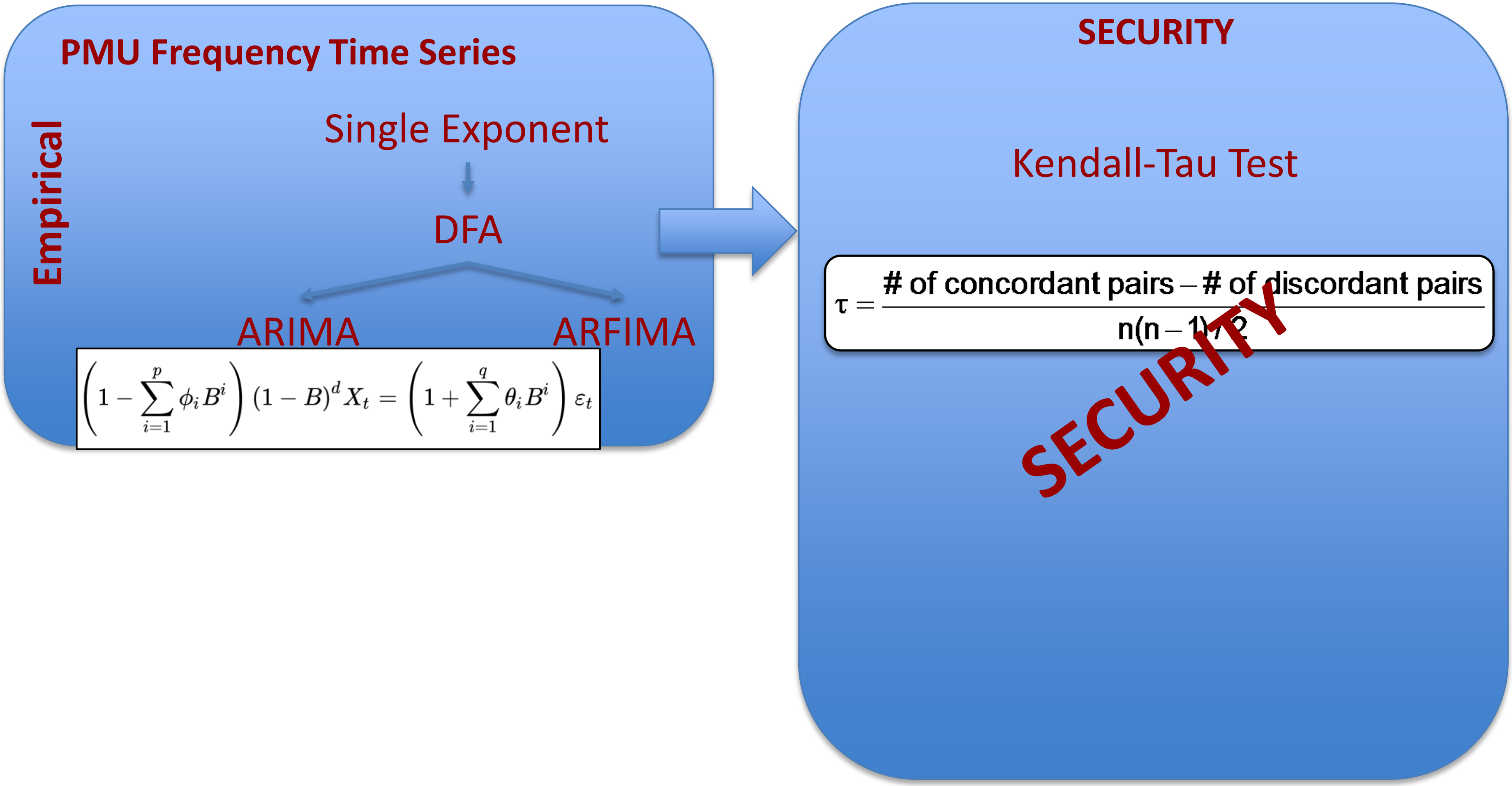

Plan of Action: Part II – Security

- Increase of Hurst exponent towards black-out
  - Kendall tau as statistical confirmation
- AR(1) versus Hurst exponent sample distribution for abnormality detection
- Falsification of swing equation by Hurst exponent
- Change Point Detection
  - Historic precedent: UDP flooding attack
  - Detection and simultaneous detection & identification
  - Threshold for False Alarm Rate
  - Indian blackout

Change Point Detection

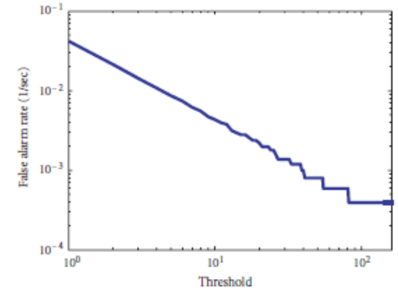

Given a time series (could be voltage, frequency)

$$y(1), y(2), y(3), \dots$$

How could we be warned that a statistically significant change has occurred, with reasonable false alarm rate???

Change point detection algorithm:

$$S_{k+1} = \max\{0, S_k + I_k - I\}, \quad S_0 = 0$$

where

- I is the nominal past/future mutual information
- I_k is the mutual information after processing $y(k)$

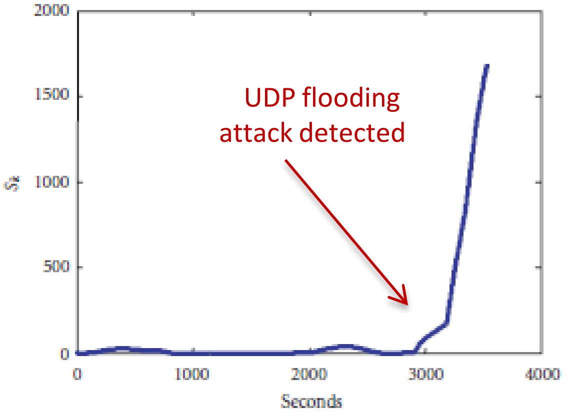

Figure 10: Time series of S_k, the cumsum of the mutual information. This data is from a backbone link. The steep increase at around the 10000th sample is due to a UDP flooding attack.

K. Shah, E. Jonckheere, and S. Bohacek, ``Dynamic Modeling of Internet Traffic for Intrusion Detection,'' EURASIP Journal on Advances in Signal Processing, The European Association for Signal, Speech and Image Processing, volume 2007, Article ID 90312, 14 pages, 2007.

Mutual Information (MI) Bound

Past at lag L: $y_-(k) = \begin{pmatrix} y(k) \\ \vdots \\ y(k-L+1) \end{pmatrix}$ Future at lag L: $y_+(k) = \begin{pmatrix} y(k+1) \\ \vdots \\ y(k+L) \end{pmatrix}$

Cholesky factorizations:

$$\mathcal{E}(y_-(k)y_-^T(k)) = L_- L_-^T \qquad \mathcal{E}(y_+(k)y_+^T(k)) = L_+ L_+^T$$

Canonical correlation:

$$\Gamma(y_-, y_+) = L_-^{-1}\mathcal{E}(y_-(k)y_+^T(k))L_+^{-T}$$

Mutual information bound:

$$I_k \geq -\frac{1}{2}\log\det\left(I - \Gamma(y_-, y_+)\Gamma^T(y_-, y_+)\right)$$

K. Shah, E. Jonckheere, and S. Bohacek, ``Dynamic Modeling of Internet Traffic for Intrusion Detection,'' EURASIP Journal on Advances in Signal Processing, The European Association for Signal, Speech and Image Processing, volume 2007, Article ID 90312, 14 pages, 2007.

Mutual information Improved Bound

Past at lag L: $y_-(k) = \begin{pmatrix} y(k) \\ \vdots \\ y(k-L+1) \end{pmatrix}$ Future at lag L: $y_+(k) = \begin{pmatrix} y(k+1) \\ \vdots \\ y(k+L) \end{pmatrix}$

Cholesky factorizations:

$$\mathcal{E}(y_-(k) y_-^T(k)) = L_- L_-^T \qquad \mathcal{E}(y_+(k) y_+^T(k)) = L_+ L_+^T$$

Canonical correlation:

$$\Gamma(y_-, y_+) = L_-^{-1} \mathcal{E}(y_-(k) y_+^T(k)) L_+^{-T}$$

Mutual information bound:

$$I_k \geq \sup_{f,g} \left(-\frac{1}{2} \log\det\big(I - \Gamma(f(y_-), g(y_+))\Gamma^T(f(y_-), g(y_+))\big) \right)$$

K. Shah, E. Jonckheere, and S. Bohacek, ``Dynamic Modeling of Internet Traffic for Intrusion Detection,'' EURASIP Journal on Advances in Signal Processing, The European Association for Signal, Speech and Image Processing, volume 2007, Article ID 90312, 14 pages, 2007.

Change Point Detection (MI) Results

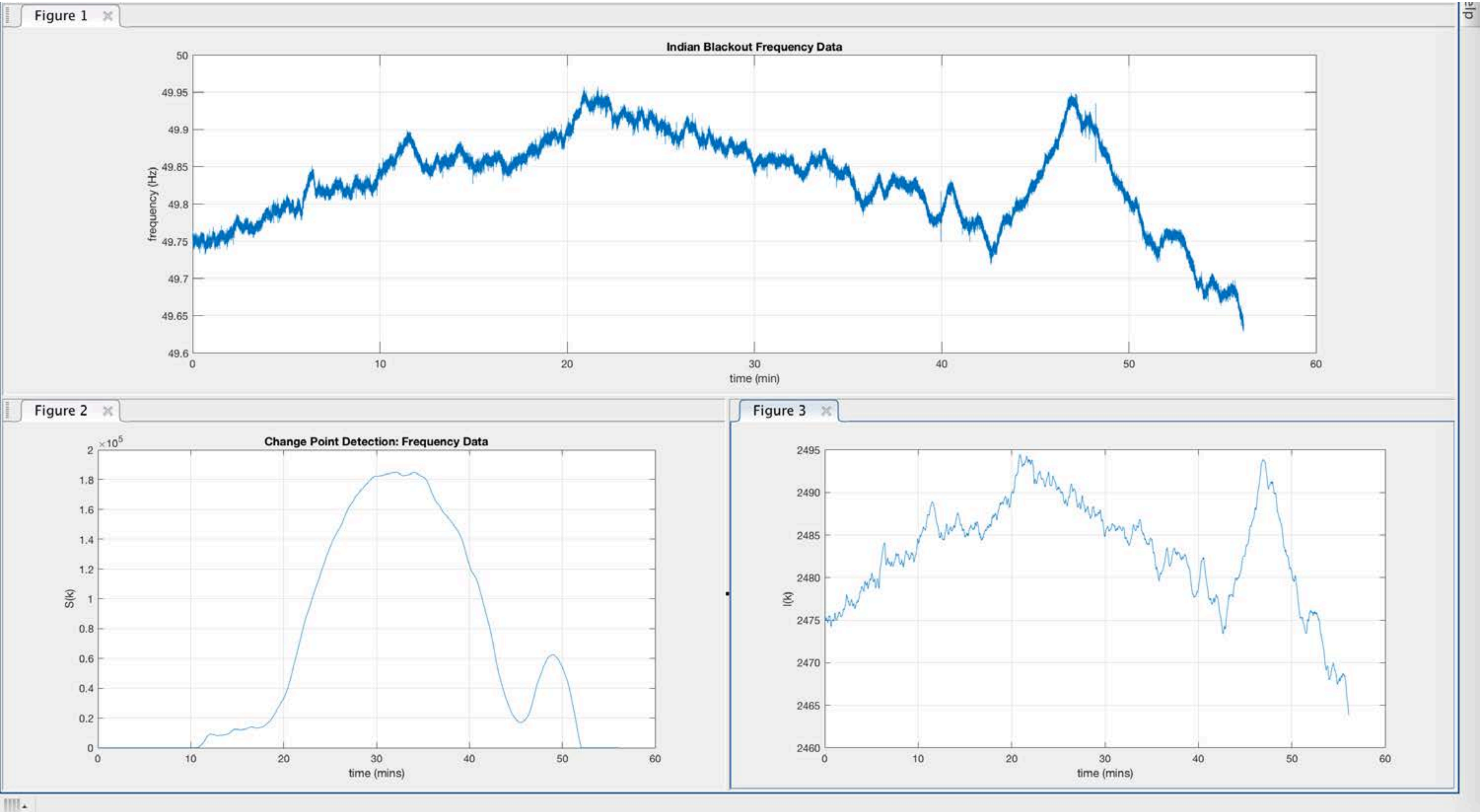

Change Point Detection Simulation

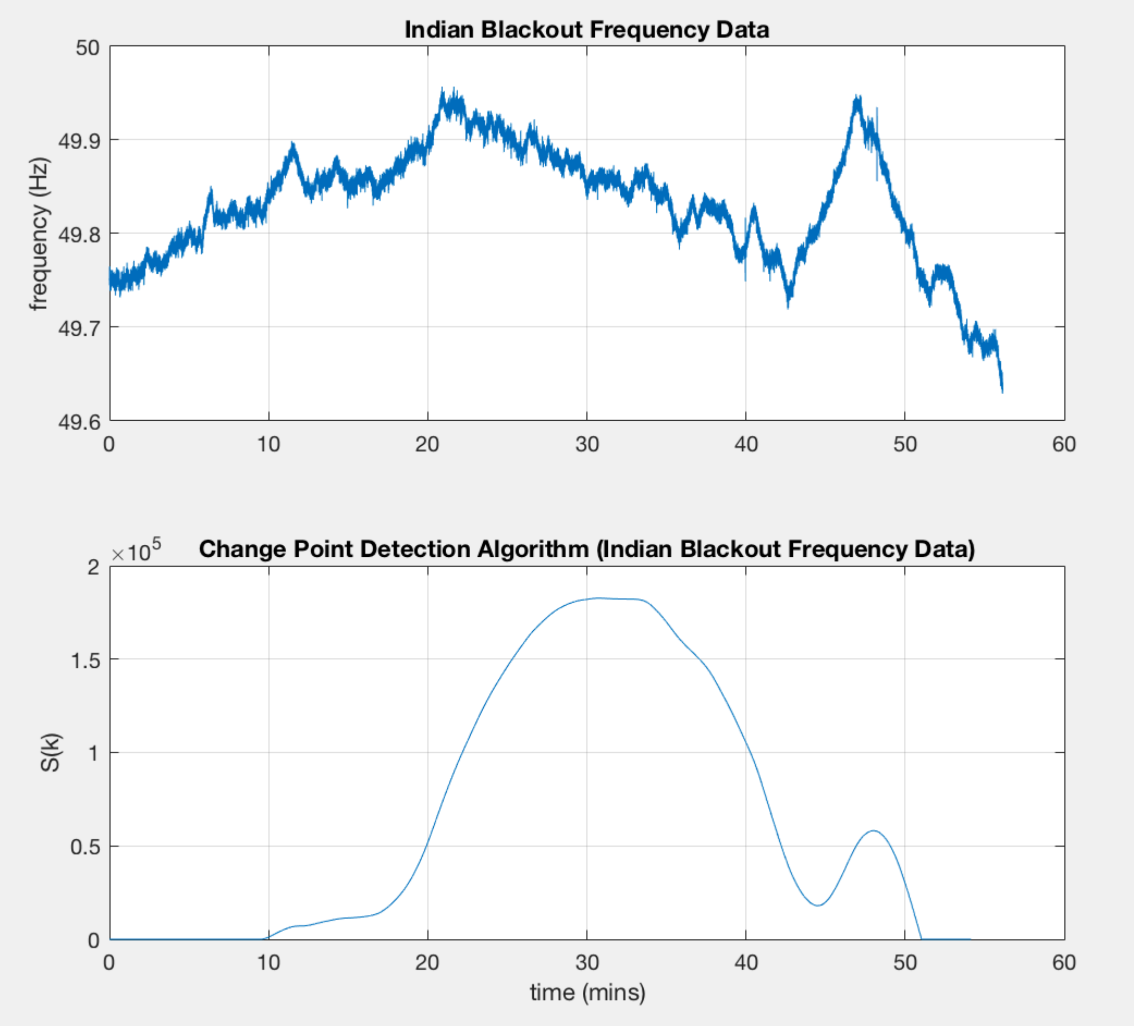

Data sampled at 50 samples/sec

L (lag) = 1 min (3000 samples)

From Shalalfe, et. al. (2016), it mentioned in the paper that the increase in the AR(1) starts around 33 mins before the blackout.

Nominal mutual information (I) is computed from time series before this time (around t<30min)

Plan of Action: Part II – Security

- Increase of Hurst exponent towards black-out
  - Kendall tau as statistical confirmation
- AR(1) versus Hurst exponent sample distribution for abnormality detection
- Falsification of swing equation by Hurst exponent
- Change Point Detection
  - Historic precedent: UDP flooding attack
  - Detection and simultaneous detection & identification
  - Threshold for False Alarm Rate
  - Indian blackout

Change Point Detection – Introduction

- Consider an iid sequence $\{X_k\}_{k=1}^{n}$
  - with "normal" regime probability density p_0 from
    $$k = [1, \lambda - 1]$$
  - and with "abnormal" probability density p_1 from
    $$k = [\lambda, n]$$
- **GOAL**: Find λ (**change point**) in the fastest possible way subject to some acceptable false alarm rates

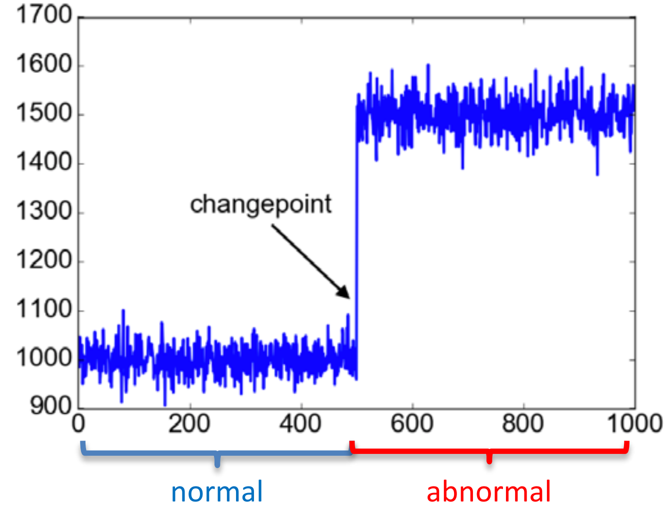

CPD Approaches

- **Shiryaev** (Bayesian) Procedure
  - λ assumed to have an a priori distribution

- Cumulative SUM (**CUSUM**) (minimax)
  - λ is deterministic, but unknown

- Goal: Minimize expected detection delay subject to false alarm rate

Change Point Detection (CUSUM)

- Change point - λ
  - considered deterministic, but unknown
- Probability measure - P_λ
  - defined as p_0 (on ‘normal’ regime) and p_1 (on “abnormal” regime)
- Null Hypothesis - H_0
  - that there has been no changes from λ up to and including n (based on the positive value of the log-likelihood ratio statistic Z_λ^n).

$$U^n = \left\{ \max_{0 \le \lambda \le n} Z_\lambda^n \right\}_+ , \quad Z_\lambda^n = \sum_{k=\lambda}^{n} \log \frac{p_1(x_k)}{p_0(x_k)},$$

- For security reasons, the statistic U^n is computed for the worst position of the change point. Note: $\{z\}_+ = \max\{0, z\}$

Recursive Form of Statistic

$$U^{n+1} = \left\{ \max_{0 \le \lambda \le n+1} \left(Z_\lambda^n + \log \frac{p_1(x_{n+1})}{p_0(x_{n+1})} \right) \right\}_+$$

$$= \left\{ \max \left\{ U^n + \log \frac{p_1(x_{n+1})}{p_0(x_{n+1})}, \log \frac{p_1(x_{n+1})}{p_0(x_{n+1})} \right\} \right\}_+$$

$$U^{n+1} = \max \left\{ 0, U^n + \log \frac{p_1(x_{n+1})}{p_0(x_{n+1})} \right\}$$

- Threshold h — $\tau(h) = \min\{n : U^n \ge h\}.$
- False Alarm Rate — $\mathrm{FAR} = 1/\mathbb{E}_{p_0}(\tau(h)) \le \overline{\mathrm{FAR}}$

Jayson Sia, Edmond Jonckheere, Laith Shalalfeh and Paul Bogdan, “PMU Change Point Detection of Imminent Voltage Collapse and Stealthy Attacks,” to appear in 2018 IEEE CDC.

Unknown "abnormal" Density p_1

- "normal" density p_0 is typically known
- "abnormal" density p_1 is not!

$$f_\theta(x) = \frac{\beta}{\eta}\left(\frac{x}{\eta}\right)^{\beta-1} \mathrm{e}^{-\left(\frac{x}{\eta}\right)^{\beta}}$$

- Solution: choose a family distributions $\{f_\theta\}$ parametrized by θ then adjust θ given some empirical knowledge on p_1
  - **Weibull Distribution**
    - where β is the shape parameter, η is the scale parameter, and the natural parameter $\theta = -1/\eta^\beta$
    - Weibull distribution is widely used in failure and reliability analysis.
    - It is also known to be the probability density that takes the least amount of data to be correctly identified

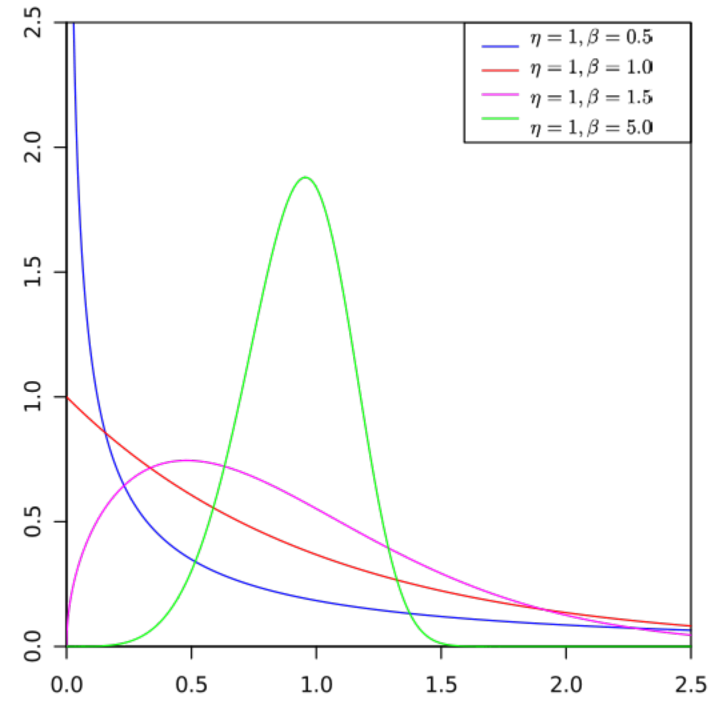

Simultaneous Detection and Estimation

- We modify the statistic U^n with a double maximization, with p_1 replaced by f_θ

$$U^n = \left\{ \max_{0 \le \lambda \le n} \max_{\theta} Z_\lambda^n \right\}_+$$

- In the security context, especially for stealthy attacks, $\max_{\theta} Z_\lambda^n$ assumes the density f_θ is the worst possible given the data.

- Does NOT have a recursive formulation.

Simultaneous Detection and Estimation

- Heuristically defined statistic

$$\widehat{U}^{n+1} = \max\left\{0, \widehat{U}^{n} + \max_{\theta} \log \frac{f_{\theta}(X_{n+1})}{p_0(X_{n+1})}\right\}, \widehat{U}^0 = 0$$

  - this dominate true statistic, $\widehat{U} > U$, and give overly conservative results with high false alarm rates

- Smoothing over $\arg\max_{\theta} \log(\cdot)$

$$\widetilde{U}^{n+1} = \max\left\{0, \widetilde{U}^{n} + \log \frac{f_{\widetilde{\theta}^{n+1}}(x_{n+1})}{p_0(x_{n+1})}\right\}, \quad \widetilde{U}^0 = 0,$$

$$\widetilde{\theta}^{n+1} = (1-\kappa)\widetilde{\theta}^{n} + \kappa \arg\max_{\theta} \log \frac{f_{\theta}(x_{k+1})}{p_0(x_{k+1})},$$

for some gain $0 < \kappa < 1$

Jayson Sia, Edmond Jonckheere, Laith Shalalfeh and Paul Bogdan, “PMU Change Point Detection of Imminent Voltage Collapse and Stealthy Attacks,” to appear in 2018 IEEE CDC.

Plan of Action: Part II – Security

- Increase of Hurst exponent towards black-out
  - Kendall tau as statistical confirmation
- AR(1) versus Hurst exponent sample distribution for abnormality detection
- Falsification of swing equation by Hurst exponent
- Change Point Detection
  - Historic precedent: UDP flooding attack
  - Detection and simultaneous detection & identification
  - Threshold for False Alarm Rate
  - Indian blackout

Threshold for False Alarm Rate

- Consider U^n as a simplified Itô diffusion process (with $b = 0$) over domain $D \subset \mathbb{R}$,

$$dU^t = b(U^t)dt + \sigma(U^t)dB_t, \qquad U^0 = x \in D,$$

- Let average time $T(x)$ for the 1-D random walk starting at x and reflecting at $-\epsilon$ to cross the absorption barrier at h is

$$T(x) = \frac{1}{\sigma^2(h^2 - x^2)} + \frac{2\epsilon}{\sigma^2}(h - x),$$

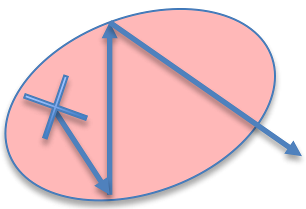

- Let $p_0 = N(\mu_0, \sigma_0)$, $p_1 = N(\mu_1, \sigma_1)$. It follows up to a good approximation ($\sigma_\alpha = \sigma_1 = \sigma_0$),

$$U^{n+1} - U^n \approx \frac{\mu_1 - \mu_0}{\sigma_\alpha^2}\left(X_{n+1} - \frac{\mu_0 + \mu_1}{2}\right)$$

Jayson Sia, Edmond Jonckheere, Laith Shalalfeh and Paul Bogdan, "PMU Change Point Detection of Imminent Voltage Collapse and Stealthy Attacks," to appear in 2018 IEEE CDC.

Threshold for False Alarm Rate

- Note that from the continuous time model (1),

$$\mathbb{E}(B_{t+\Delta t} - B_t)^2 = \Delta t,\ 1/\Delta t = \text{PMU sampling rate}$$

- The discrete- and continuous-time processes yields,

$$\sigma^2 = \frac{2(\mu_1 - \mu_0)^2}{\sigma_\alpha^2 \Delta t}$$

- Setting $\epsilon = 0$ in (2), and recall that

$$\text{FAR} = 1/T(x = 0) = \sigma^2/h^2$$

- Threshold estimate

$$h = \frac{\sqrt{2}(\mu_1 - \mu_0)}{\sigma_\alpha \sqrt{\Delta t}} \frac{1}{\sqrt{\text{FAR}}}$$

Jayson Sia, Edmond Jonckheere, Laith Shalalfeh and Paul Bogdan, "PMU Change Point Detection of Imminent Voltage Collapse and Stealthy Attacks," to appear in 2018 IEEE CDC.

Empirical PMU Data

EPFL Campus Data under normal operating conditions

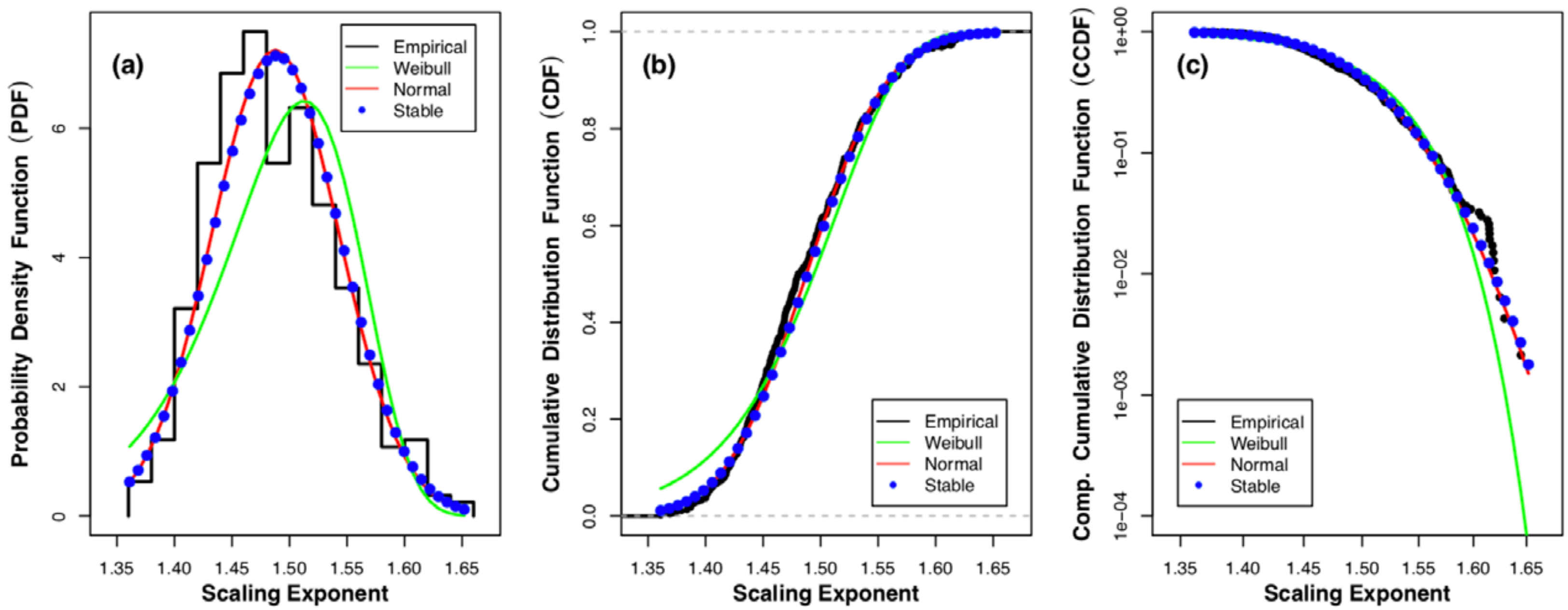

Distribution of the Frequency Scaling Exponent under Normal Conditions

Normal distribution fit (EPFL data)

$$\mu_0 = 1.488, \quad \sigma_0 = 0.055 \quad \text{(EPFL)}$$

Plan of Action: Part II – Security

- Increase of Hurst exponent towards black-out
  - Kendall tau as statistical confirmation
- AR(1) versus Hurst exponent sample distribution for abnormality detection
- Falsification of swing equation by Hurst exponent
- Change Point Detection
  - Historic precedent: UDP flooding attack
  - Detection and simultaneous detection & identification
  - Threshold for False Alarm Rate
  - Indian blackout

2012 Indian Blackout

Empirical estimates for pre- and post-distributions

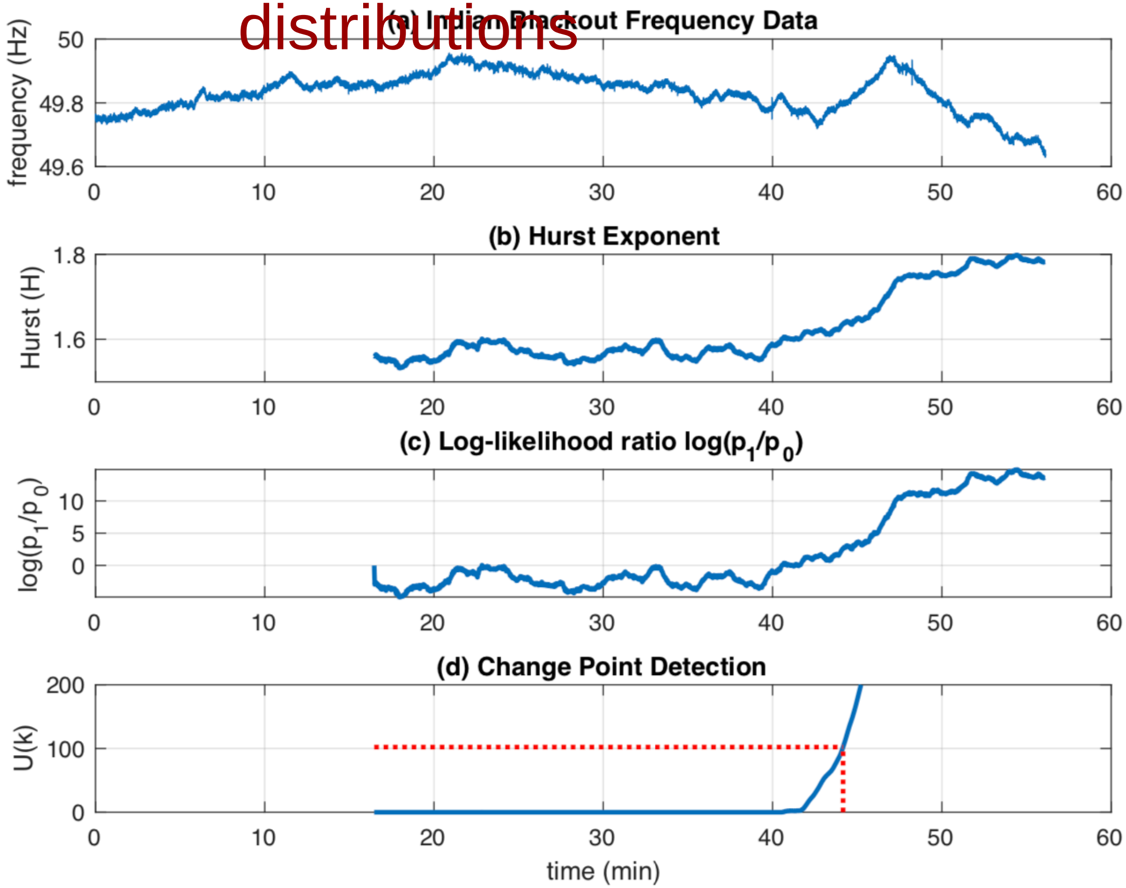

Normal regime p_0
(from empirical data)

$$p_0 \sim N(\mu_0, \sigma_0) = N(1.488, 0.055)$$

Abnormal regime p_1
normal distribution shifted in mean

$$p_1 \sim N(\mu_1, \sigma_1) = N(1.7, 0.055)$$

Threshold
$\Delta t = 0.033, \mathrm{FAR} = 0.1$
$h = 101.9$
Crosses at $t = 44.17$ min

Unknown Distribution p_1

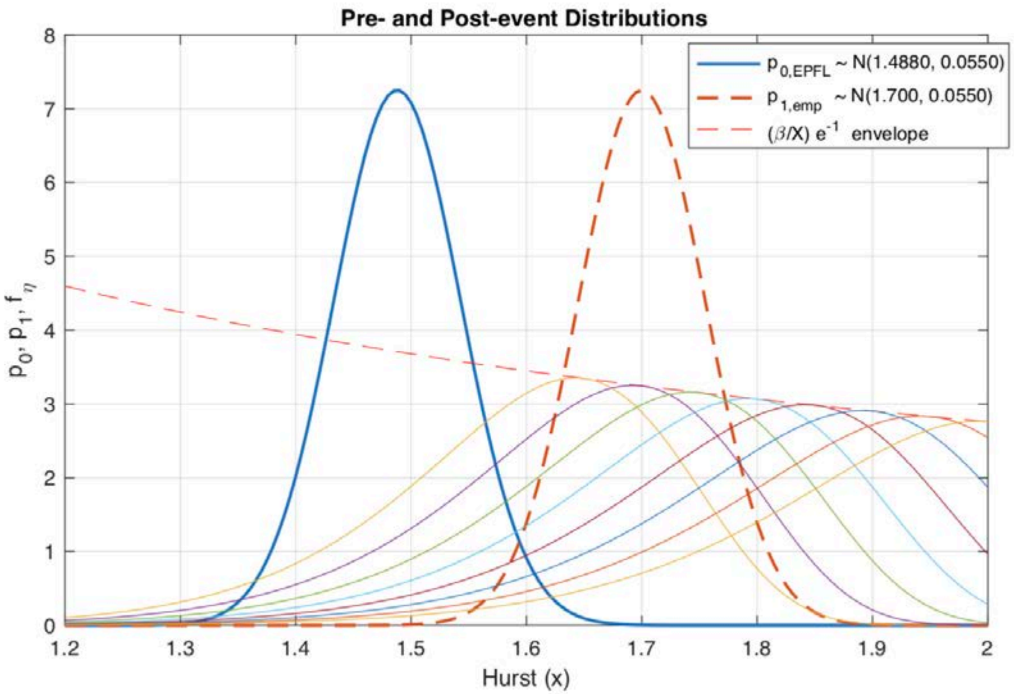

Normal distributions $p_0(x)$ and $p_{1,emp}(x)$, family of Weibull distributions $f_\eta(x)$ with $\beta = 15$, and envelope of Weibull distributions

p_1 as Weibull distribution parametrized by natural parameter $\theta = -1/\eta^\beta$

For fixed β, distribution is only parametrized by the scaling parameter η which is related to the mean as

$$\mathbb{E}(x) = \eta\Gamma(1 + 1/\beta)$$

2012 Indian Blackout

Simultaneous detection and estimation

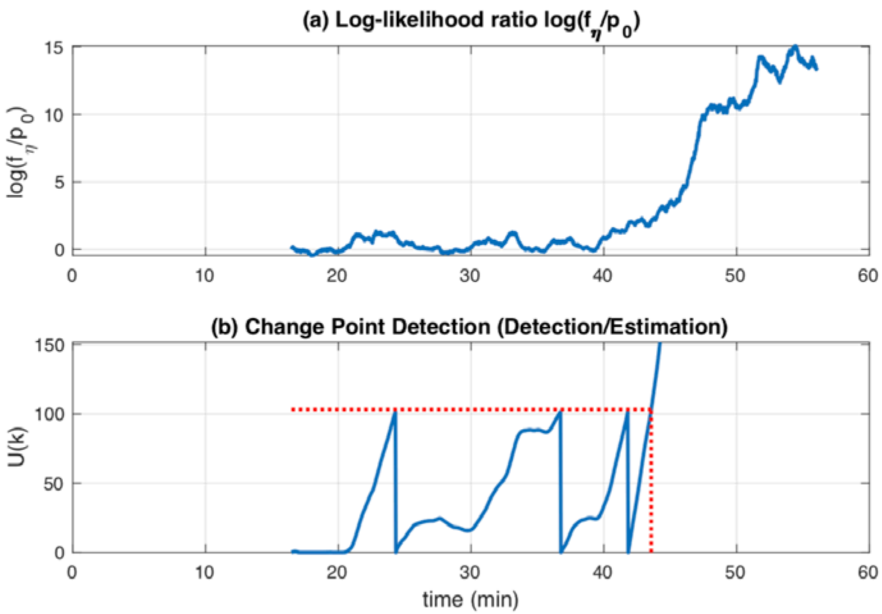

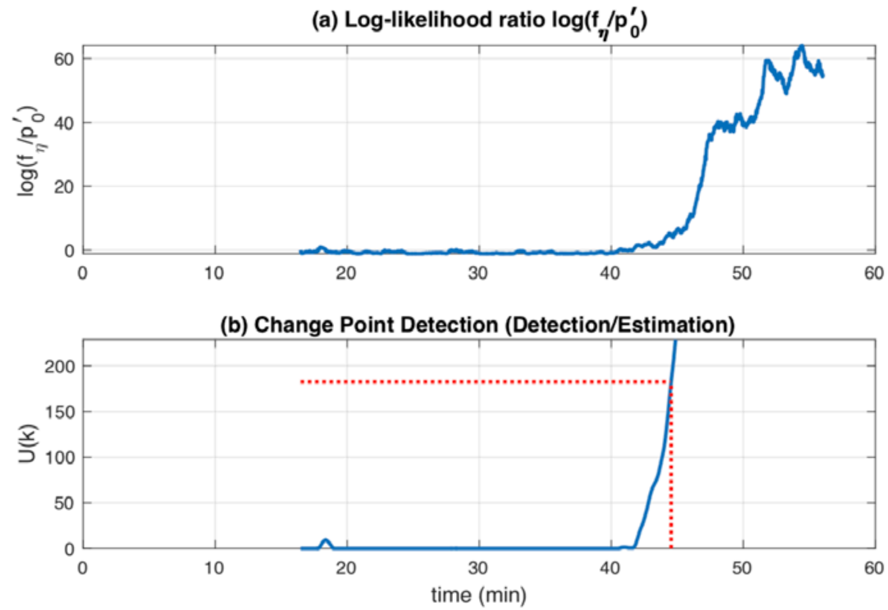

$\mu_0 = 1.488, \sigma_0 = 0.055$ (EPFL)

$h = 101.9$

False alarms, alarm at $t = 43.56$ min

$\mu_0' = 1.5733, \sigma_0' = 0.0198$ (Indian pre-blackout)

$h = 178.76$

No false alarm, alarm at $t = 44.53$ min

Part II: Summary

PMU Frequency Time Series

Empirical

Single Exponent

↓

DFA

ARIMA | ARFIMA

$$\left(1-\sum_{i=1}^{p}\phi_i B^i\right)(1-B)^d X_t = \left(1+\sum_{i=1}^{q}\theta_i B^i\right)\varepsilon_t$$

SECURITY

Offline

Kendall-Tau Test

$$\tau = \frac{\text{\# of concordant pairs} - \text{\# of discordant pairs}}{n(n-1)/2}$$

Online

Change Point Detection

$$U^{n+1} = \max\left\{0, U^n + \log\frac{p_1(x_{n+1})}{p_0(x_{n+1})}\right\}$$

Conclusions

- Power grid is a Cyber-Physical System (CPS)
- Security on both the Cyber and the Physical layers can be approached using Change Point Detection (CPD)
- On the physical side, best results are achieved by CPD on the Hurst exponent of the frequency data

References

- L. Shalalfe, P. Bogdan and E. Jonckheere, **Evidence of Long-Range Dependence in Power Grid**, IEEE Power and Energy Society General Meeting, 2016.
- L. Shalalfe, P. Bogdan and E. Jonckheere, **Kendall's Tau of Frequency Hurst Exponent as Blackout Proximity Margin**, IEEE International Conference on Smart Grid Communications (SmartGridComm), 2016.
- L. Shalalfe and E. Jonckheere, **Load Aggregation Effect in Power Grid**, IEEE 55th Conference on Decision and Control (CDC), 2016.
- L. Shalalfe and E. Jonckheere, **The Existence of a Voltage Collapse Solution in the Static-Dynamic Gap**, American Control Conference (ACC), 2016.
- Y. Xue and P. Bogdan, **Constructing Compact Causal Mathematical Models for Complex Dynamics**, 8th ACM/IEEE International Conference on Cyber-Physical System (ICCPS), 2017.
- J. Sia, E. Jonckheere, L. Shalalfeh and P. Bogdan, **PMU Change Point Detection of Imminent Voltage Collapse and Stealthy Attacks**, to appear in the IEEE 57th Conference on Decision and Control (CDC), 2018.
- L. Shalalfeh, P. Bodgan, and E. Jonckheere, ``Modeling of PMU data using ARFIMA models, Clemson University Power System Conference, Paper Session T-M II: Phasor Measurement Units (PMUs), Charleston, SC, September, 2018.

Towards a Cyber-Physical Simulation Platform

Physical Layer ← - - - - - - - - - - - - - - - → Cyber Layer

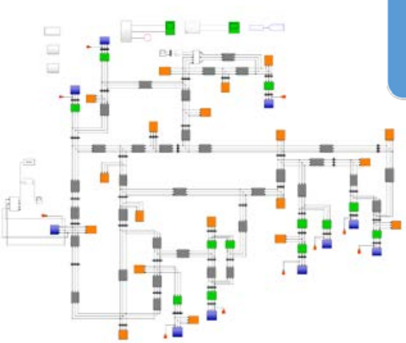

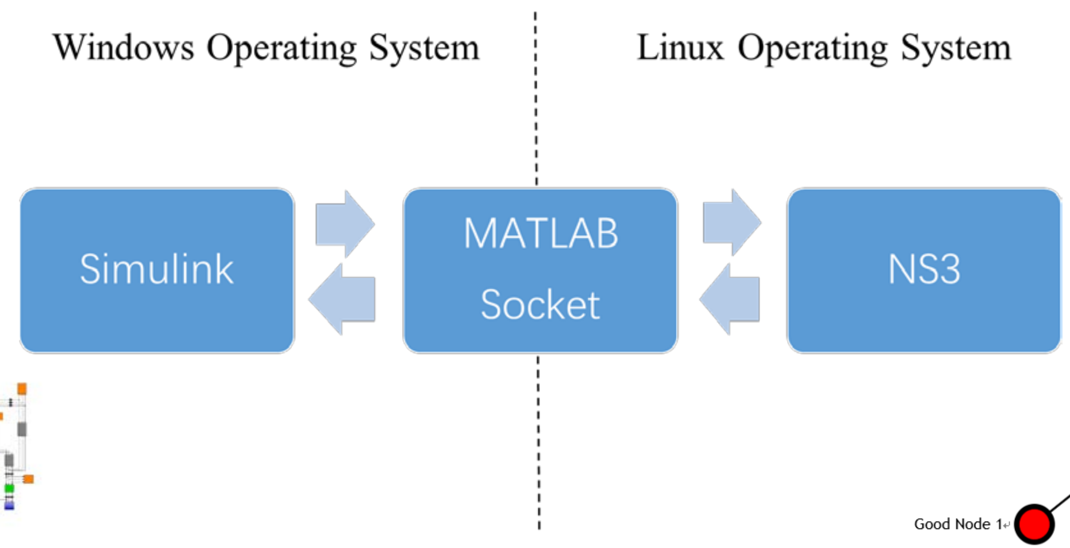

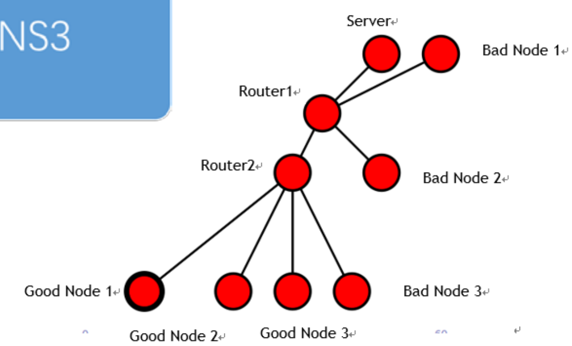

Thank you!
Questions?